Spring 2021

Studies of the Chemistry of Pentaruthenium Carbido Carbonyl Cluster Complexes with Aldehydes, Azobenzene and Alkynes

Humaiara Akter

Studies of the Chemistry of Pentaruthenium Carbido Carbonyl Cluster Complexes with Aldehydes, Azobenzene and Alkynes

by

Humaiara Akter

Bachelor of Science
University of Dhaka, 2011

Master of Science
University of Dhaka, 2013

Submitted in Partial Fulfillment of the Requirements

For the Degree of Doctor of Philosophy in

Chemistry

College of Arts and Sciences

University of South Carolina

2021

Accepted by:

Richard D. Adams, Major Professor

Dmitry V. Peryshkov, Committee Member

Linda S. Shimizu, Committee Member

Christopher Williams, Committee Member

Tracey L. Weldon, Interim Vice Provost and Dean of the Graduate School

Dedication

To my parents for their unconditional love and support.

Acknowledgements

I would like to express my deepest gratitude to Dr. Richard D. Adams for his great supervision and guidance. Your inspiration and support allowed me to accomplish my educational goals and focus on my academic pursuits. Thank you for always being there to answer all my questions whenever I ran into trouble or had a question. I truly appreciate you for all the knowledge and skills you taught me that will shape my future career.

I would like to thank the members of my PhD committee: Professors Dmitry Peryshkov, Linda Shimizu, and Christopher Williams for accepting to review my work and for taking the time to be there for all my comprehensive exams and dissertation defense. I would also like to thank Professor Thomas Bryson for the support and guidance at the beginning of my PhD studies. I am thankful to Dr. Jonathan Tedder who taught me all the techniques to carry out experiments in a chemistry lab. I am thankful to Dr. Joseph Kiprotich, Dr. Poonam Dhull, Morteza Maleki, Nutan Wakdikar and Meenal Kaushal for their encouragement and help.

I am forever grateful to my parents for their unconditional love, support, and prayer throughout my journey here at UofSC. I wish my father (Abbu) is here to see me accomplish of what I have dreamt for. I am thankful to my husband Mohammad Jahirul Islam for all his love, care, and encouragement. Your support made my journey easy and accomplishable. I am thankful to the little one Ruaydaa Zaarin. Your smile gave me strength to achieve my goal. Lastly, I am thankful to my siblings Raihan Mahmud, Fayzunnesa Maria and Bilkis Akter for always supporting me and being there for me.

Abstract

Polynuclear metal carbonyl complexes serve as the bridging model between heterogeneous catalysis and homogeneous catalysis for the activation of small molecules. $Ru_5(\mu_5\text{-}C)(CO)_{15}$ has been found to exhibit superior reactivity due to its unusual polynuclear metal geometry. possibilities of interconversions of ligand bonding modes, and the formation of the electronically unsaturated metal species. C-H activation in aldehydes and azobenzene of pentaruthenium cluster complexes is described in chapters 2 and 3 respectively. The formation of new hydrocarbyl zwitterions and C – C coupling ethyne to the carbido carbon in the complex, and the alkyne insertion reactions with pentaruthenium cluster complexes are described in chapters 4, 5, and 6 respectively.

Aldehydic C-H activation of biomass derived important aldehydes such as furfural and 5-hydroxymethylfurfural by $Ru_5(\mu_5\text{-}C)(CO)_{15}$ is reported in chapter 2. The reaction $Ru_5(\mu_5\text{-}C)(CO)_{15}$ with furfural yielded $Ru_5(\mu_5\text{-}C)(CO)_{14}(\mu\text{-}\eta^2\text{-}O{=}CC_4OH_3)(\mu\text{-}H)$, **2.2** which has an η^2-bridging furoyl ligand coordinated across the open edge of a Ru wingtip-bridged Ru_4C cluster, whereas the hydrido ligand bridges the hinge metal atoms. Similarly, the reaction $Ru_5(\mu_5\text{-}C)(CO)_{15}$ with furfural yielded $Ru_5(\mu_5\text{-}C)(CO)_{14}[\mu\text{-}\eta^2\text{-}O{=}CC_4OH_2(CH_2OH)](\mu\text{-}H)$, **2.3**.

The activation and coordination of azobenzene with $Ru_5(\mu_5\text{-}C)(CO)_{15}$ and its derivative is discussed in chapter 3. The reaction of $Ru_5(\mu_5\text{-}C)(CO)_{15}$ with azobenzene,

PhN=NPh, yielded the pentaruthenium carbido cluster compound $Ru_5C(CO)_{13}(C_6H_4N{=}NC_6H_5)(\mu\text{-}H)$, **3.4** containing a chelating ortho-metalated azobenzene ligand on one of the ruthenium atoms in a opened square-pyramidal Ru_5C cluster. Compound **3.4** is electronically unsaturated and it readily adds one CO ligand at 25 °C to yield the electronically saturated complex $Ru_5C(CO)_{14}(C_6H_4N{=}NC_6H_5)[\mu\text{-}H]$, **3.5**. $Ru_5C(CO)_{13}(\mu\text{-}\eta^2\text{-}Ph)[\mu\text{-}Au(NHC)]$ reacts with azobenzene to yield the azobenzene complex $Ru_5C(CO)_{13}(\mu\text{-}\eta^2\text{-}PhN{=}NPh)(\eta^1\text{-}Ph)[\mu\text{–}Au(NHC)]$, **3.6**, NHC = 1,3-bis(2,6-diisopropylphenyl-imidazole-2-ylidene), which contains a novel bridging di-σ-η^2-N,N coordinated azobenzene ligand across an open edge of an Ru_5C cluster. Compound **3.6** eliminated benzene and was transformed to the new compound $Ru_5C(CO)_{13}(C_6H_4N{=}NC_6H_5)[\mu\text{-}Au(NHC)]$, **3.7** when heated to 105 °C for 3 h. Compound **3.7** is similar to **3.4** except that it has an Au(NHC) group in the place of the bridging hydrido ligand in **3.4**. Compound **3.7** is also formally electronically unsaturated like **3.4**.

The formation of zwitterionic, hydrocarbylonium ligands from a combination of alkynes and Me_3N with pentaruthenium cluster complexes is reported in chapter 4. Reactions of the pentaruthenium cluster complexes $Ru_5(\mu_5\text{-}C)(CO)_{15}$, $Ru_5(\mu_5\text{-}C)(CO)_{14}[\mu\text{-}\eta^2\text{-}O{=}C(NMe_2)](\mu\text{-}H)$, **4.6**, and $Ru_5(\mu_5\text{-}C)(CO)_{15}Cl(\mu\text{-}H)$, **4.7** with ethyne ($C_2H_2$) in the presence of Me_3NO yielded the zwitterionic complexes $Ru_5(\mu_5\text{-}C)(CO)_{13}[\mu\text{-}\eta^2\text{-}CHCH(NMe_3)]$ **4.8**, $Ru_5(\mu_5\text{-}C)\text{-}(CO)_{13}[\mu\text{-}\eta^2\text{-}O{=}C(NMe_2)](\eta^1\text{-}\textit{E}\text{-}CH{=}CH(NMe_3)(\mu\text{-}H)$ **4.9**, and $Ru_5(\mu_5\text{-}C)(CO)_{13}Cl[\eta^1\text{-}\textit{E}\text{-}CH{=}CH(NMe_3)](\mu\text{-}H)$ **4.11**. Each product contains a positively-charged, trimethylammonioethenyl ligand, $CH{=}CH(^{+}NMe_3)$, that is derived from a 2-trimethylammonioethenide, $^{-}CH{=}CH(^{+}NMe3)$, zwitterion that formally has a positive charge on the nitrogen atom and a negative charge on the terminal enyl carbon

atom. The trimethylammonioethenyl ligand, CH=CH($^{+}$NMe$_3$) in **4.8** is a η^2-ligand that bridges a Ru−Ru bond on a basal edge of the square-pyramidal Ru_5 cluster by a combination of $\sigma + \pi$ coordination of the ethenyl group. Compounds **4.9** and **4.11** each contain a η^1-terminally-coordinated [η^1-*E*-CH=CH($^{+}$NMe$_3$)] ligand with an *E* stereochemistry at the C=C double bond in open Ru_5 cluster complexes. Compound **4.9** was decarbonylated to yield the compound $Ru_5(\mu_5\text{-C})(CO)_{12}[\mu\text{-}\eta^2\text{-O=C(NMe}_2)][\mu\text{-}\eta^2\text{-CH=CH(NMe}_3)](\mu\text{-H})$ **4.10** containing a η^2-bridging CHCH($^{+}$NMe$_3$) ligand. Compound **4.10** was converted back to **4.9** by the addition of CO. Two zwitterionic products, $Ru_5(\mu_5\text{-C})(CO)_{14}[\eta^1\text{-E-CH=CH(NMe}_3)]$ **4.12** and $Ru_5(\mu_5\text{-C})(CO)_{15}[\eta^1\text{-E-CH=CH(NMe}_3)]$ **4.13**, were obtained by the addition of CO to **4.8**. Compound **4.12** is an intermediate en route to **4.13**. Compound **4.12** contains a terminally-coordinated η^1-*E*-CH=CH($^{+}$NMe$_3$) ligand on one of the basal Ru atoms of a square-pyramidal Ru_5 cluster. Compound **4.13** also contains a terminally coordinated η^1-*E*-CH=CH($^{+}$NMe$_3$) ligand on the wing-tip bridging Ru atom of a butterfly Ru_4C cluster. Treatment of **4.6** with methyl propiolate (HC=CCO$_2$Me) yielded the zwitterionic complex $Ru_5(\mu_5\text{-C})(CO)_{13}[\mu\text{-}\eta^2\text{-O=C(NMe}_2)][\eta^1\text{-}E\text{-(MeO}_2\text{C)C=C(H)NMe}_3](\mu\text{-H})$ **4.14** that is structurally similar to **4.9** but contains a η^1-*E*-(MeO$_2$C)C=C(H)($^{+}$NMe$_3$) ligand. Compound **4.14** eliminated its NMe$_3$ group to yield the compounds $Ru_5(\mu_5\text{-C})(CO)_{13}[\mu\text{-}\eta^2\text{-O=C(NMe}_2)][\mu\text{-}\eta^2\text{-(MeO}_2\text{C)HC=CH}]$ **4.15** which contains a bridging methoxycarbonyl-substituted alkenyl ligand and the known compound $Ru_5(\mu_5\text{-C})(CO)_{13}[\mu\text{-}\eta^2\ \text{O=C(NMe}_2)](\text{HNMe}_2)(\mu\text{-H})$ **4.16**.

The reactivity of a (μ_5-C) carbido carbon in the pentaruthenium carbonyl cluster, $Ru_5(\mu_5\text{-C})(CO)_{15}$ with the unsaturated molecule ethyne (C_2H_2) is reported in chapter 5. The thermal reaction at 48 °C yielded four new ethyne-bound cluster complexes, $Ru_5[\mu_4\text{-}\eta^3\text{:}\eta^1\text{-}$

CC(H)C(H)C(H)C(H)](CO)$_{13}$(μ_4-η^2:η^1:η^2:η^1-HCCH), **5.2**; Ru_5[μ_4-η^4:η^1-CC(H)C(H)C(H)C(H)](CO)$_{12}$(μ_4-η^2:η^1:η^2:η^1-HCCH), **5.3**; Ru_5[μ_4-η^4:η^1-CC(H)C(H)C(H)C(H)](CO)$_{12}$(μ_4-η^2:η^1:η^2:η^1-HCCH), **5.4**; and $Ru_4(CO)_{11}$(μ_4-η^2:η^1:η^2:η^1-HCCH)Ru(CO)$_3$(C_5H_4), **5.5**. All four compounds contain a quadruply-bridging ethyne ligand coordinated to four metal atoms. Compound **5.3** has a bridging metalla-penta-1,3-dienyl ligand, RuCC(H)C(H)C(H)C(H), where two C_2H_2 molecules have been coupled to the carbido carbon of the cluster by forming a C – C bond. Upon carbonylation of **5.3**, the bridging metalla-penta-1,3-dienyl ligand, CC(H)C(H)C(H)C(H) changes its coordination mode from η^4:η^1 to η^3:η^1 in **5.2**. When **5.2** was treated with CO thermally**,** the bridging metalla-penta-1,3-dienyl ligand changed its coordination mode from bridging η^3:η^1 mode to a η^5–metalla-cyclopenta-1,3-dienyl ligand in **5.5**. The thermal decomposition of **5.5** in presence of water yielded the known compounds: a quadruply-bridged $Ru_4(CO)_{12}$(μ_4-C_2H_2), **5.6** and the dimer [Ru(η^5-C_5H_5)(CO)$_2$]$_2$, **5.7**.

In continuation of the study of alkynes with the pentaruthenium carbonyl cluster complex, we studied the insertion of alkynes into the Ru-phenyl bond of Ru_5(μ_5–C)(CO)$_{13}$(μ–η^2–Ph)[μ–Au(NHC)], **6.3** in chapter 6. The reaction of C_2H_2 and HC_2Ph with Ru_5(μ_5–C)(CO)$_{13}$(μ–η^2–Ph)[μ–Au(NHC)], **6.3** where NHC = 1,3-bis(2,6-diisopropylphenyl-imidazol-2-ylidene) yielded the new alkenyl complexes Ru_5(μ_5–C)(CO)$_{13}$[μ-η^2-*E*-C(H)C(H)Ph)][μ-Au(NHC)], **6.2** and $Ru_5C(CO)_{13}$[μ-η^2-*E*-C(Ph)C(H)Ph][μ-Au(NHC)], **6.3** by insertion of the alkyne into the metal – carbon σ-bond of the phenyl ring in **6.1**.

Table of Contents

Dedication iii

Acknowledgements iv

Abstract v

List of Tables x

List of Figures xi

Chapter 1: Introduction 1

Chapter 2: CH Activations in Aldehydes in Reactions with $Ru_5(\mu_5\text{-}C)(CO)_{15}$ 24

Chapter 3: The Coordination and Activation of Azobenzene by $Ru_5(\mu_5\text{-}C)$ Cluster Complexes 40

Chapter 4: Synthesis, Structures and Transformations of Bridging and Terminally-Coordinated Trimethylammonioalkenyl Ligands in Zwitterionic Pentaruthenium Carbido Carbonyl Complexes 66

Chapter 5: A (μ_5-C) Carbido Carbon Initiated C - C Coupling of Ethyne on $Ru_5(\mu_5\text{-}C)(CO)_{15}$ Cluster 114

Chapter 6: *Trans*-Stereochemistry from the Insertion of Alkynes into a Bridging-Phenyl Ruthenium Bond in a Pentaruthenium Cluster Complex 140

Appendix A: Copyright Releases 158

List of Tables

Table 2.1 Crystal data, data collection parameters for compounds **2.2** and **2.3** 36

Table 3.1 Crystal data, data collection parameters for compounds **3.4** and **3.5** 57

Table 3.2 Crystal data, data collection parameters for compounds **3.6** and **3.7** 58

Table 4.1 Crystal data, data collection parameters for compounds **4.7** and **4.8** 99

Table 4.2 Crystal data, data collection parameters for compounds **4.10** and **4.11** 100

Table 4.3 Crystal data, data collection parameters for compounds **4.12** and **4.13** 101

Table 4.4 Crystal data, data collection parameters for compounds **4.14** and **4.15** 102

Table 5.1 Crystal data, data collection parameters for compounds **5.2** and **5.3** 133

Table 5.2 Crystal data, data collection parameters for compounds **5.4** and **5.5** 134

Table 6.1 Crystal data, data collection parameters for compounds **6.2** and **6.3** 154

List of Figures

Figure 2.1. An ORTEP diagram of the molecular structure of $Ru_5(\mu_5\text{-}C)(CO)_{14}(\mu\text{-}\eta^2\text{-}O{=}CC_4OH_3)(\mu\text{-}H)$, **2.2** 37

Figure 2.2 An ORTEP diagram of the molecular structure of $Ru_5(\mu_5\text{-}C)(CO)_{14}(\mu\text{-}\eta^2\text{-}O{=}CC_4OH_2CH_2OH)(\mu\text{-}H)$, **2.3** 38

Figure 3.1 An ORTEP diagram of the molecular structure of $Ru_5C(CO)_{13}(C_6H_4N{=}NC_6H_5)(\mu{-}H)$, **3.4**.....59

Figure 3.2 Selected molecular orbitals (MOs) with calculated energies in eV for compound **3.4**.....60

Figure 3.3 An ORTEP diagram of the molecular structure of $Ru_5C(CO)_{14}(C_6H_4N{=}NC_6H_5)(\mu{-}H)$, **3.5**.....61

Figure 3.4 Selected molecular orbitals (MOs) with calculated energies in eV for compound **3.5**.....62

Figure 3.5 An ORTEP diagram of the molecular structure of $Ru_5C(CO)_{13}(\mu{-}\eta^2{-}PhN{=}NPh)(\eta^1{-}Ph)[\mu{-}Au(NHC)]$, **3.6** 63

Figure 3.6 An ORTEP diagram of the molecular structure of $Ru_5C(CO)_{13}(C_6H_4N\text{-}NC_6H_5)[\mu{-}Au(NHC)]$, **3.7**.....64

Figure 4.1 An ORTEP diagram of the molecular structure of $Ru_5(\mu_5\text{-}C)(CO)_{13}[\mu\text{-}\eta^2\text{-}HC{=}CH\text{-}N(CH_3)_3]$, **4.8** 103

Figure 4.2 An ORTEP diagram of the molecular structure of $Ru_5(\mu_5\text{-}C)(CO)_{13}[\mu\text{-}\eta^2\text{-}O{=}C(NMe_2)][\eta^1\text{-}\textit{E}\text{-}CH{=}CH(NMe_3)](\mu\text{-}H)$, **4.9**.....104

Figure 4.3 An ORTEP diagram of the molecular structure of $Ru_5(\mu_5\text{-}C)(CO)_{12}(\mu\text{-}\eta^2\text{-}O{=}CN(CH_3)_2)(\mu\text{-}\eta^2\text{-}CH{=}CHNMe_3)(\mu\text{-}H)$, **4.10**.....105

Figure 4.4 An ORTEP diagram of the molecular structure of $Ru_5(\mu_5\text{-}C)(CO)_{15}Cl(\mu\text{-}H)$, **4.7**.....106

Figure 4.5 An ORTEP diagram of the molecular structure of $Ru_5C(CO)_{14}[\eta^1\text{-}\textit{E}\text{-}HC{=}CHN(CH_3)_3]Cl(\mu\text{-}H)$, **4.11** 107

Figure 4.6 An ORTEP diagram of the molecular structure of $Ru_5(\mu_5\text{-}C)(CO)_{14}(\eta^1\text{-}E\text{-}CH{=}CHNMe_3)$, **4.12** 108

Figure 4.7 An ORTEP diagram of the molecular structure of $Ru_5(\mu_5\text{-}C)(CO)_{15}(\eta^1\text{-}E\text{-}CH{=}CHNMe_3)$, **4.13** 109

Figure 4.8 An ORTEP diagram of the molecular structure of $Ru_5(\mu_5\text{-}C)(CO)_{13}[\mu\text{-}\eta^2\text{-}O{=}CN(CH_3)_2](\mu\text{-}H)[\eta^1\text{-}HC_2(CO_2CH_3)N(CH_3)_3]$, **4.14** 110

Figure 4.9 An ORTEP diagram of the molecular structure of $Ru_5(\mu_5\text{-}C)(CO)_{13}[\mu\text{-}\eta^2\text{-}O{=}CN(CH_3)_2][\mu\text{-}\eta^2\text{-}(CH_3O_2C)HC{=}CH]$, **4.15**.....111

Figure 5.1 An ORTEP diagram of the molecular structure of $Ru_5[\mu_4\text{-}\eta^3{:}\eta^1\text{-}CC(H)C(H)C(H)C(H)](CO)_{13}(\mu_4\text{-}\eta^2{:}\eta^1{:}\eta^2{:}\eta^1\text{-}HCCH)$, **5.2** 135

Figure 5.2 An ORTEP diagram of the molecular structure of $Ru_5[\mu_4\text{-}\eta^4{:}\eta^1\text{-}CC(H)C(H)C(H)C(H)](CO)_{12}(\mu_4\text{-}\eta^2{:}\eta^1{:}\eta^2{:}\eta^1\text{-}HCCH)$, **5.3** 136

Figure 5.3 An ORTEP diagram of the molecular structure of $Ru_5(CO)_{13}[\mu_4\text{-}\eta^1{:}\eta^3{:}\eta^1{:}\eta^4\text{-}C(H)C(H)CC(H)C(H)C(H)C(H)]$, **5.4** 137

Figure 5.4 An ORTEP diagram of the molecular structure of $Ru_4(CO)_{11}(\mu_4\text{-}\eta^2{:}\eta^1{:}\eta^2{:}\eta^1\text{-}HCCH)Ru(CO)_3(C_5H_4)$, **5.5** 138

Figure 6.1 An ORTEP diagram of the molecular structure of $Ru_5C(CO)_{13}(\mu\text{-}\eta^2\text{-}E\text{-}CHCHPh)[\mu\text{-}Au(NHC)]$, **6.2** 155

Figure 6.2 An ORTEP diagram of the molecular structure of one of the two similar, independent molecules in the unit cell of $Ru_5C(CO)_{13}(\mu\text{-}\eta^2\text{-}E\text{-}C(Ph)C(H)Ph)[\mu\text{-}Au(NHC)]$, **6.3**.....156

Chapter 1

Introduction

The major constituents of natural gas, and petroleum are lighter alkanes such as, methane, ethane, propane and butane.[1] Currently, methane and coal are converted to methanol or longer chain hydrocarbon via synthesis gas intermediates (CO with H_2), which requires energy intensive conditions.[2] Ultimately, this industrial process contributes to the large-scale CO_2 emission and becomes a potential source of global warming.[3]

The difficulty arises from the constituent atoms of the alkane itself due to the presence of strong and localized C-C and C-H bonds. In particular, the C-H bond dissociation energy (BDE) in methane is 105 Kcal/mol.[4] Very low acidity and basicity of the C-H bond arises from the small difference between their electronegativities ($\chi_C = 2.55$; $\chi_H = 2.20$) and thus estimated pK_a is about 45-60.[5] Therefore the activation of C-C and C-H bonds in hydrocarbons remains the key challenge for obtaining value added chemicals from natural gas and petroleum.

1.1 Challenges of C-H bond Activation and Functionalization

Although C-H bonds in alkanes are strong and localized, they are known to undergo a variety of free radical oxidation processes which are not selective. More often the functionalized product is more reactive than the alkane itself leading to overoxidation and ultimately yielding mixtures of products.[6] Hence, selective catalysis is required to achieve

desired products. To date, two distinctive types of catalysis are being applied to carry out C-H activation and functionalization. One is heterogeneous catalysis, where most of the catalysts are precious metals or metal oxides on a solid support.[7] Industrial applications are mostly based upon heterogeneous catalysis and require high temperatures and high-pressure conditions. Hence, research tends to be focused on performing catalysis under milder conditions than conventional heterogeneous catalyses. Homogeneous catalysis is an alternative where both the reactant and catalyst are in same phase, for example in a solution. The first example of homogeneous CH activation catalysis was reported in 1960 by Shilov, involving the addition of alkanes including methane, to a mixture of H_2PtCl_6 and Na_2PtCl_4 which yielded the formation of alkyl halides and alcohols, although it requires an equivalent amount of Pt(IV) salt (Scheme 1.1).[8] Later, Periana showed that a Pt(II) metal complex can be used to selectively oxidize methane, but it requires the use of harsh chemicals such as, H_2SO_4 that complicate the product purification steps.[9]

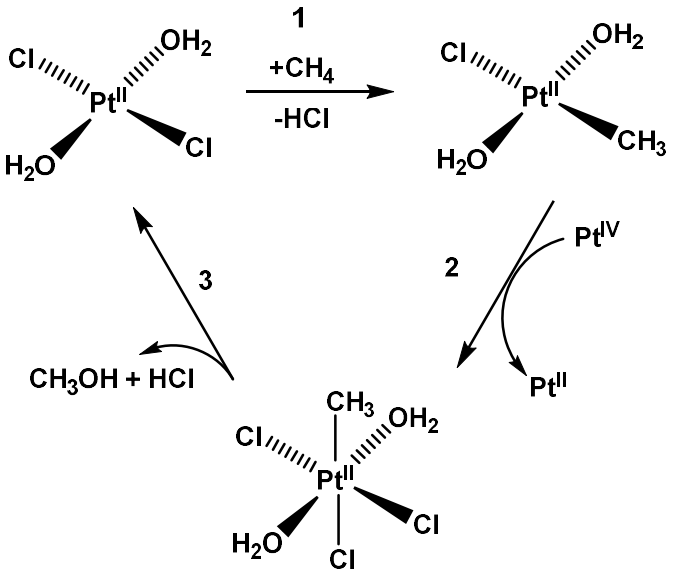

Scheme 1.1 Mechanism of C-H activation in methane by the Shilov system.[8]

1.2 Transition-metal (TM) complex mediated C −H bond activation

The practical application of C-H activation means, targeting C-H bonds in the hydrocarbon by a reagent such that the following step would yield a C-X bond, where X could be N, O or C on another hydrocarbon molecule. To date, pathways by which transition metal-catalyzed C-H activations have been observed include oxidative addition,[10] σ-bond metathesis,[11] and electrophilic addition to a π system.[12] Among them our understanding of the alkane C-H activation mechanisms has been mostly obtained from the oxidative addition process. The initial process makes a sigma bond complex at the metal center which resembles the activation of the dihydrogen molecule by a metal center.[13] The activation process is depicted below in the scheme 1.2.

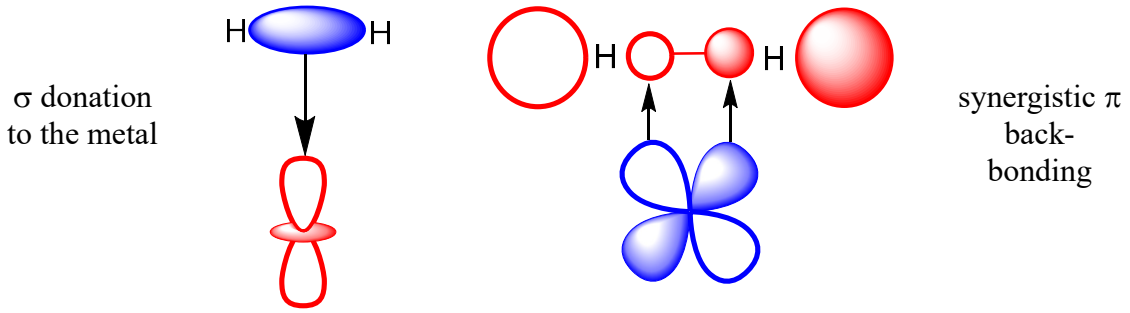

Homolytic H_2 activation by Transition metal complexes

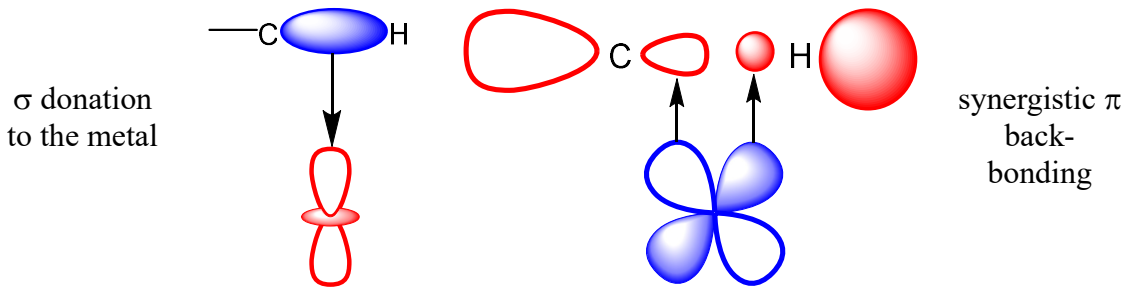

Oxidative C-H bond activation by TM complexes

Scheme 1.2 Orbital view of H-H and C-H bond activation of transition metal complex.

The act of donation of electron density from H-H or C-H bond to a metal atom (sigma (σ)→M) and the reverse π-back bonding M→σ* electron transfer weakens the σ–bond leading to the formation of a M-H and/or M-C bonds. A bonding interaction between a filled σ orbital of H-H or C-H bond and an empty metal orbital (σ donation), followed by rearrangement of the electron density at the metal center eventually yields cleavage of the H-H or C-H bond and the formation of two M-H bonds.[14]

1.4 Transition metal cluster complex mediated C −H bond activation

Polynuclear metal complexes containing metal-metal bonds, also known as cluster compounds, might serve as models for bridging the gap between heterogeneous catalysts involving reactions on surfaces (a) and homogeneous catalysts using single metal atom sites of mononuclear metal complexes (b), see (Scheme 1.3).[15] Metal clusters have been shown to exhibit unique properties regarding C-H and C-C bond activation and coordination of the ligands to the metal and in catalysis.[16]

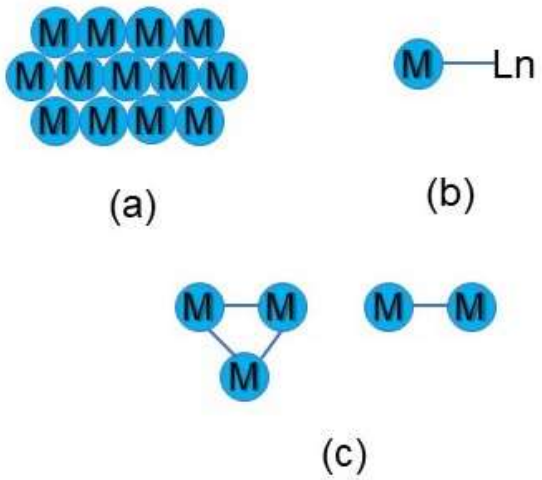

Scheme 1.3 Schematic diagram of (a) metal surface, (b) mononuclear metal complex and (c) metal cluster compounds (M_n), where number of n is 2 or more than 2.

Polynuclear metal carbonyl complexes are among the metal cluster complexes having properties that provide a basis for the development of a new class of transition-metal catalysts. Not only do they represent multinuclear sites on close-packed arrays of metal surfaces, but also polynuclear coordination and reaction at the metal-metal bond makes it possible for cooperativity and synergism in reactivity.[17] In addition, reactivity towards a small molecule can involve unusual electronic configurations including unsaturation (less than 18 electrons around a metal center) that can be found in the metal cluster.[18]

In 1983, Johnson and Lewis showed that the triosmium carbonyl complex $Os_3(CO)_{10}(NCMe)_2$ can activate CH bonds in arenes to yield the complexes $Os_3(CO)_{10}(\mu_3\text{-}C_6H_2R_1R_2)(\mu\text{-}H)_2$ that contain triply-bridging aryne ligands (Scheme 1.4).[19] Little was initially known about mechanism of how these bridging benzyne ligands were formed. Sigma-coordinated singly activated benzenes were suspected as intermediates in the benzyne formation.

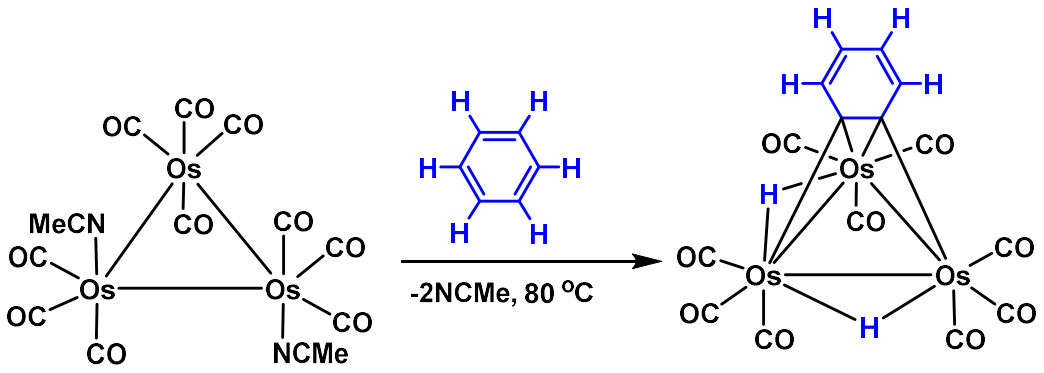

Scheme 1.4 Multiple C-H activation and oxidative addition of C_6H_6 on a triosmium carbonyl cluster complexes.

After 29 years, Adams *et al.* were able to find such a sigma coordinated group, but it was for an Au-C bond. They applied the concept of isolobality of H-C and Au-C bond to the cluster compound and successfully isolated the intermediate (Scheme 1.5).[20, 21] Multiple CH activations were also observed in furan ring systems by the same triosmium carbonyl complexes $Os_3(CO)_{10}(NCMe)_2$.[22]

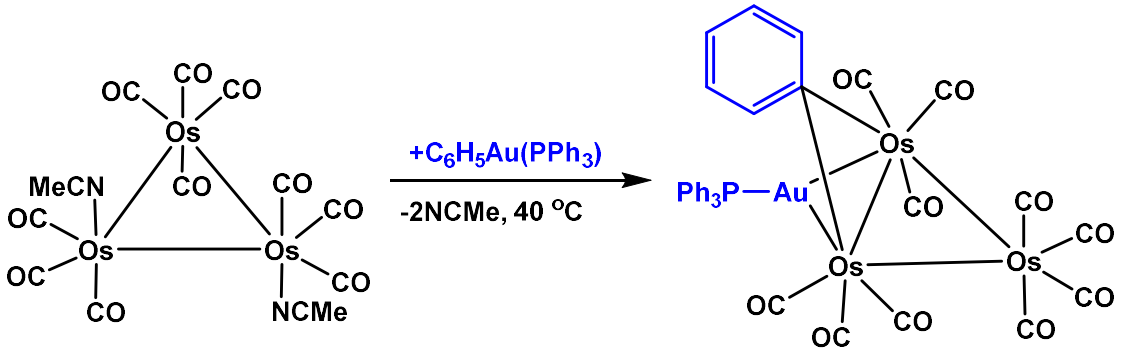

Scheme 1.5 Oxidative addition of an Au-C bond across an Os-Os metal-metal bond and formation of bridging η^1–C_6H_5 ligand.[22]

Interestingly, other metal cluster complexes were found to exhibit C-H activations on different classes of organic compounds. $[Re_2(CO)_8(\mu\text{-}H)(\mu\text{-}Ph)]$ is a good example of an electronically unsaturated binuclear metal cluster complex that can oxidatively add benzene by C-H activation and also reductively eliminate benzene by C-H bond formation.[16(c), 23] The mechanism of the aromatic C-H activation process by $[Re_2(CO)_8(\mu H)(\mu\text{-}Ph)]$ was investigated by using density-functional theory (DFT) calculations. The transformation is initiated by approach of an uncoordinated benzene solvent molecule to the cluster in the region proximate to its bridging hydride ligand (Scheme 1.6). The approaching solvent molecule donates some electron density from one of its π bonds to one of the rhenium atoms. A shift of the bridging phenyl ligand to a terminal position on the neighboring rhenium atom, via transition state **TS1**, yields the Intermediate **I1**. This

Intermediate is subsequently converted into an η^2-CH coordinated C_6H_6 ligand in the Intermediate **I2** by a C-H bond-forming shift of the bridging hydrido ligand to the carbon atom of the terminally coordinated phenyl ligand via the transition state **TS2**. The Intermediate **I2** subsequently rearranges into a centrosymmetrical bis[η^2-(C,C)-C_6H_6] Intermediate **I3**.[16(c), 23] To summarize, formation of C-H bond takes place largely on one metal atom but the second metal atom is not a spectator. The second metal atom assists the C-H activation step by delivering the H atom from the carbon atom to the M-M bond (Scheme 1.7).

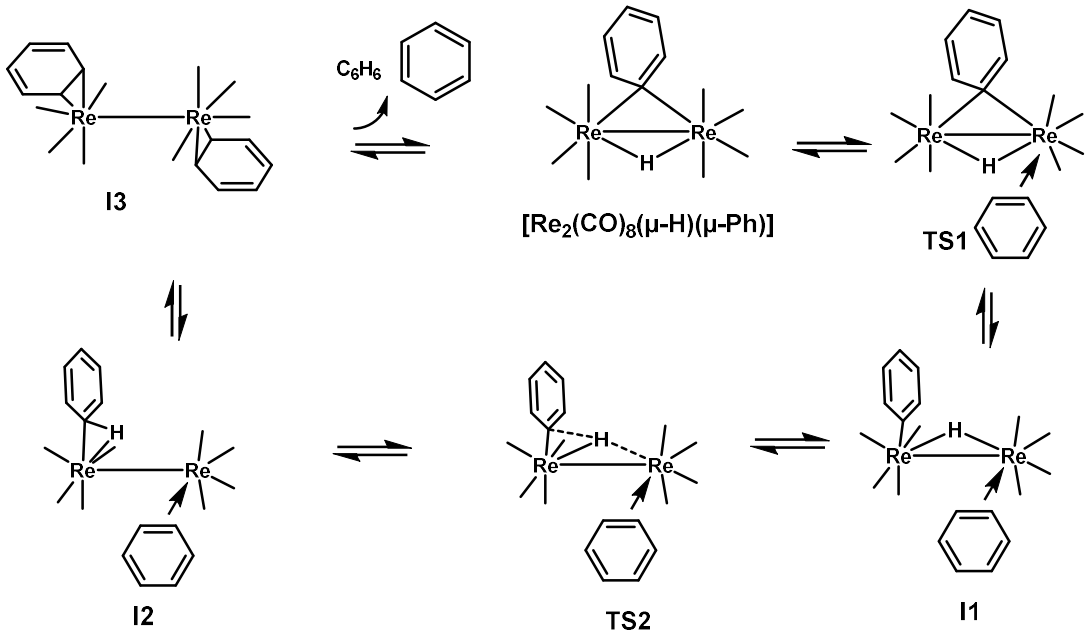

Scheme 1.6 C-H bond activation and formation of benzene (C_6H_6) in the [$Re_2(CO)_8$(μ-H)(μPh)] complex.[16(c), 23]

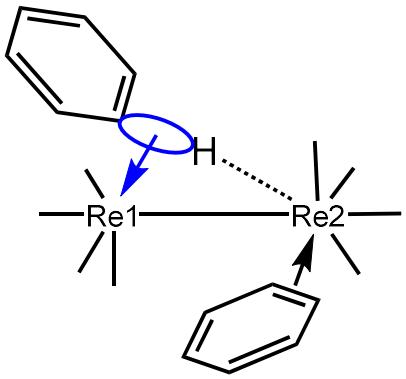

CH σ-bond donation to Re1

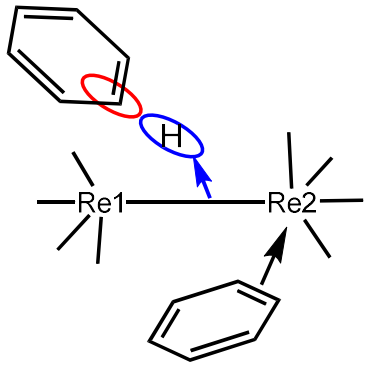

Re2 donation to CH σ*-bond

Scheme 1.7 Schematic for the C-H coordination and synergistic bond cleavage process.[16(c), 23]

1.5 Synthesis and Reactivity of $Ru_5(\mu_5\text{-}C)(CO)_{15}$

Ruthenium-based metal complexes have been used for a wide variety of reactions in organic synthesis, e. g., C–C bond formation reactions.[24] Among them ruthenium carbido carbonyl complexes are considered as important intermediates in olefin metathesis and for Fischer–Tropsch syntheses.[25]

In an attempt, to activate C-H bonds in small unsaturated molecules we chose to investigate the square-pyramidal pentaruthenium cluster compound $Ru_5(\mu_5\text{-}C)(CO)_{15}$, **1.1** with a variety of small organic molecules. The structure of **1.1** was established by single-crystal X-ray diffraction analysis many years ago.[26] The square-pyramidal cluster of Ru atoms each contains three linear terminal carbonyl ligands on each metal atom. A penta-coordinated carbido ligand resides in the center of the square-planar base and is displaced by 0.11(2) Å out of the Ru_4 plane. The average bond length for Ru-Ru bonds is reported to be 2.84 Å, whereas the average bond length for Ru-carbide bond is 2.04 Å.

Compound **1.1** is a 74 valence electron cluster[27] and exhibits a remarkable chemistry based on its ability to add ligands by cluster opening cleavage of one of its Ru-Ru bonds between the apical positioned Ru atom and one of the basal positioned Ru atoms. For example, upon addition of MeCN to **1.1** the cluster compound opens to a bridged butterfly ruthenium atom geometry (Scheme 1.8).[26, 28]

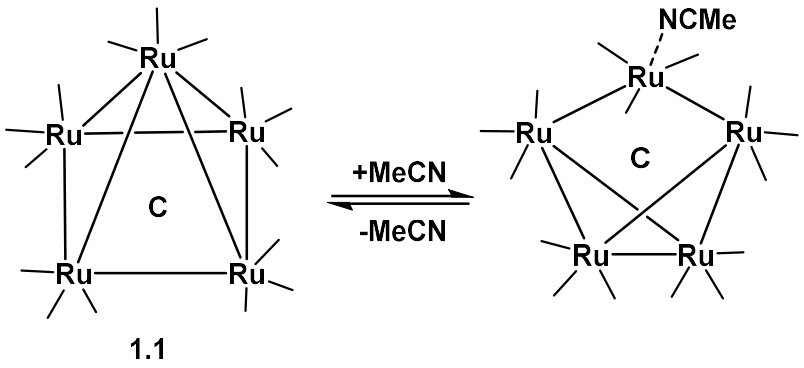

1.1

Scheme 1.8 Reversible addition of MeCN to the cluster complex **1.1** shows a switch between a square-pyramidal structure to bridged butterfly structure.

In addition, ligands can add to two metal atoms of the cluster **1.1** across the edge of Ru-Ru bond showing different modes of coordination. In recent studies, different bond modes of a benzoate ligand were found in the reaction between benzoic acid and **1.1**. In bonding mode **A**, the benzoate ligand donates three electrons to the metal center through a η^2-chelating coordination mode. The carboxylate hydrogen atom serves as a one-electron donor and was shifted to the cluster and adopted a bridging position across the hinge bond of the Ru_4 butterfly tetrahedral portion of the cluster. Overall, the five ruthenium atoms in **A** contain a total of 76 valence electrons. The formation of **A** and **B** from **1.1** lead to a net increase in the cluster valence electron count by two electrons. This requires the cleavage of one Ru–Ru bond which turns out to be one of the bonds between the apical Ru atom and one of the Ru atoms in the square base[29] (Scheme 1.9). Carbonylation and decarbonylation

of the derivative of cluster complex **1.1** plays a vital role in the coordination mode of the activated ligand. The activated cluster can further react with unsaturated hydrocarbons to leading to C-C bond formation reactions.[17(b), 30]

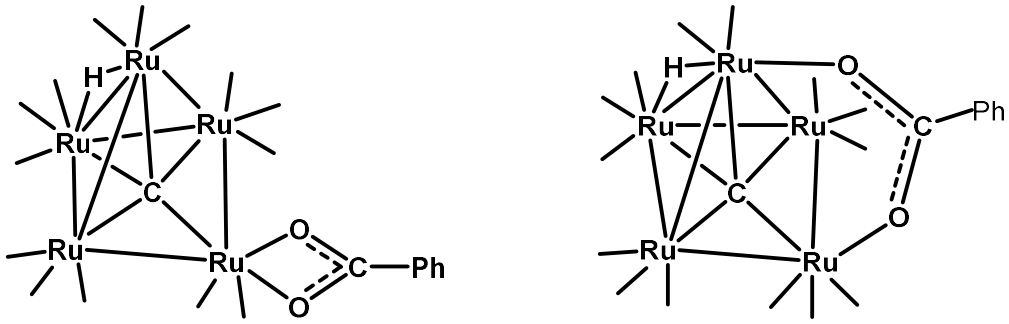

A η^2–chelate **B** μ–η^2 bridging

Scheme 1.9 Different coordination modes of compound **1.1** with a benzoate ligand.

The carbido ligand in compound **1.1** holds the cluster together while cleaving the metal- metal bond upon addition of substrate. However, being buried below 0.11(2) Å from the Ru_4 plane of compound **1.1** it might also show reactivity towards unsaturated organic molecules. Chapter 6 will be focused upon the reactivity of the carbido ligand in compound **1.1**. The synergism and cooperativity transformations of ligands upon addition and removal of CO ligand, formation of electronically unsaturated cluster upon addition of bulky ligand, formation of higher nuclearity cluster[31] of the compound **1.1** prompted us to study its chemistry further.

A brief description of preparation of compound **1.1** will be discussed here. Compound **1.1** was made from its parent cluster $Ru_6(\mu_6\text{-}C)(CO)_{17}$, **1.2** by a degradative carbonylation reaction in heptane at 80 °C. The route by which compound is made in Adams lab is depicted below:

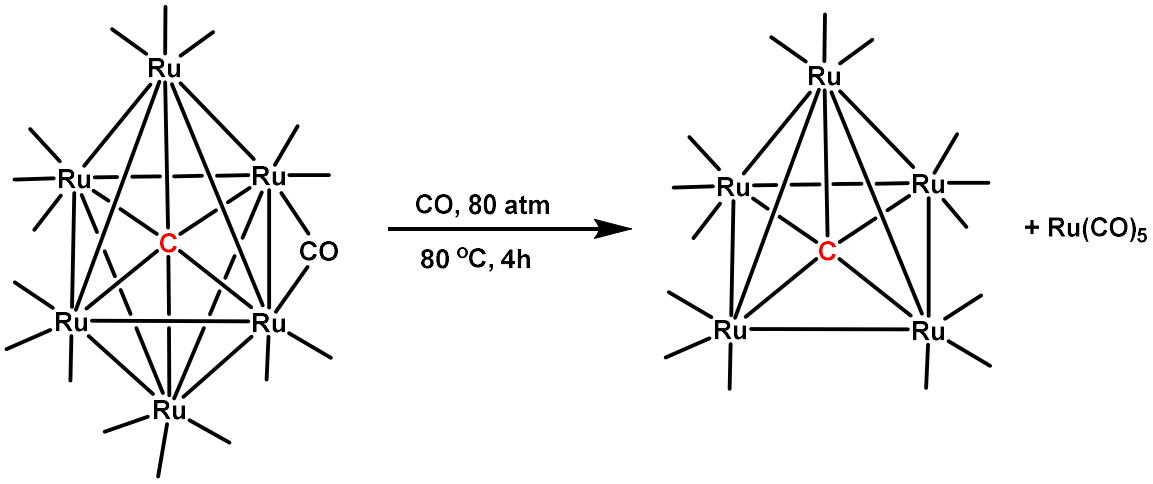

Scheme 1.10 Synthesis of $Ru_5(\mu_5\text{-}C)(CO)_{15}$, **1.1** from $Ru_6(\mu_6\text{-}C)(CO)_{17}$, **1.2** by a degradative thermal carbonylation method.

1.6 Zwitterion chemistry

Hydrocarbyl onium zwitterions were first reported in 1950s by Wittig, where a primary or secondary alkyl halide and an aldehyde or ketone were used to make an olefin by using triphenylphosphine and a base (Scheme 1.11).[32]

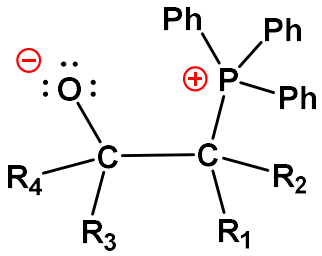

Scheme 1.11 First example of hydrocarbyl onium zwitterion reported in Wittig reaction.

The term zwitterion is derived from the German word zwitter, meaning a hybrid. According to IUPAC, zwitterion is a neutral compound having formal units of electrical charge of opposite sign located on different atoms in the same molecule.[33] Ylides of phosphorus and sulfur are an important class of zwitterions used in wide range of organic

syntheses (Scheme 1.12). More often they are reported as intermediates in certain reactions.[34, 35]

Phosphorus Ylide **Sulfur Ylide**

Scheme 1.12 General formula of a phosphorus and a sulfur ylide.

These ylides can serve as ligands by complexation to metal atoms. The coordinating atom is almost exclusively the carbon atom. In these cases, the formal negative charge is shifted to the metal atom (Scheme 1.13).[36]

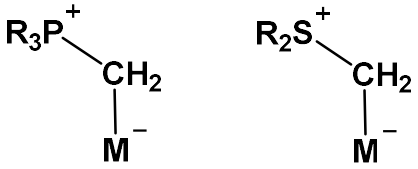

Scheme 1.13 Zwitterions complexed to a metal atom through the carbon atom.

A true hydrocarbyl onium zwitterion could also have formal unit electrical charges of opposite sign located on nonadjacent atoms. In all of these instances, they are ligands complexed to metal atoms. Selected examples include phosphonioalkenyl zwitterions complexed to one or two metal atoms (Scheme 1.14).[37] Here, the point of attachment is the carbon atom, and the formal negative charge is located on a metal atom. Thus, the charge separation gives overall stabilization on phosphonioalkenyl zwitterionic ligands.

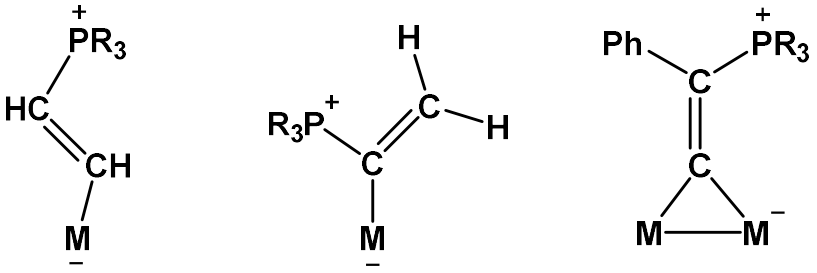

Scheme 1.14 Examples of phosphonioalkenyl zwitterionic ligands complexed to metal atoms.

There are a few examples of ammonioalkenyl ligands reported in the literature (Scheme 1.15).[38, 39]

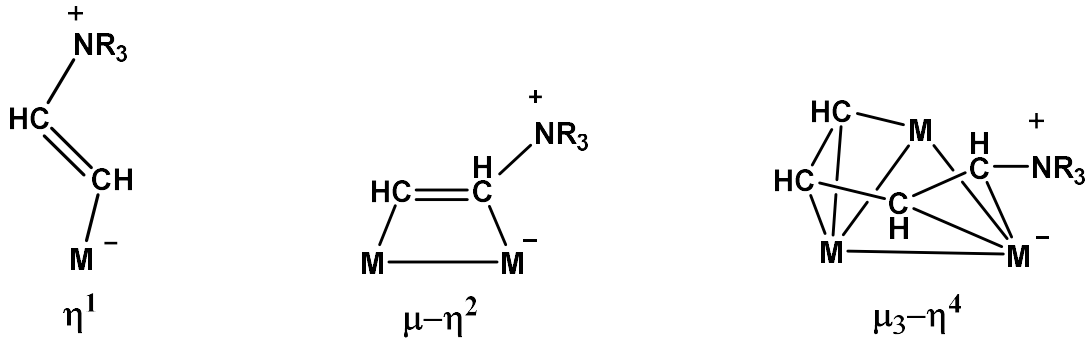

Scheme 1.15 Examples of ammonioalkenyl zwitterionic ligand complexed to metal atoms.

An example of formation of a trimethylammonioethenyl ligand from trimethylamine and ethyne is shown in Scheme 1.16.

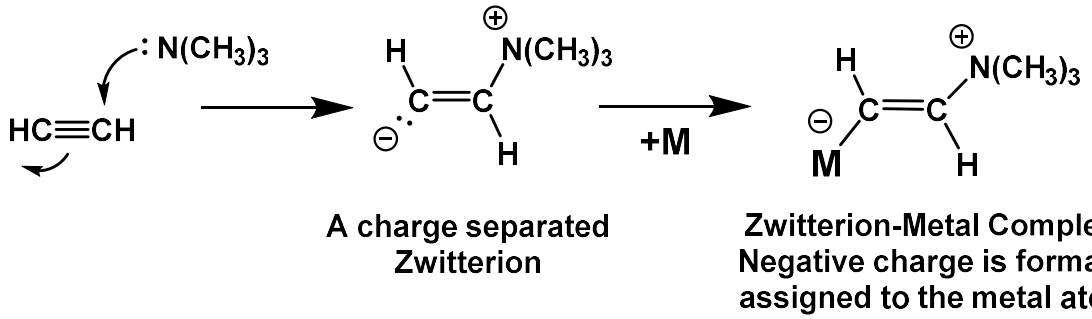

Scheme 1.16 Formation of a metal complexed trimethylammonioethenyl zwitterion from NMe_3 and C_2H_2.

Chin et al. reported an example of intramolecular C−N bond formation to produce a triethylammonioethenyl ligand in an iridium complex.[38(b)] Adams et al. recently showed not only that NMe_3 and C_2H_2 forms a zwitterionic species, but also the NMe_3 group serves as activator for the C-C coupling process in ethyne at room temperature.[39] Thus, zwitterionic ligands could also serve as a new route to create compounds containing C-N and C-P bonds. The newly formed M-C and C-N bonds could also be utilized for the formation of C-C and C=C bonds in carbon-carbon bond formation reactions.

Finally, the zwitterionic organometallic compounds could be used as reagents for organic syntheses. Heterocyclic compounds of natural products containing nitrogen, oxygen, and sulfur can be synthesized by phosphine-assisted intra- and intermolecular annulation reactions with electron-deficient alkenes, alkynes and allene carbonates. Several groups have proposed zwitterionic compounds as intermediates in reactions that do not involve metals.[40] Metal-assisted formation of zwitterions could lead to additional ways of performing new reactions.

1.7 The Chemistry of Carbido Carbon and C-C Coupling of Acetylene in Metal Complexes

Carbido ligands are of great interest because of their participation in C-C bond forming reactions in Fischer-Tropsch processes.[41] A simple carbido TM complex would be a terminal carbide having M≡C units[42] where the carbon atom coordinates to metal fragments via σ-donating and π-accepting bonding interactions.[43] They are not very common.[44] The first TM complex with a singly coordinated carbon atom was reported by Cummins and co-workers in 1997[44(a)]. It is an anionic complex, $[(NRAr)_3Mo(C)]^-$ (R = $C(CD_3)_2$-CH_3, Ar = $C_6H_3Me_2$-3,5). The first neutral TM compound with a terminal carbon

as ligand was reported by Heppert and co-workers.[44(d)] The terminal carbide mainly acts as a ligand in late transition metal complexes via formation of M≡C−M′ complexes.[45] Depending on the bonding mode of the carbon in between two metal atoms, it can be described as alkylidyne like μ_2– carbido (type **II**) or a dimetallaallene like μ_2– carbido (type **III**) ligand.

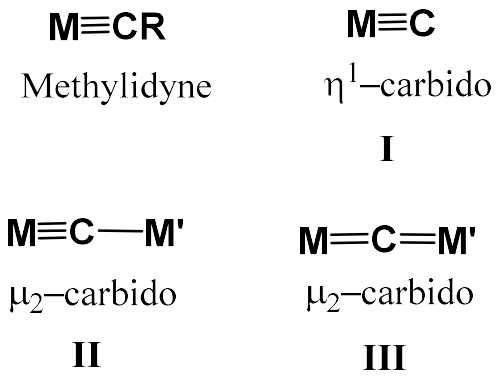

The carbido ligand can expand its coordination to up to six metal atoms by using its four valence electrons. Takemoto and his group reported the synthesis and structure of a bimetallic Ru_2Pt complex that contains a trigonal-planar μ_3-carbido ligand (type **IV**).[46(a)] Shriver et al. concluded formation of a μ_3-trigonal pyramidal carbido ligand on a Fe_3 metal cluster that was found to form C-C bond (type **V**).[46(b)]

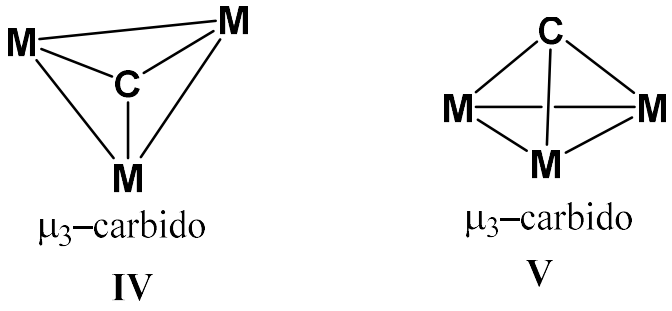

There are plenty of examples of μ_4-carbido ligands (type **VI**) in TM cluster complexes in the literature.[47] The μ_4-carbido ligand being well exposed can show a great deal of reactivity.

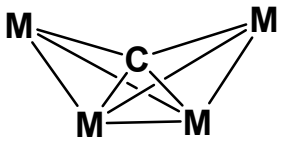

μ_4–carbido

VI

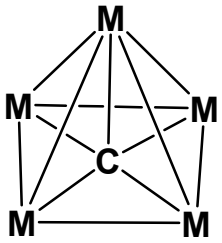

μ_5–carbido

VII

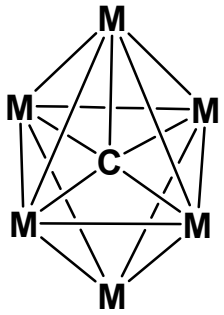

μ_6–carbido

VIII

For example, the formation of a C-C bond between the carbide ligand and an alkyne was demonstrated by Chung et al. (Scheme 1.17).[47(e)]

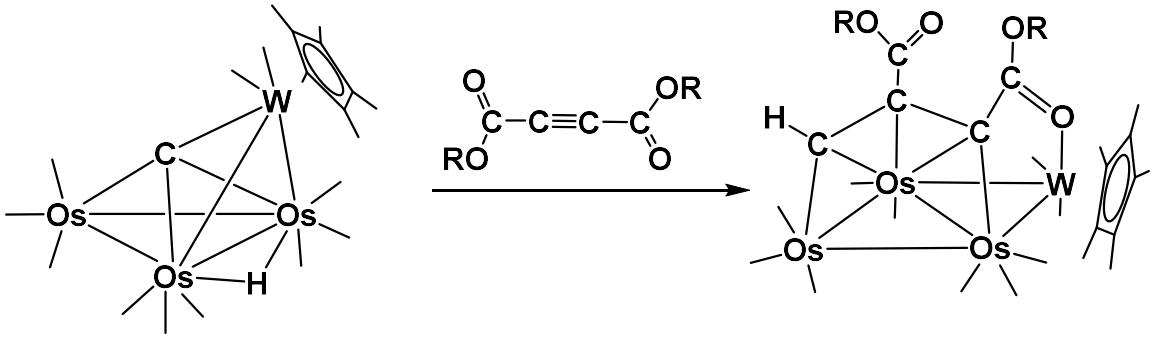

Scheme 1.17 C-C bond formation between a carbido carbon ligand and an alkyne (R= Pr^i).[47(e)]

The next in the series are μ_5- and μ_6-carbido ligands. The μ_6-carbido ligand is completely encapsulated by the cluster metal atoms (type **VIII**) and is only available to show reactivity only after removal of one of the vertex atoms. Adams *et al.* showed that a high nuclearity Ru_5C cluster containing μ_5-carbido ligand (type **VII**) was able to form a C-

C bond with a phenyl group to yield a bridging benzylidyne ligand on the cluster (Scheme 1.18).[31]

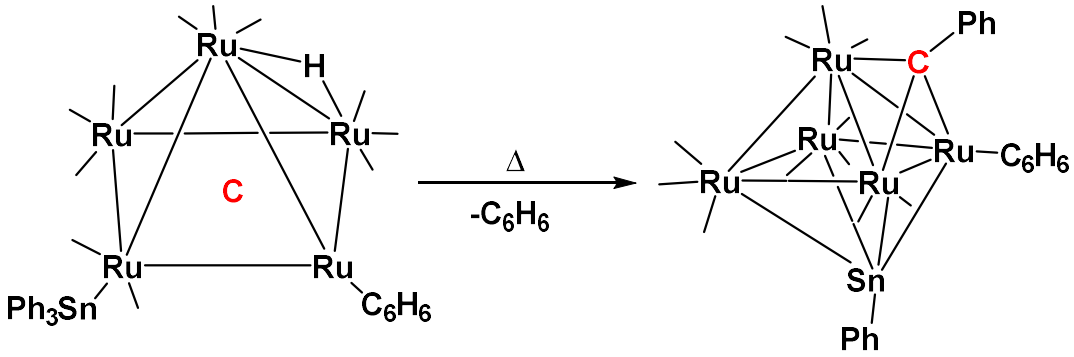

Scheme 1.18 C-C bond formation between a carbido carbon and a phenyl group.

Thus, the reactivity observed of carbido ligands in metal cluster complexes provides opportunities to further study of its chemistry with unsaturated organic molecule such as acetylenes.

1.9 References

1. (a) Holmen, A. *Catal. Today* **2009**, 142, 2–8. (b) Alvarez-Galvan, M. C.; Mota, N.; Ojeda, M.; Rojas, S.; Navarro, R. M.; Fierro, J. L. G. *Catal. Today* **2011**, 171, 15–23.
2. (a) Maitlis, P. M.; Zanotti, V. *Chem. Commun.* **2009**, 1619–1634. (b) Olah, G. A.; Goeppert, G. K.; Surya, G. K., "Beyond Oil and Gas: The Methanol Economy, Wiley-VCH Pub., Weinheim, 2006.
3. (a) Guo, X.; Fang, G.; Li, G.; Ma, H.; Fan, H.; Yu, L.; Ma, C.; Wu, X.; Deng, D.; Wei, M.; Tan, D.; Si, R.; Zhang, S.; Li, J.; Sun, L.; Tang, Z.; Pan, X.; Bao, X. *Science* **2014**, 344, 616–619. (b) Horn, R.; Schlögl, R. *Catal. Lett*. **2014**, 145, 23–39. (c) Neelis, M.; Patel, M.; Blok, K.; Haije, W.; Bach, P. *Energy* **2007**, 32, 1104–1123.

4. Luo, Y.-R. *Comprehensive Handbook of Chemical Bond Energies*, CRC Press, Boca Ratón, Fl, **2007**.

5. Arndtsen, B. A.; Bergman, R. G.; Mobley, T. A.; Peterson, T. H. *Acc. Chem. Res.* **1995**, 28, 154–162.

6. (a) Crabtree, R. H. *Chem. Rev.* **2010**, 110, 2, 575-575. (b) Hartwig, J. F. *J. Am. Chem. Soc.* **2016**, 138, 2−24.

7. (a) Li, Z.; Ji, S.; Liu, Y.; Cao, X.; Tian, S.; Chen, Y.; Niu, Z.; Li, Y. *Chem. Rev.* **2020**, 120, 623−682. (b) Friend, C. M.; Xu, B. *Acc. Chem. Res.* **2017**, 50, 517−521. (c) Schauermann, S.; Freund, H.-J. *Acc. Chem. Res*. **2015**, 48, 2775−2782.

8. (a) Shilov, A. E. *Activation of Saturated Hydrocarbons by Transition Metal Complexes*, Reidel: Dordrecht, **1984**; Chapter V. (b) Gol'dshleger, N. F.; Es'kova, v. V.; Shilov, A. E.; Shteinman, A. A. *Zh. Fiz. Khim*. **1972**, 46, 1358.

9. Mironov, O. A.; Bischof, S. M.; Konnick, M. M.; Hashiguchi, B. G.; Ziatdinov, V. R.; Goddard, W. A.; Ahlquist, M.; Periana, R. A. *J. Am. Chem. Soc.* **2013**, 135, 14644−14658.

10. Janowicz, A. H.; Bergman, R. G. *J. Am. Chem. Soc.* **1982**, 104, 352-354.

11. (a) Goldman, A. S.; Roy, A. H.; Huang Z.; Ahuja, R.; Schinski, W.; Brookhart, M. *Science*, **2006**, 312, 257-261. (b) Vidal, V.; Theolier, A.; ThivolleCazat, J.; Basset, J. M. Science **1997**, 276, 99.

12. Davies, H. M. L.; Beckwith, R. E. J. *Chem. Rev.* **2003**, 103, 2861-2903.

13. (a) Brookhart, M.; Green, M. L. H. *J. Organomet. Chem.* **1983**, 250, 395-408. (b) Whittlesey, M. K.; Mawby, R. J.; Osman, R.; Perutz, R. N.; Field, L. D.; Wilkinson, M. P.; George, M. W. *J. Am. Chem. Soc.* **1993**, 115, 8627-8637.

14. (a) Shilov, A. E.; Shul'pin, G. B. *Chem. Rev*. **1997**, 97, 2879−2932. (b) Labinger, J. A.; Bercaw, J. E. *Nature* **2002**, 417, 507−514.

15. Muetterties, E. L.; Rhodin, T. N.; Band, E.; Brucker, C. F.; Pretzers, W. R. *Chem. Rev.* **1979**, 79, 91 – 137.

16. (a) Adams, R. D. *Acc. Chem. Res*. **1983**, 16, 67-72. (b) Adams, R. D.; Captain, B.; Smith, M. D.; Beddie, C.; Hall, M. B. *J. Am. Chem. Soc*. **2007**, 129, 5981-5991. (c) Adams, R. D.; Rassolov, V.; Wong, Y. O. *Angew. Chem., Int. Ed.* **2016**, 55, 1324−1327.

17. (a) Adams, R. D.; Dhull, P.; Kaushal, M.; Smith, M. D. *Inorg. Chem.* **2019**, 58, 6008-6015. (b) Adams, R. D.; Tedder, J. D. *Inorg. Chem*. **2018**, 57, 5707−5710. (c) Adams, R. D.; Kiprotich, J.; Peryshkov, D.V.; Wong, Y. O. *Inorg. Chem.* **2016**, 55, 8207−8213.

18. Schaefer, H. F., III; King, R. B. *Pure Appl. Chem.* **2001**, 73, 1059−1073.

19. Goudsmit, R. J.; Johnson, B. F. G.; Lewis, J.; Raithby, P. R.; Rosales, M. J. *J. Chem. Soc., Dalton Trans.* **1983**, 2257−2261.

20. Adams, R. D.; Rassolov, V.; Zhang, Q. *Organometallics* **2012**, 31, 2961−2964.

21. Raubenheimer, H. G.; Schmidbaur, H. *Organometallics* **2012**, 31, 2507−2522.

22. Adams, R. D.; Kiprotich, E. J.; Smith, M. D. *Chem. Commun.* **2018**, 54, 3464-3467.

23. Adams, R. D.; Rassolov, V.; Wong, Y. O. *Angew. Chem. Int. Ed.* **2014**, 53, 11006–11009.

24. Naota, T.; Takaya, H.; Murahashi, S.-I.; *Chem. Rev.* **1998**, 98, 2599−2660.

25. (a) de Smit, E.; Weckhuysen, B. M. *Chem. Soc. Rev.* **2008**, 37, 2758–2781. (b) Schulz, H. *Applied Catalysis A: General* **1999**, 186, 3–12. (c) Takemoto, S.; Matsuzaka, H. *Coord. Chem. Rev.* **2012**, 256, 574–588.

26. Johnson, B. F. G.; Lewis J.; Nicholls, J. N.; Puga, J.; Raithby, P. R.; Rosales, M. J.; McPartlin, M.; Clegg, W. *J. Chem. Soc. Dalton Trans*. **1983**, 277−290.

27. Mingos, D. P. M. *Acc. Chem. Res.* **1984**, 17, 311-319.

28. (a) Johnson, B. F. G.; Lewis, J.; Nicholls, J. N.; Oxton, I. A.; Raithby, P. R.; Rosales, M. J. *J. Chem. Soc., Chem. Commun.* **1982**, 289. (b) Farrar, D. H.; Poë, A. J.; Zheng, Y. *J. Am. Chem. Soc.* **1994**, 116, 6252-6261.

29. Adams, R. D.; Smith, M.; Tedder J. *J. Cluster Sci.* **2017**, 28, 695-702.

30. Adams, R. D.; Smith, M. D.; Tedder, J. D.; Wakdikar, N. D. *Inorg. Chem.* **2019**, 58, 8357−8368.

31. Adams, R. D.; Captain, B.; Fu, W.; Smith, M. D. *Inorg. Chem.* **2002**, 41, 5593-5601.

32. (a) Wittig, G.; Schöllkopf, U. *Chem. Ber.* **1954**, 87, 1318−1330. (b) Wittig, G.; Haag. W. *Chem. Ber.* **1955**, 88, 1654−1666.

33. IUPAC. Compendium of Chemical Terminology, 2nd ed. (the "Gold Book"); Compiled by McNaught, A. D., Wilkinson, A. Blackwell Scientific Publications: Oxford, 1997; Online version (2019-) created by Chalk, S. J. ISBN 0-9678550-9-8. DOI: 10.1351/goldbook.

34. (a) Maryanoff, B. E.; Reitz, A. B. *Chem. Rev.* **1989**, 89, 863−927. (b) Bart, J. C. J. *J. Chem. Soc. (B)*, **1969**, 350 – 365.

35. (a) Lu, L.-Q.; Li, T.-R.; Wang, Q.; Xiao, W.-J. *Chem. Soc. Rev.* **2017**, 46, 4135−4149. (b) Burtoloso, A. C. B.; Dias, R. M. P.; Leonarczyk, I. A. *Eur. J. Org. Chem.* **2013**, 5005−5016. (c) Zhang, Y.; Wang, J. *Coord. Chem. Rev.* **2010**, 254, 941−953. (d) Li, A.-H.; Dai, L.-X.; Aggarwal, V. K. *Chem. Rev*. **1997**, 97, 2341−2372. (e) Trost, B. M.; Melvin, L. S., "Sulfur Ylides. Emerging Synthetic Intermediates", Academic Press,

New York, **1975**. (f) Neuhaus, J. D.; Oost, R.; Merad, J.; Maulide, N. *Top. Curr. Chem*. **2018**, 376, 15.

36. (a) Churchill, M. R.; Wasserman, H. J. *Inorg. Chem.* **1982**, 21, 3913−3916. (b) Hoover, J. F.; Stryker, J. M. *Organometallics* **1988**, 7, 2082−2084. (c) O'Connor, E. J.; Helquist, P. *J. Am. Chem. Soc.* **1982**, 104, 1869−1874. (d) Hevia, E.; Perez, J.; Riera, V.; Miguel, D. *Organometallics* **2002**, 21, 5312−5319.
37. (a) Hoffman, D. M.; Huffman, J. C.; Lappas, D.; Wierda, D. A. *Organometallics* **1993**, 12, 4312−4320. (b) Chin, C. S.; Lee, S.; Oh, M.; Won, G.; Kim, M.; Park, Y. J. *Organometallics* **2000**, 19, 1572−1577. (c) Chin, C. S.; Park, Y.; Kim, J.; Byeongno Lee, B. *J. Chem. Soc., Chem. Commun.* **1995**, 1495−1496. (d) Takats, J.; Washington, J.; Santarsiero, B. D. *Organometallics* **1994**, 13, 1078−1080. (e) Yang, K.; Bott, S. G.; Richmond, M. G. *J. Organomet. Chem.* **1996**, 516, 65−80. (f) Bott, S. G.; Shen, H.; Senter, R. A.; Richmond, M. G. *Organometallics* **2003**, 22, 1953−1959. (g) Henrick, K.; McPartlin, M.; Deeming, A. J.; Hasso, S.; Manning, P. *J. Chem. Soc., Dalton Trans.* **1982**, 899−906.
38. (a) Chin, C. S.; Lee, H.; Oh, M. *Organometallics* **1997**, 16, 816−818. (b) Chin, C. S.; Cho, H.; Won, G.; Oh, M.; Ok, K. M. *Organometallics* **1999**, 18, 4810−4816.
39. Adams, R. D.; Smith, M. D.; Wakdikar, N. D. *Inorg. Chem*. **2020**, 59, 1513−1521.
40. (a) Sankar, M. G.; Garcia-Castro, M.; Golz, C.; Strohmann, C.; Kumar, K. *RSC Adv.* **2016**, 6, 56537–56543. (b) Guan, X.-Y.; Shi, M. *J. Org. Chem.* **2009**, 74, 1977–1981. (c) Chen, X. Y.; Ye, S. *Eur. J. Org. Chem.* **2012**, 5723–5728. (d) Zhang, Y. S.; Sun, Y. L.; Wei, Y.; Shi, M. *Adv. Synth. Catal.* **2019**, 361, 2129–2135. (e) Waldmann, H.; Khedkar, V.; Duckert, H.; Schumann, M.; Oppel, I. M.; Kumar, K. *Angew. Chem., Int.*

Ed. **2008**, 47, 6869–6872. (f) Meng, W.; Zhao, H. T.; Nie, J.; Zheng, Y.; Fu, A. P.; Ma, J. A. *Chem. Sci.* **2012**, 3, 3053–3057.

41. (a) Schulz, H. *Applied Catalysis A: General* **1999**, 186, 3–12. (b) de Smit, E.; Weckhuysen, B. M. *Chem. Soc. Rev.* **2008**, 37, 2758–2781. (c) Maitlis, P. M. *J. Organomet. Chem.* **2004**, 689, 4366–4374. (d) Fontenelle Jr., A. B.; Fernandes, F. A. N. *Chem. Eng. Technol.* **2011**, 34, 963–971. (e) Filot, I. A. W.; van Santen, R. A.; Hensen, E. J. M. *Catal. Sci. Technol.* **2014**, 4, 3129–3140.
42. Bruce, M. I. Low, P. J. *Adv. Organomet. Chem.* **2004**, 50, 179.
43. (a) Krapp, A.; Pandey, K. K.; Frenking, G. *J. Am. Chem. Soc.* **2007**, 129, 7596−7610. (b) Krapp, A.; Frenking, G. *J. Am. Chem. Soc.* **2008**, 130, 16646−16658. (c) Frenking, G.; Tonner, R.; Klein, S.; Takagi, N.; Shimizu, T.; Krapp, A.; Pandey, K. K.; Parameswaran, P. *Chem. Soc. Rev.* **2014**, 43, 5106−5139.
44. (a) Peters, J. C.; Odom, A. L.; Cummins, C. C. *Chem. Commun.* **1997**, 1995. (b) Greco, J. B.; Peters, J. C.; Baker, T. A.; Davis, W. M.; Cummins, C. C.; Wu, G. *J. Am. Chem. Soc.* **2001**, 123, 5003-5013. (c) Enriquez, A. E.; White, P. S.; Templeton, J. L. *J. Am. Chem. Soc.* **2001**, 123, 4992-5002. (d) Carlson, R. G.; Gile, M. A.; Heppert, J. A.; Mason, M. H.; Powell, D. R.; Vander Velde, D.; Vilain, J. M. *J. Am. Chem. Soc.* **2002**, 124, 1580. (e) Hejl, A.; Trnka, T. M.; Day, M. W.; Grubbs, R. H. *Chem. Commun.* **2002**, 2524. (f) Romero, P. E.; Piers, W. E.; McDonald, R. *Angew. Chem., Int. Ed.* **2004**, 43, 6161. (g) Caskey, S. R.; Stewart, M. H.; Kivela, J. E.; Sootsman, J. R.; Johnson, M. J. A.; Kampf, J. W. *J. Am. Chem. Soc.* **2005**, 127, 16750-16750.
45. (a) Mansuy, D.; Lecomte, J. P.; Chottard, J. C.; Bartoli, J. F. *Inorg. Chem.* **1981**, 20, 3119−3121. (b) Goedken, V. L.; Deakin, M. R.; Bottomley, L. A. *J. Chem. Soc., Chem.*

Commun. **1982**, 11, 607−608. (c) Rossi, G.; Goedken, V. L.; Ercolani, C. *J. Chem. Soc., Chem. Commun.* **1988**, 1, 46−47. (d) Beck, W.; Knauer, W.; Robl, C. *Angew. Chem., Int. Ed. Engl.* **1990**, 29, 318−320. (e) Miller, R. L.; Wolczanski, P. T.; Rheingold, A. L. *J. Am. Chem. Soc.* **1993**, 115, 10422−10423. (f) Caselli, A.; Solari, E.; Scopelliti, R.; Floriani, C. *J. Am. Chem. Soc.* **2000**, 122, 538−539. (g) Hong, S. H.; Day, M. W.; Grubbs, R. H. *J. Am. Chem. Soc.* **2004**, 126, 7414−7415. (h) Solari, E.; Antonijevic, S.; Gauthier, S.; Scopelliti, R.; Severin, K. *Eur. J. Inorg. Chem.* **2007**, 367−371. (i) Hill, A. F.; Sharma, M.; Willis, A. C. *Organometallics* **2012**, 31, 2538−2542. (j) Borren, E. S.; Hill, A. F.; Shang, R.; Sharma, M.; Willis, A. C. *J. Am. Chem. Soc.* **2013**, 135, 4942−4945.

46. (a) Takemoto, S.; Morita, H.; Karitani, K.; Fujiwara, H.; Matsuzaka, H. *J. Am. Chem. Soc.* **2009**, 131, 18026−18027. (b) Kolis, J. W.; Holt, E. M.; Drezdzon, M.; Whitmire, K. H.; Shriver, D. F. *J. Am. Chem. Soc.* **1982**, 104, 6134-6135.

47. (a) Fehlner, T. P.; Housecroft, C. E. *Organometallics* **1984**, 3, 764-774. (b) Bradley, J. S.; Harris, S.; Newsam, J. M.; Hill, E. W.; Leta, S.; Modrick, M. A. *Organometallics* **1987**, 6, 2060-2069. (c) Dutton, T.; Johnson, B. F. G.; Lewis, J.; Owen, S. M.; Raithby, P. R. *J. Chem. Soc., Chem. Commun.* **1988**, 1423-1424. (d) Meng, X.; Rath, N. P.; Fehlne, T. P. *Organometallics* **1991**,10, 1986-1993. (e) Chung, C.; Tseng, W.-C.; Chi, Y.; Peng, S.-M.; Lee, G.-H. *Organometallics* **1998**, 17, 2207-2214.

Chapter 2

CH Activations in Aldehydes in Reactions with $Ru_5(\mu_5\text{-}C)(CO)_{15}$ [1]

[1] Adams, R. D.; Akter, H.; Tedder, J. D. *J. Organomet. Chem.* **2018**, *871*, 159-166. Reprinted here with permission from publisher.

2.1 Introduction

The ability to activate and functionalize C-H bonds in hydrocarbons to produce higher-value organic chemicals is of great importance to the chemical industry. Accordingly, the activation and functionalization of C-H bonds by metal complexes has received considerable research attention in recent years. Most studies have been focused on the activation of aliphatic[1] and aromatic[2] C-H bonds.

The activation of aldehydic C-H bonds has also received considerable attention and is a key step in reactions known generally as the hydroacylation of alkenes and alkynes that are catalyzed by transition metal complexes[3] (eq. (2.1)).

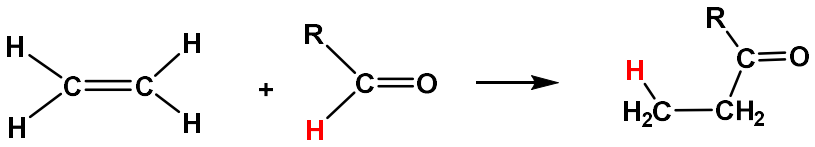

(2.1)

The oxidative addition of aldehydic C-H bonds to a metal complex will yield a metal complex **I** containing acyl and hydrido ligands that can undergo further transformations such as decarbonylation with subsequent formation of C-H bonds to yield a RH product by reductive elimination[4], or by coupling with an unsaturated substrate, e. g. C_2H_4, to yield a ketone by hydroacylation[5], (eq. (2.2)).

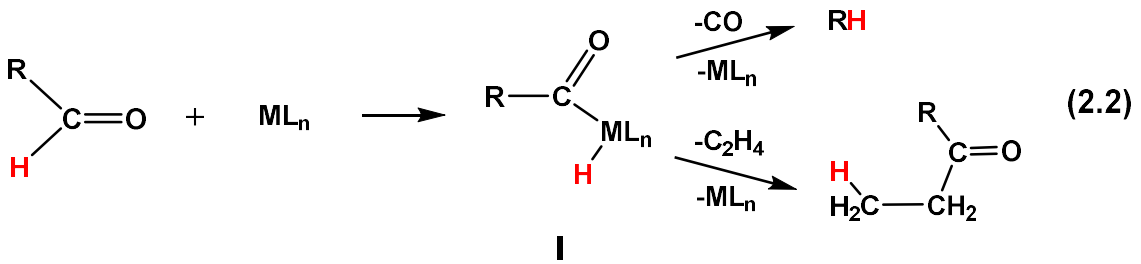

I

(2.2)

The competing decarbonylation process can significantly limit the usefulness of the more valuable hydroacylation reaction.

In recent studies, we have shown that the pentaruthenium cluster complex $Ru_5(\mu_5\text{-}C)(CO)_{15}$, **2.1**, is able to activate the formyl C-H bond of N,N-dimethylformamide to yield the complex $Ru_5(\mu_5\text{-}C)(CO)_{14}[\mu\text{-}\eta^2\text{-}O{=}CN(CH_3)_2](\mu\text{-}H)$ that contains a bridging formamido $\eta^2\text{-}O{=}CN(CH_3)_2$ ligand formed by opening of the Ru_5C square pyramid cluster of metal atoms via oxidative addition of the formyl C-H bond, eq. (2.3)[6].

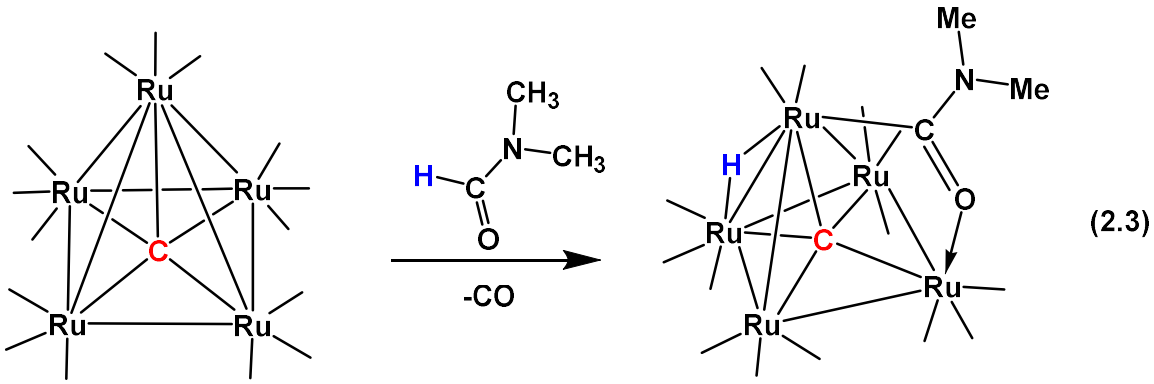

2.1

(2.3)

We have now investigated the reactions of **2.1** with selected biomass derived aldehydes: furfural and 5- hydroxymethylfurfural and have observed some similar cluster opening C - H bond activations at the formyl functional groups. Herein we report on our new studies of the activation of aldehydic C-H bonds by the cluster complex **2.1**.

2.2 Experimental Section

General Data

All reactions were performed under an atmosphere of nitrogen. Reagent grade solvents were dried by standard procedure and were freshly distilled prior to use. Infrared spectra were recorded on a Thermo Scientific Nicolet IS10. ^{1}H NMR spectra was recorded on a Varian Mercury 300 spectrometer operating at 300.1 MHz. Mass spectrometric (MS)

measurements were performed by a direct-exposure probe by using electron impact (EI) ionization. $Ru_3(CO)_{12}$ was obtained from STREM and was used without further purification. $Ru_5(\mu_5\text{-}C)(CO)_{15}$, **2.1** was prepared from $Ru_3(CO)_{12}$ according to a previously reported procedure.[7] Furfural was purchased from Sigma Aldrich and was used without further purification. 5-Hydroxymethyl-2-furaldehyde (5-Hydroxymethylfurfural) was purchased from Sigma Aldrich and was used without further purification. Product separations were performed by TLC in air on Analtech 0.25 mm and 0.50 mm silica gel 60 Å F254 glass plates and silica gel column chromatography on silica gel 60, 0.606 -0.2 mm (70 – 230 mesh).

Reaction of $Ru_5(\mu_5\text{-}C)(CO)_{15}$, 2.1 with furfural at 80 °C

49.8 mg (0.05312 mmol) of **2.1** was added to a 50 mL three-neck flask with a solution of 200 μL of furfural in 25 mL of degassed cyclohexane. After refluxing for 43 h, the solvent was removed in vacuo and the product was isolated by TLC by using a hexane to methylene chloride mixture to yield 25.5 mg of $Ru_5(\mu_5\text{-}C)(CO)_{14}(\mu\text{-}\eta^2\text{-}O{=}CC_4OH_3)(\mu\text{-}H)$, **2.2** (48%). Spectral data for **2.2**: IR νCO (cm^{-1} in hexane): 2105(w), 2077(s), 2060(vs), 2053(s), 2033(w), 2020(vw), 2014(vw), 2002(vw), 1993(vw), 1982(vw), 1972(vw). ^{1}H NMR (in acetone-d_6 solvent, δ in ppm) d = 7.87 (s, 1H, OCH=CH-C**H**), 6.76 (d, 1H, OC**H**=CH-CH, $^3J_{H\text{-}H}$ = 3 Hz), 6.55 (dd, 1H, OCH=C**H**-CH, $^3J_{H\text{-}H}$ = 3 Hz), -20.84 (s, 1H, hydride). EI/MS *m/z*. M^+ = 1005. The isotope distribution pattern is consistent with the presence of five ruthenium atoms.

Reaction of $Ru_5(\mu_5\text{-}C)(CO)_{15}$, 2.1 with 5-hydroxymethylfurfural at 80 °C

43.4 mg (0.04629 mmol) of **2.1** was added to a 50 mL three-neck flask with a solution of 124.7 mg of 5-hydroxymethylfurfural in 25 mL of degassed benzene. After refluxing for 32.5 h, the solvent was removed in vacuo and the product was isolated by TLC by using a hexane to methylene chloride mixture to yield 16.5 mg of $Ru_5(\mu_5\text{-}C)(CO)_{14}[\mu\text{-}\eta^2\text{-}O{=}CC_4OH_2(CH_2OH)](\mu\text{-}H)$, **2.3** (34%). Spectral data for **2.3**: IR νCO (cm^{-1} in hexane): 2105(vw), 2078(s), 2060(vs), 2054(m), 2034(w), 2018(vw), 2014(vw), 2003(vw), 1994(vw), 1979(vw), 1972(vw). ^1H NMR (CD_2Cl_2, in ppm) d = 6.60 (d, $^3J_{H\text{-}H}$ = 3 Hz, 1H, OCCC**H**-CH), 6.32(d, $^3J_{H\text{-}H}$ = 3 Hz, 1H, OCCCH-C**H**), 4.60 (d, $^3J_{H\text{-}H}$ = 9 Hz, 2H, C**H**$_2$OH), 1.91 (t, $^3J_{H\text{-}H}$ = 6 Hz, 1H, CH_2O**H**), -20.80 (s, 1H, hydride). EI/MS *m/z*. M^+ = 1035. The isotope distribution pattern is consistent with the presence of five ruthenium atoms.

Thermal decomposition of 2.2 at 108 °C

10.0 mg (0.0099 mmol) of **2.2** was added to an NMR tube in deuterated toluene solution. After heating for 21 h at 108 °C in a constant temperature oil bath. The solvent was removed in vacuo, and the products were then isolated by column chromatography on silica gel by using a hexane/methylene chloride mixture which yielded 5.8 mg (62% yield) of **2.1**. Formation of furan was confirmed in the ^1H NMR spectrum.

Thermal decomposition of 2.3 at 108 °C

15.1 mg (0.01146 mmol) of **2.3** was added to an NMR tube in deuterated toluene solution. After heating for 11 h at 108 °C in a constant temperature oil bath. The solvent was removed in vacuo, and the products were then isolated by TLC by using a hexane/

methylene chloride mixture to provide in order of elution: 2.3 mg (18% yield) of **2.1** and 1.9 mg of **2.3**. $Ru_5C(CO)_{15}$, **2.1**, decomposes during TLC reducing the amount of recoverable product.

Crystallographic analyses

Crystals of compound **2.2** suitable for X-ray diffraction analyses were obtained by slow evaporation of solvent from a solution of the pure compound in a hexane/methylene chloride solvent mixture. Crystals of compound **2.3** suitable for X-ray diffraction analyses were obtained by slow evaporation of solvent from a solution of the pure compound in an octane/benzene solvent mixture. X-ray intensity data for compounds **2.2** and **2.3** was measured by using a Bruker D8 QUEST diffractometer equipped with a PHOTON100 CMOS area detector and an Incoatec microfocus source (Mo Ka radiation, λ = 0.71073 Å).[8] The raw area detector data frames were reduced, scaled, and corrected for absorption effects by using the SAINT[8] and SADABS[9] programs. All structures were solved by a combination of direct Methods and difference Fourier syntheses, and refined by full-matrix least squares refinement on F^2 by using the SHELXTL software package.[10] All hydrogen atoms were placed in geometrically idealized positions and were included as standard riding atoms during the final least-squares refinements with C-H distances fixed at 0.96 Å. The hydrido ligands in compounds **2.2** and **2.3** were located and refined in each analysis. Compound **2.2** crystallized in the monoclinic crystal system. The space group $P2_1/c$ was identified for compound **2.2** on the basis of systematic absences observed in the intensity data. Compound **2.3** crystallized in the triclinic crystal system. The space group P-1 was assumed for compound **2.3** and was confirmed by successful solutions and refinements of

the structures. Crystal data, data collection parameters, and results of the refinements for each analysis are listed in Table 2.1.

2.3 Results and Discussion

Furans are one of the most common families of compounds obtained from the chemical upgrading of biomass.[11] Because of this interest, we investigated the reactions of two of the most common of these furan compounds, furfural and 5-hydroxymethyl-2-furfural[12], with **2.1**. The reaction of **2.1** with furfural in cyclohexane solvent yielded only one product $Ru_5(\mu_5\text{-}C)(CO)_{14}(\mu\text{-}\eta^2\text{-}O{=}CC_4OH_3)(\mu\text{-}H)$, **2.2** in 48% yield after 43 h at reflux. Compound **2.2** was characterized by IR, and ^1H NMR spectroscopy, mass spectrometry and single-crystal X-ray diffraction analyses. An ORTEP diagram of the molecular structure of **2.2** is shown in Figure 2.1. Compound **2.2** contains an O=C coordinated, η^2-bridging furoyl, η^2-$O{=}CC_4OH_3$, ligand across the open edge of a Ru wingtip-bridged Ru_4C cluster. The acyl carbon atom C1 is bonded to Ru1 and to oxygen atom O1 bonded to Ru4, Ru1-C1 = 2.062(2) Å, Ru4-O1 = 2.1190(15) Å, C1-O1 = 1.268(3) Å. The hydrido ligand bridges the hinge metal atoms Ru1 and Ru2, Ru1 – H1 = 1.91(3) Å, Ru2 – H1 = 1.79(3) Å, δ = -20.84. With fourteen CO ligands, compound **2.2** contains a total of 76 cluster valence electrons which is consistent with that of an 'open' Ru_5C square pyramidal cluster of five metal atoms.[7, 13]

Similarly, the reaction of **2.1** with 5-hydroxymethyl-2-furfural in cyclohexane solvent yielded only one product $Ru_5(\mu_5\text{-}C)(CO)_{14}[\mu\text{-}\eta^2\text{–}O{=}CC_4OH_2(CH_2OH)](\mu\text{-}H)$, **2.3** in 34% yield after 32.5 h at reflux. Compound **2.3** was characterized by single crystal X-ray diffraction analyses. ORTEP diagram of the molecular structures of compounds **2.3** is

shown in Figure 2.2. Compound **2.3** contains an η^2-O=C, 5-hydroxymethylfuroyl, η^2 -O=C$C_4OH_2(CH_2OH)$, ligand bridging the opened edge of the Ru_5C cluster. The acyl carbon atom C1 is bonded to Ru1 and to oxygen atom O1 bonded to Ru4, Ru1-C1 = 2.024(3) Å, Ru4-O1 = 2.140(2) Å, C1-O1 = 1.267(4) Å. The hydrido ligand bridges the hinge metal atoms Ru1 and Ru2, Ru1 – H1 = 1.85(3) Å, Ru2 – H1 = 1.80(3) Å, δ = -20.80. With fourteen CO ligands, compound **2.3** also contains a total of 76 cluster valence electrons which is consistent with that of an 'open' Ru_5C square pyramidal cluster of five metal atoms. [7, 13]

The reductive decarbonyation of the bridging furyol ligand in **2.2**, and hydroxymethylfuroyl ligand in **2.3** were also investigated at 108 °C and this treatment decarbonylated the bridging acyl ligand and regenerated **2.1** in the yields 62%, and 18%, respectively.

2.4 Conclusion

A summary of the reactions and products studied in this work is shown in Scheme 2.1. It has been shown that **2.1** possesses the ability to activate the formyl C-H bonds in selected biomass derived aldehydes via reactions that lead to an opening of the Ru_5 cluster of **2.1** by cleavage of one of the apical-basal Ru - Ru bonds. The reactions of each of the aldehydes studied in this work with **2.1** have yielded products formed by the activation of the formyl CH bonds with the formation of opened Ru_5 clusters with a η^2-O=C acyl group bridging the opened edge of the cluster. Thermal decomposition of the complexes with the bridging acyl groups led to decarbonylation and reductive elimination of the unsaturated hydrocarbon and regeneration of **2.1**. The activation of the formyl C-H bonds of aldehydes

by $Ru_5(\mu_5\text{-}C)(CO)_{15}$, **2.1** could pave the way to new hydroacylation reactions for the functionalization of alkenes and alkynes in a manner similar to that observed in the hydrocarbamoylation of C_2H_2 by N,N-dimethylformamide by **2.1**.[6]

2.5 References

1. (a) Yang, Y.; Lan, J.; You, J. *Chem. Rev.* **2017**, 117, 8787-8863. (b) Eisenstein, O.; Milani, J.; Perutz, R.N. *Chem. Rev.* **2017**, 117, 8710-8753. (c) Xue, X.-S.; Ji, P.; Zhou, B.; Cheng, J.-P. *Chem. Rev.* **2017**, 117, 8622-8648. (d) Balcells, D.; Clot, E.; Eisenstein, O. *Chem. Rev.* **2010**, 110, 749-823. (e) Crabtree, R. H. *J. Organomet. Chem.* **2004**, 689, 4083-4091. (f) Shilov, A. E.; Shul'pin, G. B. *Chem. Rev.* **1997**, 97, 2879-2932. (g) Labinger, J. A.; Bercaw, J. E. *Nature* **2002**, 417, 507-514. (h) Bergman, R. G. Nature **2007**, 446, 391-393. (i) Caballero, A.; Perez, P. J. *Chem. Soc. Rev.* **2013**, 42, 8809-8820. (j) Gunay, A.; Theopold, K.H. *Chem. Rev.* **2010**, 110, 1060-1081. (k) Hall, C.; Perutz, R. N. *Chem. Rev.* **1996**, 96, 3125-3146. (l) Rudakov, E. S.; Shul'pin, G. B. *J. Organomet. Chem.* **2015**, 793, 4-16. (m) Labinger, J. A.; Bercaw, J. E. *J. Organomet. Chem.* **2015**, 793, (2015) 47-53. (n) Webb, J. R.; Bolaño, T.; Gunnoe, T. B. *ChemSusChem* **2011**, 4, 37-49.
2. (a) Lersch, M.; Tilset, M. *Chem. Rev.* **2005**, 105, 2471-2526. (b) Jones, W. D.; Feher, F. J. *Acc. Chem. Res.* **1989**, 22, 91-100. (c) Jones, W. D. *Acc. Chem. Res.* **2003**, 36, 140-146. (d) Koppaka, A.; Captain, B. *Inorg. Chem.* **2016**, 55, 2679-2681. (e) Adams, R. D.; Rassolov, V.; Wong, Y.O. *Angew. Chem. Int. Ed.* **2016**, 55, 1324-1327.
3. (a) Willis, M. C. *Chem. Rev.* **2010**, 110, 725-748. (b) Coxon, T. J.; Fernández, M.; Barwick-Silk, J.; McKay, A. I.; Britton, L. E.; Weller, A. S.; Willis, M. C. *J. Am. Chem. Soc.* **2017**, 139, 10142-10149. (c) Kondo, T.; Akazome, M.; Tsuji, Y.; Watanabe, Y. *J.*

*Org. Chem.***1990**, 55, 1286-1291. (d) Kondo, T.; Hiraishi, N.; Morisaki, Y.; Wada, K.; Watanabe, Y.; Mitsudo, T. *Organometallics* **1998**, 17, 2131-2134. (e) Dyker, G. *Angew. Chem. Int. Ed.* **1999**, 38, 1698-1712. (f) Jun, C. -H.; Moon, C. W.; Lee, D. -Y. *Chem. Eur. J.* **2002**, 8, 2423-2428. (g) Willis, M. C.; McNally, S. J.; Beswick, P. J. *Angew. Chem. Int. Ed.* **2004**, 43, 340-340. (h) Lochow, C. F.; Miller, R. G. *J. Am. Chem. Soc.***1976**, 98, 1281-1283. (i) Tanaka, K.; Fu, G. C. *J. Am. Chem. Soc.* **2001**, 123, 11492-11493. (j) Tanaka, M.; Sakai, K.; Suemune, H. *Org. Chem.* **2003**, 7, 353-367.

4. (a) Suggs, J.W. *J. Am. Chem. Soc.* **1978**, 100, 640-641. (b) Saunder, M.; Kates, M. R. *J. Am. Chem. Soc.* **1978**, 100, 7083-7085. (c) Beck, C. M.; Rathmill, S. E.; Park, Y. J.; Chen, J. Y.; Crabtree, R. H.; Liable-Sands, L. M.; Rheingold, A. L. *Organometallics*, **1999**,18, 5311-5317. (d) Kreis, M.; Palmelund, A.; Bunch, L.; Madsen, R. *Adv. Synth. Catal.* **2006**, 348, 2148-2154. (e) Fristrup, P.; Kreis, M.; Palmelund, A.; Northby, P. O.; Madsen, R. J. *J. Am. Chem. Soc.* **2008**, 130, 5206-5215.
5. (a) Campbell Jr. R. E.; Lochow, C. F.; Vora, Miller, R.G. *J. Am. Chem. Soc.* **1980**, 102, 5824-5830. (b) Campbell Jr. R. E.; Miller, R. G. *J. Organomet. Chem.* **1980**, 186, C27-C31. (c) Fairlie, D. P.; Bosnich, B. *Organometallics* **1988**, 7, 946-954. (d) Moxham, G. L.; Randell-Sly, H. E.; Brayshaw, S. K.; Woodward, R. L.; Weller, A. S.; Willis, M. C. *Angew. Chem. Int. Ed.* **2006**, 45, 7618-7622. (e) Moxham, G. L.; Randell-Sly, H. E.; Brayshaw, S. K.; Weller, A. S.; Willis, M. C. *Chem. Eur. J.* **2008**, 14, 8383-8397.
6. Adams, R. D.; Tedder, J. D. *Inorg. Chem.* **2018**, 57, 5707-5710.
7. Johnson, B. F. G.; Lewis, J.; Nicholls, J.; Puga, J.; Raithby, P. R.; Rosales, M. J.; McPartlin, M.; Clegg, W.; *J. Chem. Soc. Dalton Trans.* **1983**, 277-290.

8. APEX3 Version 2016.5-0 and SAINT Version 8.34A, Bruker AXS, Inc. Madison, WI, USA.
9. SADABS Version 2016/2, Krause, L.; Herbst-IrMer, R.; Sheldrick, G. M.; Stalke, D. *J. Appl. Cryst.* **2015**, 48, 3-10.
10. Sheldrick, G. M. SHELXTL, Version 6.1, Bruker Analytical X-ray Systems, Inc, Madison, WI, **1997**.
11. (a) Mika, L. T.; Csefalvay, E.; Nemeth, A. *Chem. Rev.* **2018**, 118, 505-613. (b) Alonso, D. M.; Wettstein, S. G.; Dumesic, J. A. *Chem. Soc. Rev.* **2012**, 41, 8075-8098. (c) Chheda, J. N.; Huber, G. W.; Dumesic, J. A. *Angew. Chem. Int. Ed.* **2007**, 46, 7164-7183. (d) Filiciotto, L.; Balu, A. M.; van der Waal, J. C.; Luque, R. *Catal. Today* **2018**, 302, 2-15. (e) Corma, A.; Iborra, S.; Velty, A. *Chem. Rev.* **2007**, 107, 2411-2502. (f) Roman-Leshkov, Y.; Barrett, C. J.; Liu, Z. Y.; Dumesic, J. A. *Nature* **2007**, 447, 982-985. (g) Tong, X. L.; Ma, Y.; Li, Y. D. *Appl. Catal. A* **2010**, 385, 1-13. (h) Zhang, X. G.; Wilson, K.; Lee, A. F. *Chem. Rev.* **2016**, 116, 12328-12368. (i) Tong, X. L.; Li, M. R.; Yan, N.; Ma, Y.; Dyson, P. J.; Li, Y. D. *Catal. Today* **2011**, 175, 524-527. (j) van Putten, R. J.; Soetedjo, J. N. M.; Pidko, E. A.; van der Waal, J. C.; Hensen, E. J. M.; de Jong, E.; Heeres, H. J. *ChemSusChem* **2013**, 6, 1681-1687. (k) Assary, R. S.; Kim, T.; Low, J. J.; Greeley, J.; Curtiss, L. A. *Phys. Chem. Chem. Phys.* **2012**, 14, 16603-16611. (l) Teixeira, I. F.; Lo, B. T. W.; Kostetskyy, P.; Ye, L. Tang, C. C.; Mpourmpakis, G.; Tsang, S. C. E. *ACS Catal.* **2018**, 8, 1843-1850.
12. (a) Climent, M. J.; Corma, A.; Iborra, S. *Green Chem.* **2014**, 16, 516-547. (b) Deuss, P.J. Barta, B.; de Vries, J. G.; *Catal. Sci. Technol.* **2014**, 4, 1174-1196.

13. (a) Johnson, B. F. G.; Lewis, J.; Nicholls, J. N.; Pruga, J.; Whitmire, K. H. *J. Chem. Soc. Dalton Trans.* **1981**, 787-797. (b) Adams, R.D.; Captain, B.; Fu, W. *Organometallics* **2000**, 19, 3670-3673. (c) Adams, R. D.; Smith, M.; Tedder, J. *J. Cluster Sci.* **2017**, 28, 695-702.

Table 2.1 Crystal data, data collection parameters for compounds **2.2** and **2.3**.

Compound	**2.2**	**2.3**
Empirical formula	$Ru_5O_{16}C_{20}H_4$	$Ru_{10}O_{34}C_{55}H_{15}$
Formula weight	1005.58	2110.27
Crystal system	Monoclinic	Triclinic
Lattice parameters		
a (Å)	8.9260(6)	9.0487(5)
b (Å)	17.0070(10)	17.9687(9)
c (Å)	17.5850(11)	18.6397(9)
α (deg)	90.00	85.535(2)
β (deg)	95.299(2)	84.640(2)
γ (deg)	90.00	75.738(2)
V ($Å^3$)	2658(3)	2919.7(2)
Space group	$P2_1/c$	*P*-1
Z value	4	2
ρ_{calc} (g / cm^3)	2.513	2.400
μ (Mo Kα) (mm^{-1})	2.852	2.605
Temperature (K)	100(2)	100(2)
$2\Theta_{max}$ (°)	50.06	50.06
No. Obs. ($I > 2\sigma(I)$)	4705	10329
No. Parameters	375	849
Goodness of fit (GOF)	1.107	1.051
Max. shift in cycle	0.003	0.002
Residuals*: R1; wR2	0.0148; 0.0294	0.0211; 0.0378
Absorption Correction, Max/min	Multi-scan 0.3577/0.2717	Multi-scan 0.564/0.449
Largest peak in Final Diff. Map ($e^- / Å^3$)	0.321	1.123

*$R1 = \Sigma_{hkl}(||F_{obs}| - |F_{calc}||)/\Sigma_{hkl}|F_{obs}|$; $wR2 = [\Sigma_{hkl}w(|F_{obs}| - |F_{calc}|)^2/\Sigma_{hkl}wF^2_{obs}]^{1/2}$; $w = 1/\sigma^2(F_{obs})$; $GOF = [\Sigma_{hkl}w(|F_{obs}| - |F_{calc}|)^2/(n_{data} - n_{vari})]^{1/2}$.

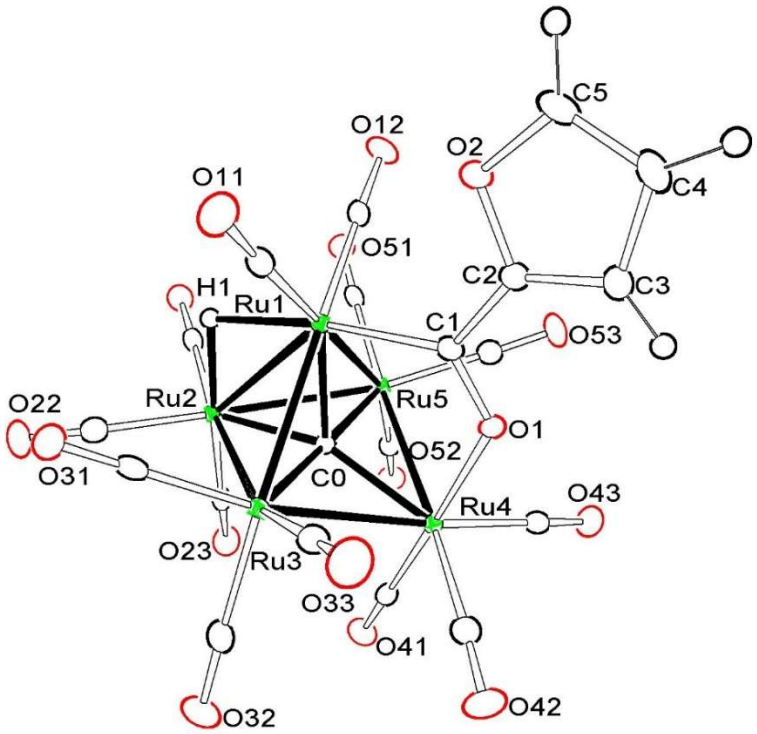

Figure 2.1 ORTEP diagram of the molecular structure of $Ru_5(\mu_5\text{-}C)(CO)_{14}(\mu\text{-}\eta^2\text{-}O{=}CC_4OH_3)(\mu\text{-}H)$, **2.2** showing 40% thermal ellipsoid probability. Selected interatomic bond distances (Å) are as follows: Ru1-Ru3 = 2.8290(3), Ru1-Ru5 = 2.8065(3), Ru1-Ru2 = 2.9050(3), Ru2-Ru5 = 2.8696(3) Ru2-Ru3 = 2.8903(3), Ru3-Ru4 = 2.8734(3), Ru4-Ru5 = 2.8670(3), Ru1-H1 = 1.91(3), Ru2-H1 = 1.79(3), Ru1-C1 = 2.026(2), Ru4-O1 = 2.1190(15), C1-O1 = 1.268(3), C1-C2 = 1.463(3), C2-C3 = 1.355(3), C2-O2 = 1.376(3), Ru1-C0 = 2.049(2), Ru2-C0 = 2.089(2), Ru3-C0 = 1.973(2), Ru4-C0 = 2.072(2), Ru5-C0 = 1.977(2).

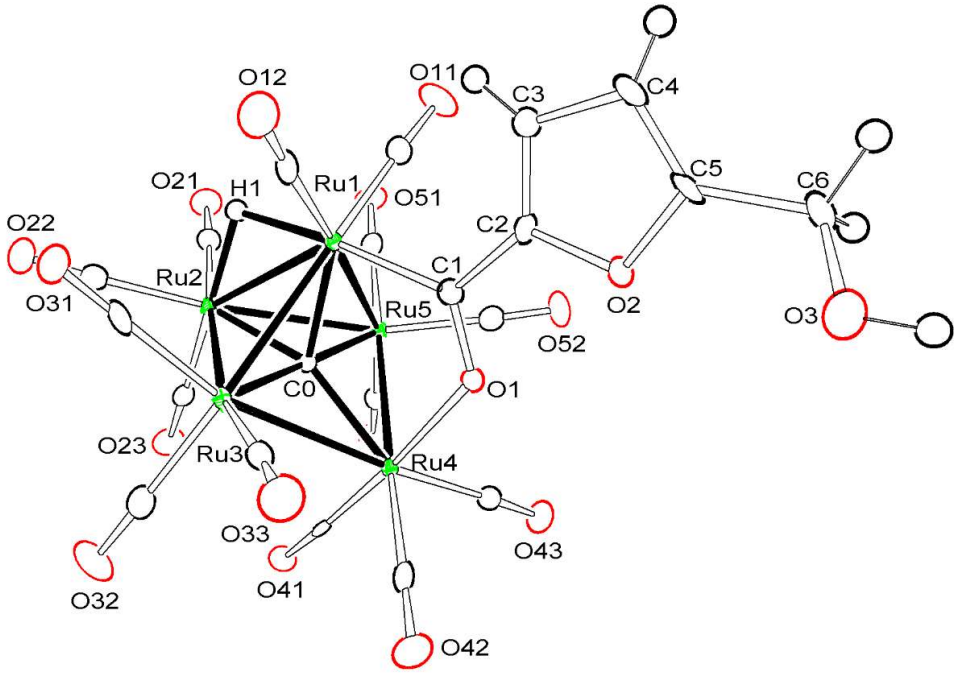

Figure 2.2 ORTEP diagram of the molecular structure of $Ru_5(\mu_5\text{-}C)(CO)_{14}(\mu\text{-}\eta^2\text{-}O{=}CC_4OH_2CH_2OH)(\mu\text{-}H)$, **2.3**, showing 50% thermal ellipsoid probability. Selected interatomic bond distances (Å) are as follows: Ru1-Ru3 = 2.8442(4), Ru1-Ru5 = 2.8137(4), Ru1-Ru2 = 2.8825(4), Ru2-Ru5 = 2.8742(4), Ru2-Ru3 = 2.8787(4), Ru3-Ru4 = 2.8764(4), Ru4-Ru5 = 2.8637(4), Ru1-H1 = 1.85(3), Ru2-H1 = 1.80(3), Ru1-C1 = 2.024(3), Ru4-O1 = 2.140(2), C1-O1 = 1.267(4), C1-C2 = 1.459(4), C2-C3 = 1.367(4), C2-O2 = 1.381(4), Ru1-C0 = 2.043(3), Ru2-C0 = 2.092(3), Ru3-C0 = 1.973(3), Ru4-C0 = 2.079(3), Ru5-C0 = 1.973(3).

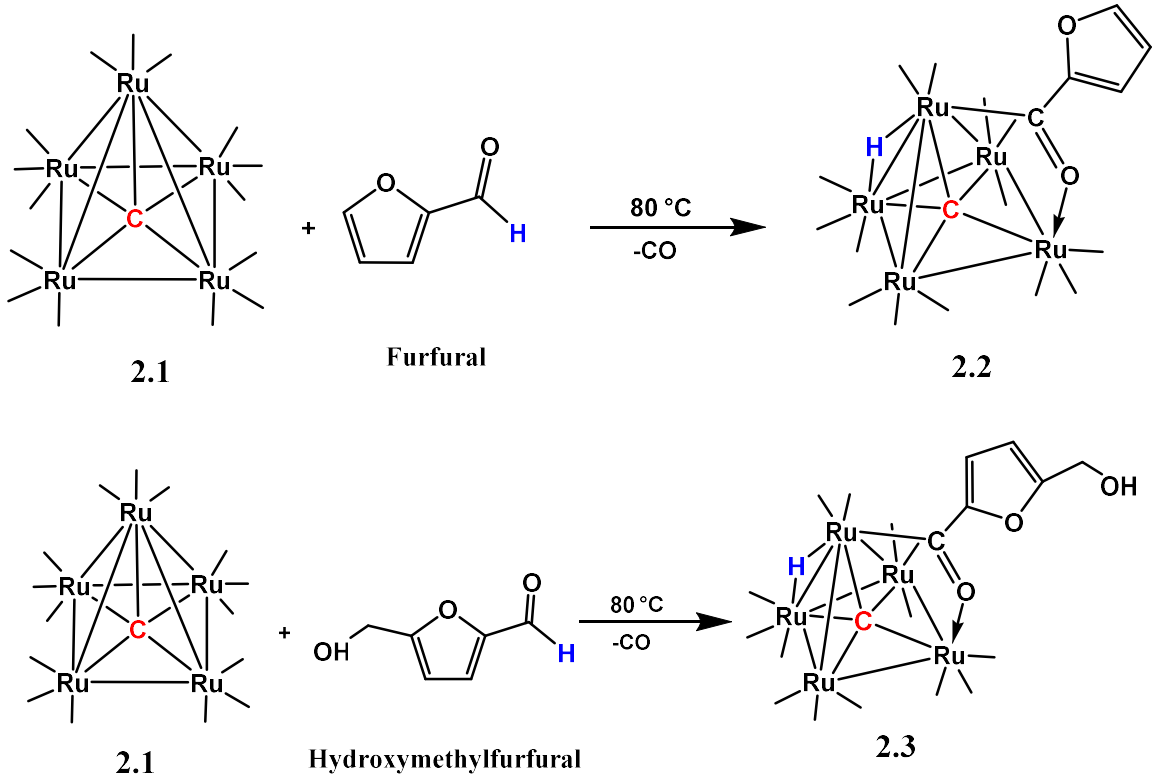

Scheme 2.1 Products formed by the oxidative addition of aldehydes to **2.1**. The CO ligands are represented only as lines from the Ru atoms.

Chapter 3

The Coordination and Activation of Azobenzene by

$Ru_5(\mu_5\text{-}C)$ Cluster Complexes [2]

[2] Adams, R. D.; Akter, H.; Smith, M. D.; Tedder, J. D. *J. Organomet. Chem.* **2018**, *878*, 77-83. Reprinted here with permission from publisher.

3.1 Introduction

Azobenzene, PhN=NPh, has attracted attention for its interesting photoisomerization properties[1] and applications ranging from those of molecular devices[2] to pharmacology.[3] Azobenzene readily undergoes ortho-metallation at its phenyl rings when it is coordinated to metal complexes[4] and today it can be easily functionalized at these ortho-positions catalytically.[5] There are only a few structurally characterized examples of azobenzene ligands in polynuclear metal carbonyl cluster complexes.[6]

In recent studies, we have been investigating the reactions of the pentaruthenium carbonyl cluster complex $Ru_5(\mu_5\text{-}C)(CO)_{15}$, **3.1** with molecules containing C-Au[7] and C-H[8] bonds. For example, we have shown that the pentaruthenium cluster complex **3.1** is able to activate the formyl C-H bond of N,N-dimethylformamide and certain aldehydes to yield the complexes $Ru_5(\mu_5\text{-}C)(CO)_{14}(\mu\text{-}\eta^2\text{ - }O{\equiv}CR)(\mu\text{-}H)$, R = NMe_2, Ph, cinnamoyl, furanyl, 5- hydroxymethylfurfuranyl that contain a bridging acyl ligand formed by opening of the Ru_5C square pyramidal cluster of metal atoms via oxidative addition of the formyl C-H bond to the metal atoms, eq. (3.1)[8].

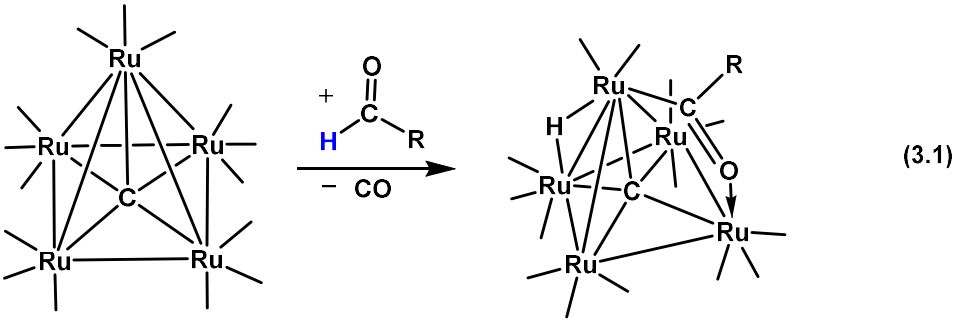

$Ru_5(\mu_5\text{–}C)(CO)_{15}$, 3.1

(3.1)

Compound **3.1** also reacts with (NHC)AuPh to yield the $AuRu_5$ complexes, $Ru_5C(CO)_{14}(Ph)[\mu\text{-}Au(NHC)]$, **3.2** and $Ru_5C(CO)_{13}(\mu\text{-}\eta^2\text{-}Ph)[\mu\text{-}Au(NHC)]$, **3.3**, NHC = dippim, by activation of the Au-C bond to the phenyl ring.[9]

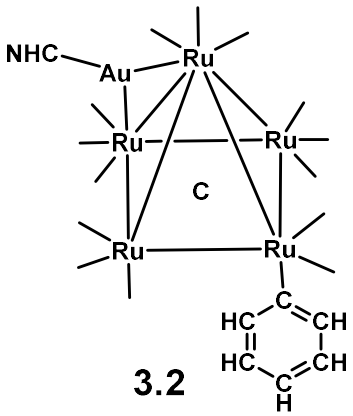

3.2

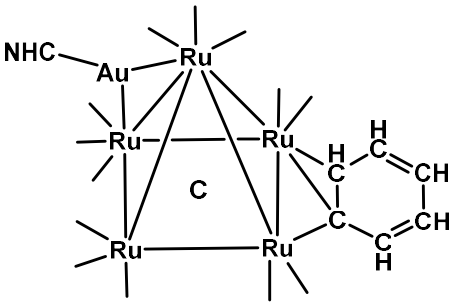

3.3

We have now investigated the reactions of **3.1** and **3.3** with azobenzene. We have obtained the first pentaruthenium complexes containing azobenzene ligands. Ortho-metallation at one of the phenyl rings has been observed. Two of the new complexes possess an unusual and unexpected electronic unsaturation which affects their structures and reactivity. The results of these studies are reported herein.

3.2 Experimental Data

General Data

All reactions were performed under nitrogen atmosphere by using standard Schlenk techniques. Reagent grade solvents were dried by the standard procedures and were freshly distilled prior to use. Infrared spectra were recorded on a Thermo Fisher Scientific Nicolet iS10 FT-IR spectrophotometer. ^{1}H NMR spectra were recorded on a Varian Mercury 300 spectrometer operating at 300.1 MHz for compounds **3.5**, **3.6** and **3.7**. ^{1}H NMR spectra for compound **3.4** was recorded on a Bruker AVANCE III spectrometer operating at 400 MHz.

Mass spectrometric (MS) measurements performed by a direct-exposure probe using electron impact ionization (EI) were made on a VG 70S instrument for compounds **3.4** and **3.5**. Positive/negative ion mass spectra were recorded on a Micromass Q-TOF instrument by using electrospray (ES) ionization for compounds **3.6** and **3.7**. Azobenzene was purchased from KODAK and was used without further purification. $Ru_5C(CO)_{15}$, **3.1**[10] and $Ru_5C(CO)_{13}(\mu-\eta^2\text{-Ph})[\mu\text{-Au(NHC)}]$, **3**, NHC = 1,3-bis(2,6- diisopropylphenyl-imidazole-2-ylidene)[9] were prepared according to previously reported procedures. Reaction products were separated by TLC in the air on Analtech 0.25 and 0.5 mm silica gel 60 Å F_{254} glass plates.

Synthesis of $Ru_5C(CO)_{13}(C_6H_4N{=}NC_6H_5)(\mu\text{-H})$, 3.4

A 59.2 mg amount of **1** (0.0631 mmol) was dissolved in heptane in a 100 mL three-neck flask. 57.5 mg of azobenzene (0.3155 mmol) was then added to the solution which was then heated to reflux for 21 h. The reaction was monitored by IR spectroscopy. The solvent was then removed in vacuo and the product was isolated by TLC by using a hexane to methylene chloride solvent mixture to yield 20.5 mg of $Ru_5C(CO)_{13}(C_6H_4N{=}NC_6H_5)(\mu\text{-H})$, **3.4** (yield 27%). Spectral Data for **3.4**: IR νCO (cm^{-1} in hexane): 2094(m), 2063(s), 2059(vs), 2044(m), 2022(m), 2007(m), 1998(w), 1991(w), 1969(w). ^1H NMR (CD_2Cl_2, in ppm) δ = 8.29 (d, J = 7.5 Hz, 1H, Ph), 8.07 (d, J = 7.5 Hz, 2H, Ph), 7.46 (d, J = 7.5 Hz, 2H, Ph), 7.16 (dt, J = 8 Hz, 2H, C_6H_4), 7.16 (d, J = 3 Hz, 1H, C_6H_4), 7.16 (d, J = 3 Hz, 1H, C_6H_4), -22.25 (s, 1H, Ru-H). EI+/MS: m/z 1064 (M+). The isotope distribution pattern was consistent with the presence of five ruthenium atoms.

Synthesis of $Ru_5C(CO)_{14}(C_6H_4N\text{-}NC_6H_5)(\mu\text{-}H)$, 3.5

1.9 mg of compound **3.4** was dissolved in 3 to 4 drops of benzene and 1 mL of heptane was added in a 20 mL glass vial. CO gas was bubbled through the solution slowly. A rapid color change from orange to yellow was observed. The vial was then stored under CO atmosphere at room temperature while the orange colored crystals were deposited overnight to yield 1.9 mg of $Ru_5C(CO)_{14}(C_6H_4N{=}NC_6H_5)(\mu\text{-}H)$, **3.5** (yield 97%). Spectral Data for **3.5**: IR νCO (cm^{-1}in hexane): 2097(w), 2066(s), 2060(vs), 2047(m), 2033(w), 2024(w), 2015(w), 2001(w), 1991(vw), 1980 (vw). ^1H NMR (CD_2Cl_2, in ppm) δ = 8.25 (dd, J = 8.4 Hz, 1H, Ph), 7.73-7.50 (m, 4H, Ph), 7.31-7.11 (m, 4H, C_6H_4), -21.78 (s,1H, Ru-H). EI+/MS: *m/z* 1093 (M+) plus ions $M^+ - n(CO)$, n = 1−14. The isotope distribution pattern was consistent with the presence of five ruthenium atoms.

Synthesis of $Ru_5C(CO)_{13}(\mu\text{-}\eta^2\text{-}PhN{=}NPh)(\eta^1\text{-}Ph)[\mu\text{–}Au(NHC)]$, 3.6

A 11.7 mg (0.0076 mmol) amount of **3.3** and 13.6 mg (0.0746 mmol) of azobenzene were dissolved in 25 mL heptane in a 50 mL three-neck flask and then heated to reflux with stirring for 11 h. The solution was then cooled, and the solvent was removed in *vacuo*. The product was isolated by TLC by using a hexane to methylene chloride solvent mixture to yield 8.9 mg of $Ru_5C(CO)_{13}(\mu\text{-}\eta^2\text{-}PhN{=}NPh)(\eta^1\text{-}Ph)[\mu\text{-}Au(NHC)]$, **3.6** (yield 68%). Spectral Data for **3.6**: IR νCO (cm^{-1} in hexane): 2071(m), 2049(w), 2039(vs), 2030(s), 2026(m), 2015(w), 1996(m), 1980(w), 1969(w), 1962(w), 1953(w), 1938(vw). ^1H NMR (CD_2Cl_2, in ppm) δ = 7.32 (t, J = 8 Hz, 2H, para $CC_2(i\text{-}Pr)_2C_2H_2C\mathbf{H}$, 7.29 (m, 7H, $CC_2(i\text{-}Pr)_2C_2\mathbf{H}_2CH$ + NPh), 6.97 (s, 2H, $C(NC_6i\text{-}Pr_2H_3)C_2\mathbf{H}_2$, 6.9-5.6 (m, 12H, NPh), 2.70 (sept, J = 6.8 Hz, 4H, $C\mathbf{H}\text{-}(CH_3)_2$), 1.16 (d, J = 6.8 Hz, 6H, $CH\text{-}(C\mathbf{H}_3)_2$), 1.15 (d, J = 6.8 Hz, 6 H,

CH-(C**H**$_3$)$_2$), 1.01 (d, J = 6.8 Hz, 6 H, CH-(C**H**$_3$)$_2$), 1.00 (d, J = 6.8 Hz, 6 H, CH-(C**H**$_3$)$_2$). ESI/MS: *m/z* 1750 $(M + Na)^+$.

Synthesis of $Ru_5C(CO)_{13}(C_6H_4N{=}NC_6H_5)[\mu\text{-}Au(NHC)]$, 3.7

A 15.3 mg amount (0.0086 mmol) of **3.6** was dissolved in d_8-toluene in a NMR tube and was then heated to 105 °C for 3 h. The product $Ru_5C(CO)_{13}(C_6H_4N{=}NC_6H_5)[\mu$-Au(NHC)], **3.7** was isolated by TLC by using a hexane to methylene chloride mixture to yield 2.8 mg of **3.7**, (yield 19%). Also 1.4 mg of **3.3** was isolated (yield 10.4%). Spectral data for **3.7**: IR νCO (cm^{-1} in hexane): 2072(vw), 2048(vs), 2039(w), 2031(m), 2015(m), 1998(m), 1991(w), 1955(vw). ^{1}H NMR (CD_2Cl_2, in ppm) δ = 8.25 (d, J = 8.7 Hz, 1H, Ph), 7.88 (d, J = 8.7 Hz, 2H, Ph), 7.43 (d, J = 8.7 Hz, 2H, Ph), 7.42 (d, J = 8.7 Hz, 2H, CC_2(i-Pr)$_2C_2H_2$C**H**), 7.29 (d, J = 7.8 Hz, 4H, CC_2(i-Pr)$_2C_2$**H**$_2$CH), 7.12 (s, 2H, C(NC_6i-Pr$_2H_3$)C_2**H**$_2$, 7.07 (dt, J = 7 Hz, 2H, C_6H_4), 6.84 (d, J = 7 Hz, 2H, C_6H_4), 6.82 (d, J = 7 Hz, 2H, C_6H_4), 2.78 (sept, J = 7 Hz, 4H, C**H**-$(CH_3)_2$), 1.37 (d, J = 7 Hz, 12H, CH-(C**H**$_3$)$_2$), 1.13 (d, J = 7 Hz, 12H, CH-(C**H**$_3$)$_2$). ESI/MS: *m/z* 1649 (M+).

Crystallographic analyses

Single crystals of **3.4** (red), **3.6** (brown), and **3.7** (orange red) suitable for X-ray analyses were obtained by slow evaporation from a hexane/methylene chloride solvent mixture at room temperature. Crystals of compound **3.5** (yellow orange) were grown from a solution in a heptane and benzene solvent mixture under a CO atmosphere. Each data crystal was glued onto the end of a thin glass fiber. For compounds **3.4**, **3.6** and **3.7**, X-ray intensity data were measured by using a Bruker SMART APEX CCD-based diffractometer by using Mo Kα radiation (λ = 0.71073 Å). The raw data frames were integrated by using

the SAINT$^+$ program with a narrow-frame integration algorithm.[11] For compound **3.5** X-ray intensity data from a yellow-orange needle of approximate dimensions 0.03 × 0.06 × 0.16 mm^3 were collected at 100(2) K by using a Bruker D8 QUEST diffractometer equipped with a PHOTON-100 CMOS area detector and an Incoatec microfocus source (Mo Kα radiation, λ = 0.71073 Å).[12] The data collection strategy consisted of seven 180° ω-scans at different φ settings and two 360° φ-scans at different ω angles, with a scan width per image of 0.5°. Corrections for Lorentz and polarization effects were also applied with SAINT+. Empirical absorption corrections based on the multiple measurements of equivalent reflections were applied by using the program SADABS. All structures were solved by a combination of direct methods and difference Fourier syntheses, and refined by full-matrix least-squares on F^2 by using the SHELXTL software package.[13] All non-hydrogen atoms were refined with anisotropic thermal parameters. Hydrogen atoms were placed in geometrically idealized positions and included as standard riding atoms during the least-squares refinements. Compound **3.4** crystallized in the monoclinic crystal system. The space group $P2_1/c$ was indicated for compound **3.4** based on the systematic absences in the data and was confirmed by the successful solution and refinement of the structure. Compound **3.5** also crystallized in the monoclinic crystal system. The space group *I*2/a (a nonstandard setting of *P*2/a) was used for the solution and refinement of this structure. Compounds **3.6** and **3.7** crystallized in the triclinic crystal system. The space group *P*-1 was assumed for the analyses of compounds **3.6** and **3.7**, and this was confirmed by the successful solution and refinement of both structures. Crystal data, data collection parameters and results of the analyses are summarized in Table 3.1.

Computational analyses

All molecular orbital calculations were performed with ADF2014 program by using the PBEsol-D3 functional with ZORA scalar relativistic correction[14] and valence triple-ζ+1 polarization, relativistically optimized (TZP) Slater-type basis set, with small frozen cores. All computations were done by using the gas phase model. This choice of computational model is based on prior testing of various functionals and basis sets.[15] The PBEsolD3 functional, which was originally developed primarily for solids, was shown to be superior to other functionals in the PBE family in the structural parameters of large organic systems[16] and for metal clusters[17]. This is also consistent with our own testing of various functionals for the structures and relative energetics in organometallic cluster complexes.[15] The dispersion corrections by Grimme et al. were included upon additional testing, once they became available in the current release of ADF.[14(h)] All calculations were geometry-optimized and were initiated with the structures obtained from the crystal structure analyses.

3.3 Results and discussion

The reaction of **3.1** with azobenzene in a heptane solution at reflux 98 °C for 21 h yielded the new pentaruthenium carbido cluster compound $Ru_5C(CO)_{13}(C_6H_4N{=}NC_6H_5)(\mu\text{-}H)$, **3.4** in 27% yield. Compound **3.4** was characterized by IR and ^{1}H NMR spectroscopy, mass spectrometry and single-crystal X-ray diffraction analysis. An ORTEP diagram of the molecular structure of **3.4** is shown in Fig. 3.1. Compound **3.4** contains a chelating, ortho-metalated azobenzene ligand coordinated to an opened square-pyramidal Ru_5C cluster. The cluster can be described as a Ru_4C butterfly

cluster that is bridged at the wingtips by the fifth Ru atom, Ru(4). The atom Ru4 contains a chelating, cyclometalated azobenzene ligand which is coordinated by the nitrogen atom N1 and the metalated carbon atom C1, Ru4–N1 = 2.087(5) Å, Ru4–C1 = 1.992(6) Å. The N1–N2 bond distance is typical of a N=N double bond, N1–N2 = 1.273(7) Å. The compound also contains one hydrido ligand H1 derived from the metalated phenyl ring. Atom H1 bridges the Ru1–Ru2 metal–metal bond, Ru1–H1 = 1.71(6) Å and Ru2–H1 = 1.82(6) Å, δ = –22.25. The metalated azobenzene ligand serves formally as a three electron donor. With a total of thirteen terminal CO ligands distributed as shown in Fig. 3.1, compound **3.4** contains a total of 74 cluster valence electrons which is two electrons less than the 76 electrons required for an 'open' Ru_5C cluster of five metal atoms;[18] thus, compound **3.4** is formally unsaturated by the amount of two electrons. Simpler electron counting procedures indicate that atom Ru4 has only 16 valence electrons. To try to obtain a better understanding of the electronic structure **3.4**, a geometry optimized PBEsolD3 ADF molecular orbital analysis of **3.4** was performed. Fig. 3.2 shows drawings of frontier orbitals in **3.4**. The highest occupied molecular orbital (HOMO) is dominated by a nonbonding d-orbital localized on the metal atom Ru4. This orbital is 65% a d_{xz}-orbital in the coordinate system that was assigned to the molecule in these calculations, see the MOs shown in Fig. 3.2. The lowest unoccupied molecular orbital (LUMO) is a delocalized π*–orbital on the metalated azobenzene ligand. The LUMO+1 is a delocalized orbital on the Ru_4C portion of the cluster. The LUMO+2 is a very interesting empty orbital that is a hybrid composed of 13% d_z^2 and 8% p_z atomic orbitals in this model that is localized on Ru4. We believe that this orbital represents the "unsaturation" site on this metal atom. Curiously, although it is much longer than the normal Ru – Ru bond distances in the

complex, Ru1– Ru3 = 2.8110(8) Å, Ru1–Ru5 = 2.8236(8) Å, Ru1–Ru2 = 2.8647(8) Å, Ru2–Ru5 = 2.8314(8) Å, Ru2–Ru3 =0 2.8692(8) Å, Ru3–Ru4 = 2.8952(8) Å, Ru4–Ru5 = 2.8854(8) Å, the Ru1···Ru4 interatomic distance of 3.461(1) Å is much shorter than the corresponding Ru2···Ru4 distance of 4.030(1) Å in this molecule which is clearly a nonbonding interaction. Thus, there may be some significant long range attractive forces between the atoms Ru1 and Ru4. Electronic unsaturation can have important implications for the reactivity of metal complexes.[19]

In order to test for unsaturation in compound **3.4**, we investigated the reaction of **3.4** with CO. A solution of **3.4** in a benzene-heptane solvent mixture was exposed to CO (1 atm) at 25 °C. The solution immediately changed color to yellow and the IR spectrum showed a complete conversion to a new compound subsequently confirmed to be $Ru_5C(CO)_{14}(C_6H_4N{=}NC_6H_5)(\mu\text{-}H)$, **5** formed by the addition of one CO ligand to **3.4**. Compound **3.5** loses CO when the CO atmosphere is removed, and it is converted back to **3.4**. Crystals of **3.5** suitable for X–diffraction analysis were grown by slow evaporation of solvent from a solution under an atmosphere of CO at room temperature. An ORTEP diagram of the molecular structure of **3.5** is shown in Fig. 3.3. Compound **3.5** is structurally similar to **3.4** except that it contains two terminally coordinated CO ligands, C41–O41 and C42–O42, on the metal atom Ru4, Ru4–C41 = 1.894(4), Ru4–C42 = 1.952(4), instead of one CO ligand as found in **3.4**. Compound **3.5** contains a single hydrido ligand that bridges the Ru1 – Ru2 metal–metal bond, δ = –21.78 in the ^{1}H NMR spectrum. Interestingly, the nonbonding Ru1···Ru4 distance in **3.5** is significantly longer, 3.929(1) Å, than the corresponding distance 3.461(1) Å found in **3.4**, Ru2–Ru4 = 3.980(1) Å. This can be explained by the differences in the electronic structures of **3.4** and **3.5**. The Ru1···Ru4 in

3.4 is short due to the electronic unsaturation on Ru4. That is, Ru4 is shifted toward Ru1 in order to share partially with some of the electrons on **3.1**, perhaps nonbonding electrons on that atom. However, the 3.461(1) Å Ru1 – Ru4 distance in **3.4** is still very long and we would hesitate to describe it as a Ru – Ru single bond. By contrast, atom Ru4 in **3.5** has a complete 18 electron configuration and it does not need additional electron sharing, so it shifts further away from Ru1 to a very long 3.929(1) Å which we would describe as completely nonbonding. The bond distances to the azobenzene ligand, Ru4–N1 = 2.072(3) Å, Ru4–C1 = 2.111(4) Å are also longer than those found in **3.4**, but the noncoordinated N–N distance, N1–N2 = 1.279(4) Å, is virtually the same as that in **3.4**.

An ADF DFT molecular orbital analysis of **3.5** was performed in order to compare with the MOs of **3.4**. Selected MOs for **3.5** are shown in Fig. 3.4. The HOMO shows the nature of the bonding of the metalated azobenzene ligand to Ru4. The LUMO shows the lowest energy π*-orbital in the azobenzene ligand. The HOMO-LUMO gap in **3.5** is 0.45 eV larger than that in **3.4**. The LUMO+1 and the LUMO+3 are delocalized orbitals on the Ru_4C portion of the metal cluster. The LUMO+2 is an antibonding orbital concentrated on the Ru3–Ru4 and the carbide carbon atom. The empty d_z^2-p_z hydrid orbital observed in the LUMO+2 of **3.4** was not found in **3.5**.

The reaction of compound **3.3** with azobenzene in heptane solvent at reflux for 11 h yielded the new azobenzene complex **3.6** in 68% yield. An ORTEP diagram of the molecular structure of **3.6** as found in the solid state is shown in Fig. 3.5. Compound **3.6** contains a bridging di-σ-η^2-N,N-coordinated azobenzene ligand across an open edge of an open Ru_5C cluster. The cluster is structurally similar to that found in **3.4** and **3.5**. Nitrogen

atom N1 of the μ-η^2-N,N-coordinated azobenzene is coordinated to Ru1 and N2 is coordinated to Ru4, Ru1–N1 = 2.064(4) Å and Ru4–N2 = 2.153(4) Å. The N–N bond distance, N1–N2=1.281(5) Å, is still short and indicative of an N–N double bond. This appears to be the first example of a di-σ-μ-η^2-N,N-coordinated azobenzene ligand. Carty reported an example of a μ_4-η^2-PhNNPh ligand in the complex $Ru_4(CO)_{10}$(μ-CO)(μ_4-PPh)(μ_4-η^2-PhNNPh) a number of years ago.[6a] In that case, each nitrogen atom was bonded to two Ru atoms and the N–N bond was very long at 1.515(4) Å. Compound **3.6** contains a η^1–coordinated phenyl group on Ru4, Ru4–C1 = 2.146(5) Å. The gold atom Au1 bridges an edge of the cluster at the Ru1–Ru2 bond, Ru1–Au1 = 2.7441(5) Å, Ru2–Au1 = 2.8671(5) Å, Ru1–Ru2 = 2.8694(6) Å and the carbene ligand is coordinated to the gold atom Au1, Au1–C60 = 2.058(5) Å. The bridging azobenzene ligand serves as a four electron donor and with 13 CO ligands, one phenyl ligand and one Au(NHC) group, compound **3.6** achieves a total of 76 cluster valence electrons which is consistent with the observed, opened square-pyramidal structure.

Compound **3.6** is somewhat similar to the compound $Ru_5(\mu_5\text{-}C)(CO)_{14}$(μ-η^2-O=CPh)[μ-Au(NHC)] that was obtained by the addition of CO to compounds **3.2** or **3.3**.[7]

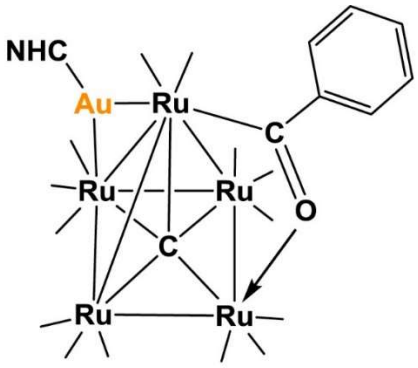

$Ru_5(\mu_5\text{-}C)(CO)_{14}$(μ-η^2-O=CPh)[μ-Au(NHC)]

When compound **3.6** was heated to 105 °C for 3 h in a NMR tube in d_8-toluene solvent, the new compound $Ru_5C(CO)_{13}(C_6H_4N{=}NC_6H_5)[\mu{-}Au(NHC)]$, **3.7** was formed in 19% yield. Compound **3.7** was also characterized structurally by single-crystal X-ray diffraction analysis. An ORTEP diagram of the molecular structure of **3.7** is shown in Fig. 3.6. Compound **3.7** is very similar to compound **3.4** except that it contains an Au(NHC) ligand bridging the Ru1–Ru2 bond of the cluster, Ru1–Au1 = 2.7889(5) Å, Ru2–Au1 = 2.8235(5) Å, Ru1···Ru4 = 3.3171(6) Å instead of a bridging hydrido ligand in the same location in **3.4**. There is a chelating ortho-metalated azobenzene ligand on the metal atom Ru4. The bonds to this ligand, Ru4–N1 = 2.098(5) Å, Ru4–C1 = 1.988(6) Å, N1–N2 = 1.284(6) Å are very similar to those in **3.4**. The formation of **3.7** involved a metalation of one of the phenyl rings of the azobenzene ligand in **3.6**. The incipient hydrido ligand from the CH activation then combined with the phenyl ligand on Ru4 and benzene was eliminated from the complex. One of the nitrogen atoms of the azobenzene ligand was released from coordination to the metal atoms and the formation of complex **3.7** was completed following a CO ligand shift to the metal atom Ru2. As result, the total valence electron count on the metal atoms in compound **3.7** is only 74, and like **3.4** it is electron deficient by the amount two electrons. As found in **3.4** the structure of the cluster appears to reflect on this deficiency. Most notably, the Ru1–Ru4 bond distance has decreased significantly Ru1···Ru4 = 3.3171(6) Å and it is even shorter than the Ru1···Ru4 distance of 3.461(1) Å in **3.4**. Unfortunately, due to the very small amounts of **3.7** that we were able to obtain, we were not able to study its reactivity with electron donors such as CO.

3.4 Conclusions

Summaries of the reactions and products studied in this work are shown in Schemes 3.1 and 3.2. The addition of azobenzene to **3.1** resulted in the formation of the electronically unsaturated compound **3.4** by the loss of two CO ligands and the addition and metalation of one of the phenyl rings of the azobenzene to the Ru5 cluster, see Scheme 3.1. The metal atom containing the metalated azobenzene ligand is formally unsaturated by the amount of two electrons. Although it is weak, there appears to be a significant long-range interaction between the unsaturated metal atom Ru4 and one of the metal atoms is the Ru_4C portion of the cluster. This long-range weak interaction between these two ruthenium atoms is represented by a dashed line shown in the line structure of compound **3.4** in Scheme 3.1. In support of its unsaturation character, compound **3.4** was found to add CO to the metal atom containing the metalated-azobenzene ligand to yield the electronically saturated complex **3.5**. In the process, the weak interaction between the two ruthenium atoms was eliminated. The CO addition reaction is reversible.

The nature of the addition of azobenzene to compound **3.3** is shown in Scheme 3.2. The cluster of **3.3** opened upon addition of the azobenzene molecule and the bridging phenyl ligand moved to a terminally coordinated position. The azobenzene ligand adopted a bridging di-σ-*N,N*-coordination mode in the product **3.6**. When compound **3.6** was heated, one of the phenyl rings of the azobenzene ligand became metalated at an ortho-position. The hydrogen atom of the metalated CH bond was shifted to a metal atom where it was combined with the phenyl ligand and benzene was then reductively eliminated from the complex. One of the nitrogen atoms of the azobenzene ligand was released from coordination and the complex became electron deficient, analogous to that of compound

3.4. As a result, a weak metal–metal interaction developed between the remote metal atom and one of the metal atoms of the Ru_4C portion of the cluster as represented by the dashed line in the structure of **3.7** in Scheme 3.2.

In this work, it has been shown that azobenzene is a viable ligand in Ru_5C cluster complexes. Ortho-metallation of a phenyl ring, a common feature of the azobenzene ligand,[4] was also observed. Most interestingly, two examples of electronically unsaturated Ru_5 complexes were observed. This property could have implications of additional reactivity toward small donor molecules.

3.5 References

1. (a) Dong, L.; Feng, Y.; Wang, L.; Feng, W. *Chem. Soc. Rev.* **2018**, 47, 7339-7368. (b) Dhammika Bandar, H. M.; Burdette, S.C. *Chem. Soc. Rev.* **2012**, 41, 1809-1825.
2. (a) Mart, R. J.; Allemann, R. K. *Chem. Commun.* (*J. Chem. Soc. Sect. D*) **2016**, 52, 12262-12277. (b) Broichhagen, J.; Frank, J. A.; Trauner, D. *Acc. Chem. Res*. **2015**, 48, 1947-1960. (c) Beharry, A. A.; Woolley, G. A. *Chem. Soc. Rev.* 2011, 40, 4422-4437.
3. Velema, W. A.; Szymanski, W.; Feringa, B. L. *J. Am. Chem. Soc.* 2014, 136, 2178-2191.
4. (a) Kleiman, J. P.; Dubeck, M. *J. Am. Chem. Soc.* **1963**, 85, 1544-1545. (b) Cope, A. C.; Siekman, R. W.; *J. Am. Chem. Soc.* **1965**, 87, 3272-3273.
5. Long Nguyen, T. H.; Gigant, N.; Joseph, D. *ACS Catal.* **2018**, 8, 1546-1579.
6. (a) Corrigan, J.F.; Doherty, S.; Taylor, N.J.; Carty, A.J. *J. Chem. Soc., Chem. Commun.* **1991**, 1640-1641. (b) Hansert, B.; Vahrenkamp, H. J. *Organomet. Chem.* **1993**, 459, 265-269.
7. Adams, R. D.; Tedder, J. D. *J. Organomet. Chem.* **2017**, 829, 58-85.

8. (a) Adams, R. D.; Tedder, J. D. *Inorg. Chem.* **2018,** 57, 5707-5710. (b) Adams, R. D.; Akter, H.; Tedder, J. D. *J. Organomet. Chem*. **2018**, 871, 159-166.
9. Adams, R. D.; Tedder, J. D.; Wong, Y. O. *J. Organomet. Chem.* **2015**, 795, 2-10.
10. Johnson, B. F. G.; Lewis, J.; Nicholls, J. N.; Puga, J.; Raithby, P.R.; Rosales, M. J.; McPartlin, M.; Clegg, W. *J. Chem. Soc. Dalton Trans*. **1983**, 277 – 290.
11. SAINT^{+}, Version 6.2a, Bruker Analytical X-ray Systems, Inc., Madison, WI, **2001**.
12. APEX3 Version 2016.5-0 and SAINT Version 8.37A. Bruker AXS, Inc. Madison, WI, USA.
13. Sheldrick, G. M. SHELXTL, Version 6.1, Bruker Analytical X-ray Systems, Inc., Madison, WI, **1997**.
14. (a) te Velde, G.; Bickelhaupt, F. M.; van Gisbergen, S. J. A.; Fonseca Guerra, C.; Baerends, E. J.; Snijders, J. G.; Ziegler, T. *J. Comput. Chem.* **2011**, 22, 931-967. (b) Fonseca Guerra, C.; Snijders, J. G.; te Velde, G.; Baerends, E. J. *Theoret. Chem. Accts.* **1998**, 99, 391-403. (c) Perdew, J. P.; Ruzsinszky, A.; Csonka, G. I.; Vydrov, O. A.; Scuseria, G. E.; Constantin, L. A.; Zhou, X.; Burke, K. *Phys. Rev. Lett.* **2008**, 100, 136406. (d) Perdew, J. P.; Ruzsinszky, A.; Csonka, G. I.; Vydrov, O. A.; Scuseria, G. E.; Constantin, L. A.; Zhou, X.; Burke, K. *Phys. Rev. Lett.* **2009**, 102, 039902. (e) van Lenthe, E.; Baerends, E. J.; Snijders, J. G. *J. Chem. Phys.* **1993**, 99, 4597. (f) van Lenthe, E.; Baerends, E. J.; Snijders, J. G. *J. Chem. Phys.* **1994**, 101, 9783. (g) van Lenthe, E.; Ehlers, A. E.; Baerends, E. J. *J. Chem. Phys.* **1999**, 110, 8943. (h) Grimme, S.; Anthony, J.; Ehrlich, S.; Krieg, H. *J. Chem. Phys.* **2010**, 132, 154104.

15. (a) Adams, R. D.; Kan, Y.; Rassolov, V.; Zhang, Q. *Organometallics* **2013**, 730, 20-31. (b) Adams, R. D.; Rassolov, V.; Wong, Y. O. *Angew. Chem. Int. Ed.* **2016**, 55, 1324-1327.

16. Csonca, G. I.; Ruzisinsky, A.; Perdew, J. P.; Grimme, S. *J. Chem. Theor. Comput.* **2008**, 4, 888-891.

17. Koitz, R.; Soini, T. M.; Genest, A.; Trickey, S. B.; Rosch, N. *J. Chem. Phys.* **2008**, 137, 034102.

18. Mingos, D. M. P.; May, A. S. in: Shriver, D. F.; Kaesz, H. D.; Adams, R. D. (Eds.), The Chemistry of Metal Cluster Complexes, VCH Publishers, New York, **1990**, Ch. 2.

19. (a) Adams, R. D.; Captain, B.; Beddie, C.; Hall, M. B. *J. Am. Chem. Soc.* **2007**, 129, 986-1000. (b) Adams, R. D.; Captain, B. *Angew. Chem. Int. Ed.* **2005**, 44, 2531-2533. (c) Adams, R. D.; Captain, B.; Zhu, L. *J. Organomet. Chem.* **2008,** 693, 819-833.

Table 3.1 Crystal data, data collection parameters for compounds **3.4**, and **3.5**.

Compound	**3.4**	**3.5**
Empirical formula	$Ru_5O_{13}N_2C_{26}H_{10}$	$Ru_5O_{14}N_2C_{27}H_{10}$
Formula weight	1063.71	1091.72
Crystal system	Monoclinic	Monoclinic
Lattice parameters		
a (Å)	10.5296(14)	14.8943(7)
b (Å)	32.997(4)	25.5563(14)
c (Å)	9.1870(19)	16.6131(13)
α (deg)	90.00	90.00
β (deg)	100.326(3)	91.499(2)
γ (deg)	90.00	90.00
V (Å^3)	3140.3(7)	6321.5(7)
Space group	$P2_1/c$	$I2/a$
Z value	4	8
ρ_{calc} (g/cm^3)	2.250	2.294
μ (Mo Kα) (mm^{-1})	2.416	2.406
Temperature (K)	294(2)	100(2)
2Θmax (°)	50.06	60.20
No. Obs. (I > 2σ(I))	5534	9265
No. Parameters	419	433
Goodness of fit (GOF)	1.158	1.029
Max. shift in cycle	0.000	0.001
Residuals*: R1; wR2	0.0441; 0.0923	0.0383, 0.0853
Absorption Correction,	Multi-scan	Multi-scan
Max/min	1.00/0.659	0.9313/0.6995
Largest peak in Final Diff. Map (e$^-$/Å^3)	0.780	2.930

*$R1 = \Sigma_{hkl}(||F_{obs}| - |F_{calc}||)/\Sigma_{hkl}|F_{obs}|$; $wR2 = [\Sigma_{hkl}w(|F_{obs}| - |F_{calc}|)^2/\Sigma_{hkl}wF^2_{obs}]^{1/2}$; $w = 1/\sigma^2(F_{obs})$; $GOF = [\Sigma_{hkl}w(|F_{obs}| - |F_{calc}|)^2/(n_{data} - n_{vari})]^{1/2}$.

Table 3.2 Crystal data, data collection parameters for compounds **3.6**, and **3.7**.

Compound	**3.6**	**3.7**
Empirical formula	$Ru_5AuO_{13}N_4C_{62}H_{58}$	$Ru_5AuO_{13}N_4C_{56}H_{52}$
Formula weight	1769.44	1691.33
Crystal system	Triclinic	Triclinic
Lattice parameters		
a (Å)	12.6764(9)	12.8392(5)
b (Å)	14.1876(10)	13.6145(5)
c (Å)	20.5509(15)	19.3942(8)
α (deg)	76.020(2)	77.330(1)
β (deg)	80.507(2)	89.300(1)
γ (deg)	68.981(2)	68.939(1)
V ($Å^3$)	3335.4(4)	3078.3(2)
Space group	*P*-1	*P*-1
Z value	2	2
ρ_{calc} (g/cm^3)	1.762	1.825
μ (Mo Kα) (mm^{-1})	3.355	3.630
Temperature (K)	294(2)	294(2)
2Θmax (°)	50.06	50.06
No. Obs. ($I > 2\sigma(I)$)	11783	10860
No. Parameters	760	706
Goodness of fit (GOF)	1.070	1.051
Max. shift in cycle	0.001	0.001
Residuals*: R1; wR2	0.0331; 0.0817	0.0323; 0.0749
Absorption Correction,	Multi-scan	Multi-scan
Max/min	1.00/0.749	0.466/0.709
Largest peak in Final Diff. Map ($e^-/Å^3$)	1.033	1.077

*$R1 = \Sigma_{hkl}(||F_{obs}| - |F_{calc}||)/\Sigma_{hkl}|F_{obs}|$; $wR2 = [\Sigma_{hkl}w(|F_{obs}| - |F_{calc}|)^2/\Sigma_{hkl}wF^2_{obs}]^{1/2}$; $w = 1/\sigma^2(F_{obs})$; $GOF = [\Sigma_{hkl}w(|F_{obs}| - |F_{calc}|)^2/(n_{data} - n_{vari})]^{1/2}$.

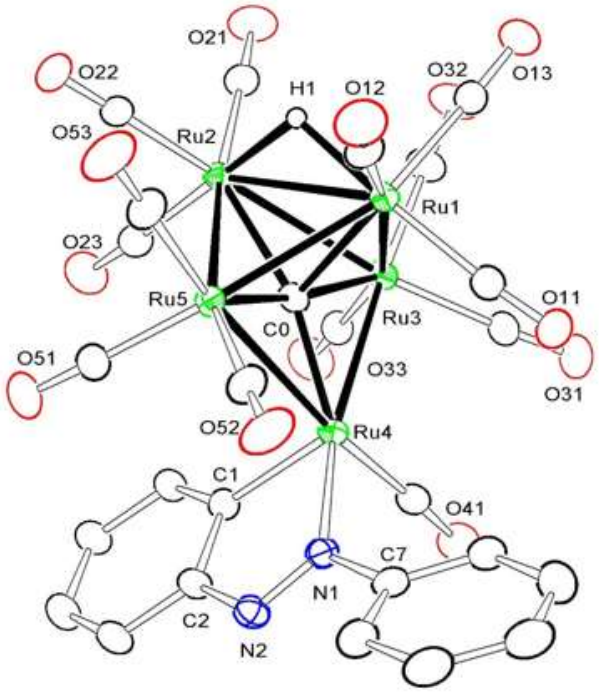

Figure 3.1 An ORTEP diagram of the molecular structure of $Ru_5C(CO)_{13}(C_6H_4N{=}NC_6H_5)$ (μ–H), **3.4** showing 20% thermal ellipsoid probability. Selected interatomic distances are (Å) as follows: Ru1–Ru2 = 2.8647(8), Ru1–Ru3 = 2.8110(8), Ru1…Ru4 = 3.461(1), Ru1–Ru5 = 2.8236(8), Ru2–Ru5 = 2.8314(8), Ru2–Ru3 = 2.8692(8), Ru3–Ru4 = 2.8952(8), Ru4–Ru5 = 2.8854(8), Ru1–H1 = 1.71 (6), Ru2–H1 = 1.82 (6), Ru4–N1 = 2.087 (5), Ru4–C1 = 1.992 (6), N1–N2 = 1.273(7).

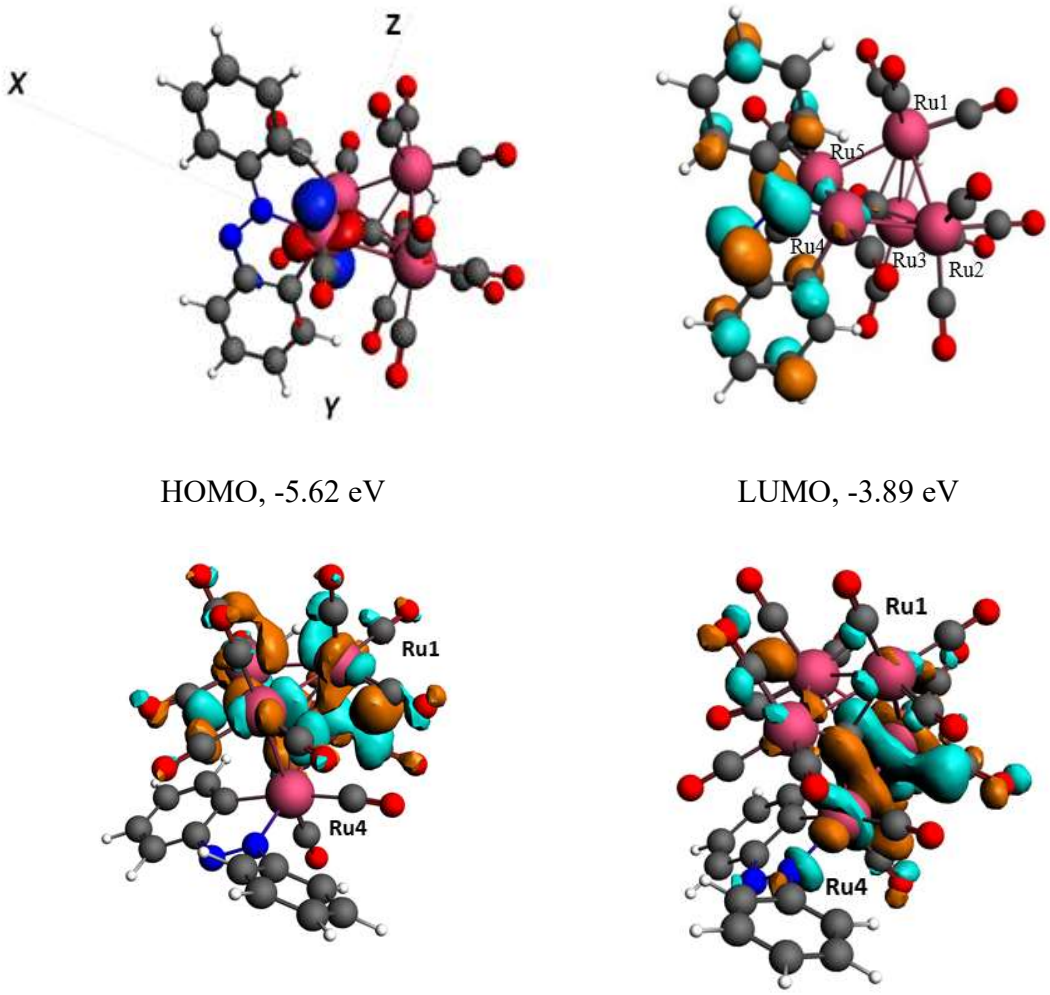

HOMO, -5.62 eV

LUMO, -3.89 eV

LUMO + 1, -3.65 eV

LUMO + 2, -3.34 eV

Figure 3.2 Selected molecular orbitals (MOs) with calculated energies in eV for compound **3.4** that show the nature of the bonding between the metalated azobenzene ligand and the interactions of ruthenium atoms in the metal cluster. The ruthenium atoms are colored as pink.

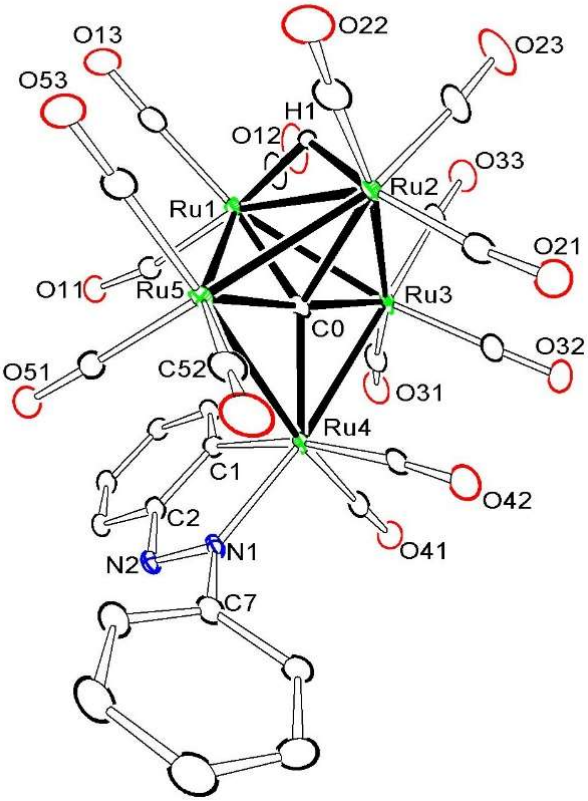

Figure 3.3 An ORTEP diagram of the molecular structure of $Ru_5C(CO)_{14}(C_6H_4N{=}NC_6H_5)(\mu{-}H)$, **3.5** showing 25% thermal ellipsoid probability. Selected interatomic distances are (Å) as follow: Ru1-Ru5 = 2.8195(5), Ru1-Ru2 = 2.8338(5), Ru1-Ru3 = 2.9143(5), Ru1···Ru4 = 3.929(1), Ru2-Ru3 = 2.8298(5), Ru2- Ru5 = 2.8536(5), Ru3-Ru4 2.9254(5), Ru1-H1 = 1.7104, Ru2-H1 = 1.7109, Ru4-C41 = 1.894(4), Ru4-C42 = 1.952(4), Ru4-N1 = 2.072(3), Ru4-C1 = 2.111(4), Ru4-Ru5 = 2.9624(5), N1 - N2 = 1.279(4).

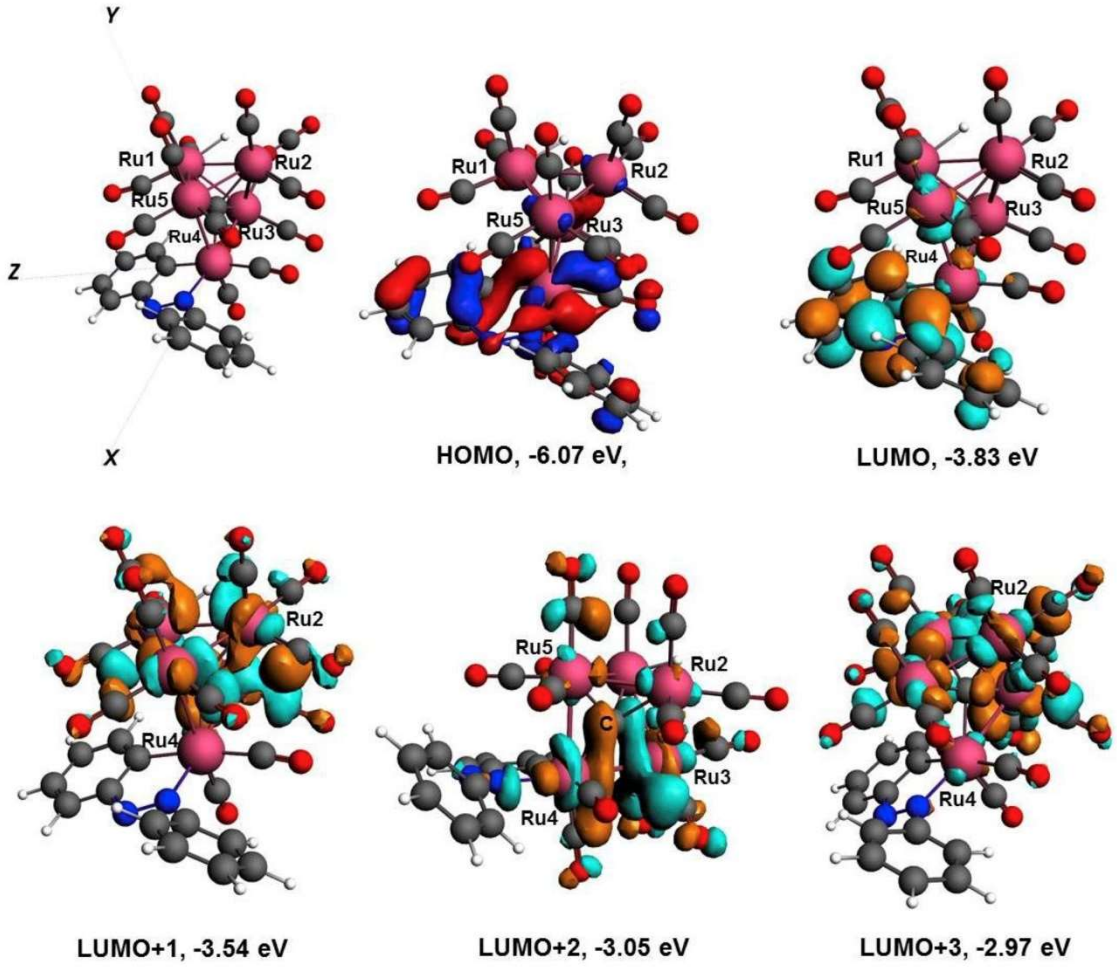

Figure 3.4 Selected molecular orbitals (MOs) with calculated energies in eV for compound **3.5** that show the nature of the bonding between the metalated azobenzene ligand and the interactions of ruthenium atoms in the metal cluster. The ruthenium atoms are colored as pink.

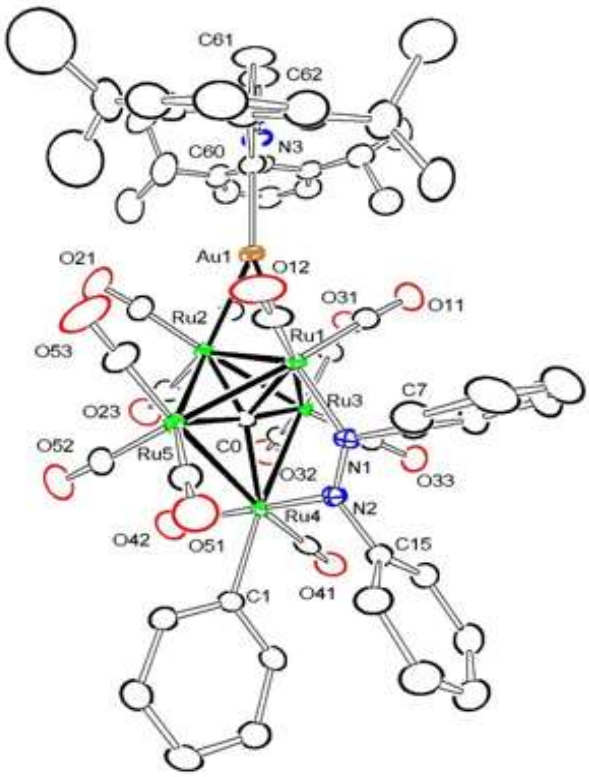

Figure 3.5 An ORTEP diagram of the molecular structure of $Ru_5C(CO)_{13}(\mu-\eta^2-PhN=NPh)(\eta^1-Ph)[\mu-Au(NHC)]$, **3.6** showing 15% thermal ellipsoid probability. The hydrogen atoms in the carbene ligand is omitted for clarity. Selected interatomic distances are (Å) as follows: Ru1−Au1 = 2.7441(5), Ru2−Au1 = 2.8671(5), Ru1−Ru2 = 2.8694(6), Au1−C60 = 2.058(5), Ru1−N1 = 2.064 (4), Ru4−N2 = 2.153 (4), Ru4−C1 = 2.146 (5), N1−N2 = 1.281(5).

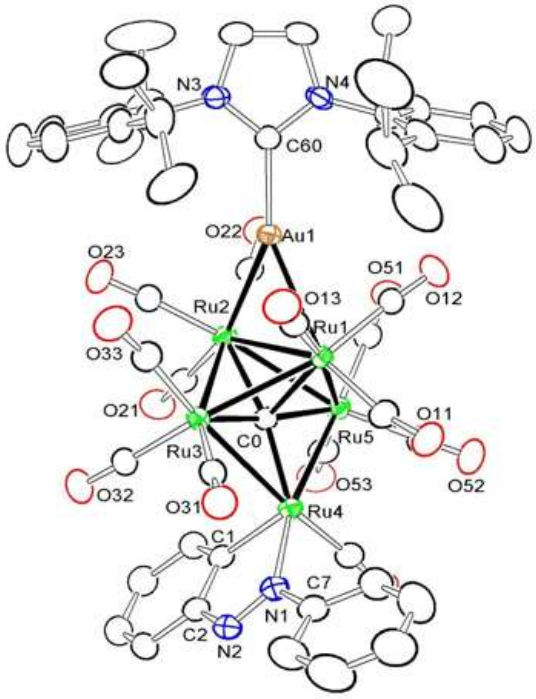

Figure 3.6 An ORTEP diagram of the molecular structure of $Ru_5C(CO)_{13}(C_6H_4N\text{-}NC_6H_5)$[μ−Au(NHC)], **3.7** showing 20% thermal ellipsoid probability. The hydrogen atoms in the carbene ligand is omitted for clarity. Selected interatomic distances are (Å) as follows: Ru1−Au1 = 2.7889(5), Ru2−Au1 = 2.8235(5), Ru1−Ru2 = 2.9113(6), Au1−C60 = 2.040(5), Ru4−N1 = 2.098 (5), Ru4−C1 = 1.988 (6), N1−N2 = 1.284(6).

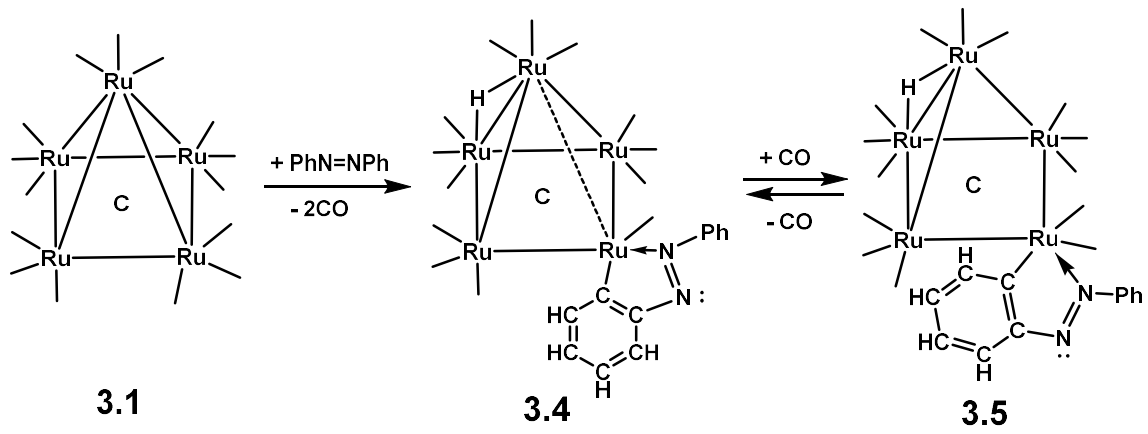

Scheme 3.1 A schematic of reactions and structures for the compounds **3.4** and **3.5** in this study. CO ligands are represented only as lines from the Ru atoms.

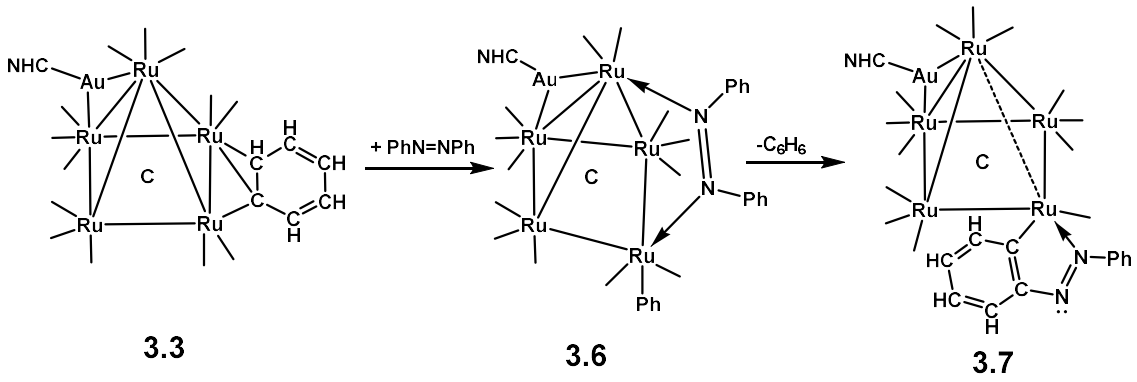

Scheme 3.2 A schematic of reaction of compound **3.3** with azobenzene. CO ligands are represented only as lines from the Ru atoms.

Chapter 4

Synthesis, Structures and Transformations of Bridging and Terminally-Coordinated Trimethylammonioalkenyl Ligands in Zwitterionic Pentaruthenium Carbido Carbonyl Complexes [3]

[3] Adams, R. D.; Akter, H.; Kaushal, M.; Smith, M. D.; Tedder, J. D. *Inorg. Chem.* **2021**, 60, 6, 3781–3793. Reprinted here with permission from publisher.

4.1 Introduction

Hydrocarbyl onium zwitterions have been of great interest for many years. The best known examples of these are the phosphorus- and sulfur-ylides **A**[1] and **B**[2] that were first reported by Wittig in the 1950s.[1] These and other ylides are valuable reagents in organic syntheses.[2,3] These ylides are well known to coordinate to metal atoms by using the negatively-charged carbon atom which formally transfers its negative charge to the metal atom upon coordination, see **C** and **D** below, and the complex becomes a zwitterion.[4,5]

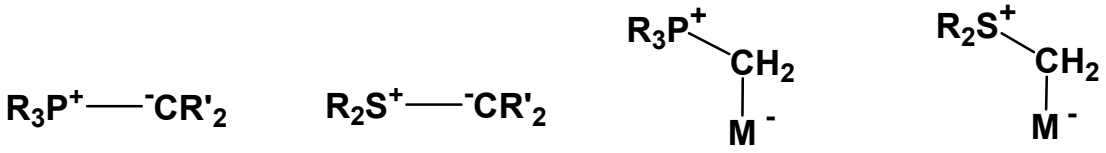

A **B** **C** **D**

In recent years, new families of unsaturated hydrocarbyl onium ligands have been synthesized in metal complexes. Some examples of these are shown in the structures **E** – **G**.[6-8] They can be obtained by the addition of tertiary phosphines to certain alkyne or vinylidene ligands. There are only a few examples of complexes containing the ammonioethenyl ligand shown in structure **H**.[9, 10]

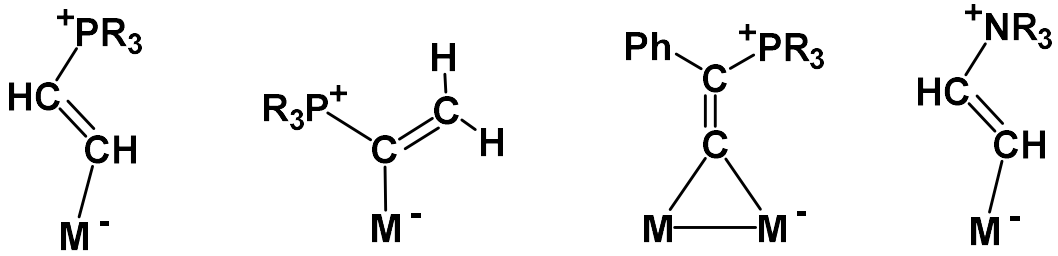

E **F** **G** **H**

In recent studies, we have synthesized the first example of a bridging η^2-trimethylammonioethenyl ligand in the zwitterionic hexaruthenium carbonyl complex $Ru_6(\mu_6\text{-}C)(CO)_{15}(\mu\text{–}\eta^2\text{–}CHCHNMe_3)$, **4.1** and have found that this bridging ligand can be readily converted to a terminally-coordinated η^1-ligand in the complex $Ru_6(\mu_6\text{-}C)(CO)_{16}[\mu\text{–}\eta^2\text{–}CH{=}CH(NMe_3)]$, **4.2** by the addition of CO to **4.1**, eq. (4.1).[10]

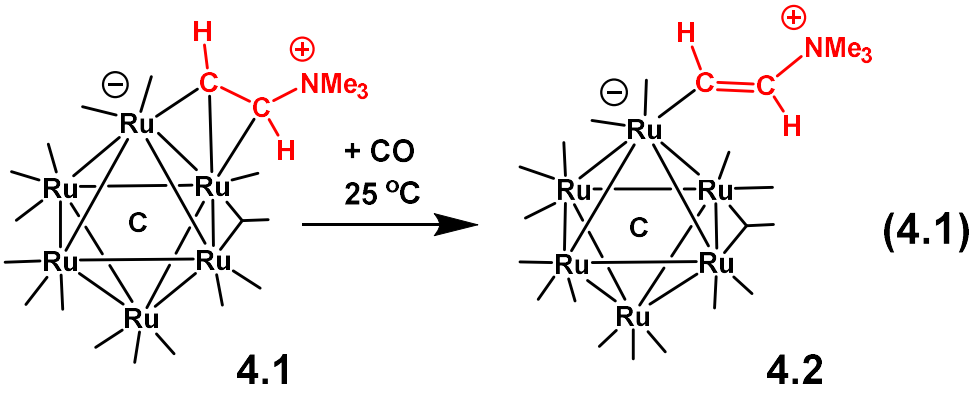

Interestingly, the bridging η^2-trimethylammonioethenyl ligand, $(\mu\text{–}\eta^2\text{–}CHCH^{+}NMe_3)$, in **4.1** can also be converted to a simple alkyne ligand in the complex $Ru_6C(CO)_{15}(\mu_3\text{-}C_2H_2)$, **4.3** by the reversible elimination of NMe_3 from the bridging η^2-ligand in **4.1**, eq. (4.2).

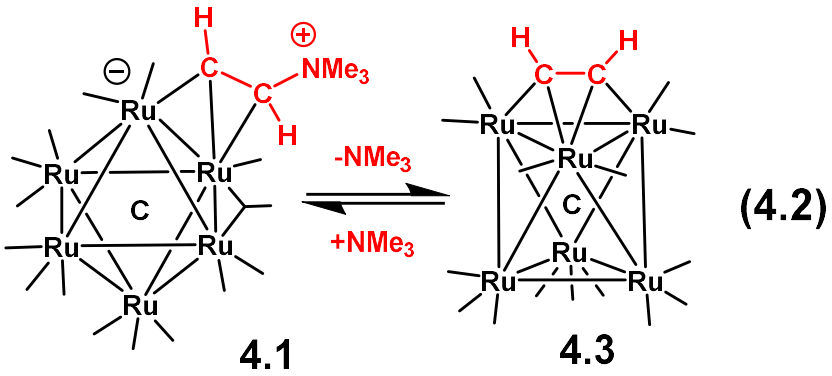

Even more interestingly, it was also found that ethyne (C_2H_2) can be added to the bridging η^2–CHCH($^+$NMe$_3$) ligand in **4.1** to form a triply-bridging η^4-trimethylammoniobutadienyl, (μ_3-η^4-CHCHCHCH$^+$NMe$_3$), ligand in the zwitterionic complex $Ru_6(\mu_6\text{-}C)(CO)_{14}[\mu_3\text{–}\eta^4\text{–}C_4H_4(NMe_3)]$, **4.4** by a C – C bond forming coupling to the η^2–CHCH$^+$NMe$_3$ ligand, eq. (4.3).

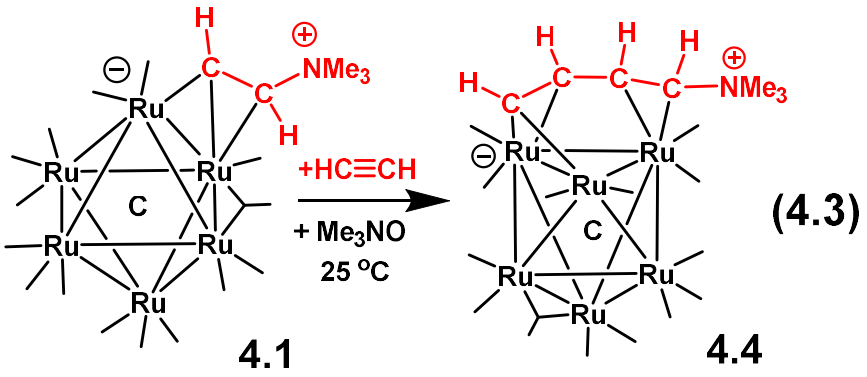

(4.3)

In hopes of finding new structures and reactivity of alkylammonioethenyl zwitterions for applications in organic synthesis, we have now investigated reactions of the pentaruthenium carbonyl complexes $Ru_5(\mu_5\text{-}C)(CO)_{15}$,[11] **4.5**, $Ru_5(\mu_5\text{-}C)(CO)_{14}[\mu\text{-}\eta^2\text{-}O{=}C(NMe_2)](\mu\text{-}H)$,[12] **4.6** and $Ru_5(\mu_5\text{-}C)(CO)_{15}Cl(\mu\text{-}H)$,[11] **4.7** with ethyne (C_2H_2) and methyl propiolate (HC≡CCO$_2$Me) in the presence of Me$_3$NO. We have obtained a series of new pentaruthenium complexes containing terminally-coordinated η^1-trimethylammonioethenyl ligands, two new complexes containing bridging η^2-trimethylammonioethenyl ligands and one complex containing a terminally-coordinated η^1-2-trimethylammonio(1-methoxycarbonyl)ethenyl ligand. The syntheses, structures and chemistry of these new complexes are described in this chapter.

4.2 Experimental Section

General Data

All reactions were performed under nitrogen atmosphere. Reagent grade solvents were dried by standard procedures and were freshly distilled prior to use. $Ru_3(CO)_{12}$ was obtained from STREM and was used without further purification. N,N-dimethylformamide, (**DMF**), $Me_2NC(=O)H$; hydrochloric acid, HCl (37%); Methyl propiolate, $HC{\equiv}C(CO_2Me)$ (**MP**); Trimethylamine-N-oxide, Me_3NO; and anhydrous trimethylamine gas (NMe_3) were purchased from Sigma Aldrich and were used without further purification. Ethyne gas (HC_2H) (industrial grade) was purchased from Praxair and was used without further purification. Research Grade Carbon Monoxide (CO) was purchased from Airgas Specialty Chemicals and was used without further purification. **WARNING**: Carbon Monoxide is a hazardous gas that should be used only in a well-ventilated fume hood. $Ru_5(\mu_5\text{-}C)(CO)_{15}$,[11] **4.5**, $Ru_5(\mu_5\text{-}C)(CO)_{14}[\mu\text{-}\eta^2\text{-}O{=}C(NMe_2)](\mu\text{-}H)$,[12] **4.6** and $Ru_5(\mu_5\text{-}C)(CO)_{15}Cl(\mu\text{-}H)$,[11] **4.7** were prepared according to previously reported procedures. Product separations were performed by TLC in the air on Analtech 0.25 mm and 0.50 mm silica gel 60 Å F254 glass plates. Column chromatography was performed by using silica gel 60, 0.606-0.2 mm (70–230 mesh).

Synthesis of $Ru_5(\mu_5\text{-}C)(CO)_{13}[\mu{-}\eta^2{-}CHCH(NMe_3)]$, 8 from reaction of 5 with NMe_3, Me_3NO, and C_2H_2 at -78 ℃.

22.2 mg (0.0237 mmol) of **4.5** was added to a 100 mL three-neck flask and then dissolved in 25 mL of degassed CH_2Cl_2. The solution was cooled to -78 ℃ temperature by using dry ice/acetone bath. 3 mL of NMe_3 (gas/1atm) were added to the solution through the rubber septum by syringe. A solution of 4.7 mg (0.0626 mmol) of Me_3NO in CH_2Cl_2

was then added to the flask. A color change from red to dark red was observed. Then, 4 mL of C_2H_2 (gas/1atm) was added to the flask and the reaction solution was allowed to stir for 30 min. The progress of the reaction was monitored by IR spectroscopy. The excess unreacted gases were then removed by flushing the solution with nitrogen. The reaction mixture warmed to room temperature and the solvent was removed in *vacuo*. The product was then isolated by TLC on silica gel by using a solvent mixture of hexane/methylene chloride to yield 1.2 mg of red orange $Ru_5(\mu_5\text{-}C)(CO)_{13}[\mu\text{–}\eta^2\text{–}CHCH(NMe_3)]$, **4.8** (5.2% yield). Spectral data for **4.8**: IR, νCO (cm^{-1} in CH_2Cl_2): 2071(w), 2033(s), 2016(s), 2006(vs). ^{1}H NMR (in acetone-d_6 solvent, δ in ppm): 11.23 (C**H**CHN$(CH_3)_3$, d, $^3J_{H\text{-}H}$ = 10.0 Hz, 1H), 5.87 (CHC**H**N$(CH_3)_3$, m, $^3J_{H\text{-}H}$ = 10.0 Hz, 1H), 3.64 (CHCHN(C**H**$_3)_3$, s, 9H). ^{13}C NMR (in $(CD_3)_2CO$, 100.66 MHz, δ in ppm): 204.33 (CO), 202.85(CO), 201.60 (CO), 199.83 (CO), 197.72 (CO), 192.73 (CO), 191.40 (CO), 170.41 (**C**HCHN$(CH_3)_3$), 94.80 (CH**C**HN$(CH_3)_3$), 54.65 (t, $^1J_{C\text{-}N}$ = 16 Hz, CHCHN(**C**$H_3)_3$). Elemental analysis: Calculated for $Ru_5NO_{13}C_{19}H_{11}$: C, 23.61%; H, 1.15%; N, 1.45%. Found: C, 23.74%; H, 0.96%; N, 1.39%.

Reaction of $Ru_5(\mu_5\text{-}C)(CO)_{14}[\mu\text{-}\eta^2\text{-}O{=}C(NMe_2)](\mu\text{-}H)$, 4.6 with C_2H_2 and Me_3NO at 25 °C.

66.5 mg (0.0677 mmol) of **4.6** in 20 mL of degassed dichloromethane was added to a 100 mL three-neck flask. A slow purge of C_2H_2 (1 atm) was then passed through the solution. 10.2 mg (0.136 mmol) Me_3NO was added to the solution while keeping the flask under C_2H_2 (1 atm) at 25 °C. Then the solution was stirred for 15 min until an IR spectrum showed no **4.6** remained. The products were then isolated by TLC by using hexane/methylene chloride solvent mixture to yield in order of elution: 34.2 mg (48%

yield) of $Ru_5(\mu_5\text{-}C)(CO)_{13}[\mu\text{–}\eta^2\text{–}O{=}C(NMe_2)](\eta^1\text{–}E\text{–}CH{=}CH(NMe_3)](\mu\text{–}H)$, **4.9**[13] and 4.4 mg (6.4% yield) of $Ru_5(\mu_5\text{-}C)(CO)_{12}[\mu\text{-}\eta^2\text{-}O{=}C(NMe_2)][\mu\text{-}\eta^2\text{-}CHCH(NMe_3)](\mu\text{-}H)$, **4.10**. Spectral data for **4.9**: Tedder (2018) reported IR, ^{1}H NMR, and X-ray analyses of the compound **4.9** in his dissertation.[13] For the current work we also obtain the ^{13}C NMR, elemental analysis, and mass spectral analyses. ^{13}C NMR ($(CD_3)_2CO$, 100.66 MHz, δ in ppm): 219.55 (d, $^2J_{C\text{-}H}$ = 1.6 Hz, **C**$ON(CH_3)_2$), 206.11 (CO), 206.09 (CO), 205.77 (CO), 205.75 (CO), 202.30 (CO), 197.92 (CO), 141.95 (**C**$HCHN(CH_3)_3$), 133.05 (CH**C**$HN(CH_3)_3$), 53.88 ($CHCHN(\mathbf{C}H_3)_3$), 43.35 (1C, $CON(\mathbf{C}H_3)_2$), 34.38 (1C, $CON(\mathbf{C}H_3)_2$). ESI/MS: *m/z* = 1040 M^+, and 996 $[M - N(CH_3)_2]^+$. Elemental analysis: Calculated for $Ru_5N_2O_{14}C_{22}H_{18}$: C, 25.41%; H, 1.74%; N, 2.69%. Found: C, 25.79%; H, 1.64%; N, 2.50%. Spectral data for **4.10**: IR νCO (cm^{-1} in CH_2Cl_2): 2075(m), 2035(s), 2014(vs), 1987(w), 1971(m). ^{1}H NMR (in acetone-d_6 solvent, δ in ppm): 10.57 (C**H**$CHN(CH_3)_3$, d, $^3J_{H\text{-}H}$ = 8.8 Hz, 1H), 4.46 ($CHC\mathbf{H}N(CH_3)_3$, m, $^3J_{H\text{-}H}$ = 8.8 Hz, 1H), 3.51 ($CHCHN(C\mathbf{H}_3)_3$, s, 9H), 3.15 ($N(CH_3)_2$, s, 3H), 2.39 ($N(CH_3)_2$, s, 3H), -21.44 (μ-H, s, 1H). Elemental analysis: Calculated for $Ru_5N_2O_{13}C_{21}H_{18}\cdot 0.79\ CH_2Cl_2$: C, 24.26%; H, 1.83%; N, 2.60%. Found: C, 24.10%; H, 1.22%; N, 2.52%.

Synthesis of 4.10 from reaction of 4.9 with Me_3NO at 25 °C

10.0 mg (0.00963 mmol) of **4.9** was taken in an NMR tube in d_6-acetone solvent. 2.9 mg (0.0386 mmol) of Me_3NO was added to the solution and mixed thoroughly. The reaction mixture kept at 25 °C for 22 h. The reaction products were then separated by TLC by using hexane/methylene chloride/acetone mixture to yield in order of elution: 2.1 mg of starting material **4.9**, 1.3 mg of **4.8** (14% yield), and 4.0 mg of **4.10** (41% yield).

Conversion of 4.9 to 4.8 by the Elimination of DMF at 60 ℃

22.0 mg (0.0212 mmol) of **4.9** was dissolved in an NMR tube in d_6-acetone. The solution in the tube was then heated in a constant temperature oil bath at 60 ℃ for 9.5 h. The reaction was monitored by ^{1}H NMR spectroscopy and DMF was observed in the solution. The cluster complexes were then isolated by TLC by using hexane/methylene chloride/acetone mixture to yield in order of elution: 2.0 mg of unreacted **4.9**, and 15.0 mg of **4.8** (73% yield).

Conversion of 4.10 to 4.8 at 50 ℃

5.5 mg (0.0054 mmol) of **4.10** was dissolved an NMR tube in d_6-acetone solvent. The NMR tube was sealed with a rubber septum and degassed under nitrogen. The tube was then heated in a constant temperature oil bath at 50 ℃ for 13 h. The formation of dimethylformamide (DMF) was observed in a ^{1}H NMR spectrum of the reaction solution. Workup by TLC using methylene chloride solvent to yield 2.6 mg of **4.8** (50% yield) and 0.3 mg of unreacted **4.10**.

Addition of CO to 4.10 at 35 ℃

4.6 mg (0.0045 mmol) of **4.10** was dissolved in d_6-acetone and then transferred to an NMR tube. The NMR tube was sealed with a rubber septum and degassed under nitrogen three times. In a fume hood, CO gas at 1 atm was bubbled through the solution for 60 s. The sample was then heated at 35 ºC. Reaction progress was monitored by ^{1}H NMR spectroscopy. After 24 h, compounds **4.9** (36% yield) and **4.13** (50% yield) were observed by ^{1}H NMR spectroscopy and resonance integrations. In addition, the resonances of DMF in approximately 34% yield were also observed.

Synthesis of $Ru_5(\mu_5\text{-}C)(CO)_{13}Cl[\eta^1\text{–}E\text{–}CH{=}CH(NMe_3)](\mu\text{–}H)$, 4.11 from 4.7 plus C_2H_2 and Me_3NO

Compound **4.7** was first prepared *in situ*: 37.4 mg (0.040 mmol) of **4.5** was placed in a 100 mL three-neck flask and then dissolved in 30 mL freshly distilled dichloromethane. 20 µL of concentrated HCl (37%) was added to the solution and stirred at room temperature for 12 h. The conversion of **4.5** to **4.7** was followed by IR spectroscopy and appeared to be complete. The solvent was removed in *vacuo* and compound **4.7** was then re-dissolved in 30 mL freshly distilled dichloromethane. A steady flow of C_2H_2 (g) was then passed through the solution at 1 atm for 5 min. After this time, 6.2 mg (0.0825 mmol) of Me_3NO was added to the solution and the solution was stirred for 15 min under an atmosphere of C_2H_2 gas at 25 ºC. The products were separated by TLC by using a solvent mixture of hexane/methylene chloride and finally with acetone to yield two bands in the order of elution: 3.6 mg of **4.8** (9 % yield), and 22.9 mg of $Ru_5(\mu_5\text{-}C)(CO)_{13}Cl[\eta^1\text{–}E\text{–}CH{=}CH(NMe_3)](\mu\text{–}H)$, **4.11** (56 % yield). Spectral data for **4.11**: IR, ν_{CO} (cm^{-1} in CH_2Cl_2): 2091(w), 2060(s), 2051(vs), 2040(m), 2025(w), 2013(w), 1975(sh). ^1H NMR (in acetone-d_6 solvent, δ in ppm): 8.51 (C**H**CHN$(CH_3)_3$, d, $^3J_{H\text{-}H}$ = 14.4 Hz, 1H), 6.17 (CHC**H**N$(CH_3)_3$, d, $^3J_{H\text{-}H}$ = 14.4 Hz, 1H), 3.51 (CHCHN(C**H**$_3)_3$, s, 9H) -22.53 (µ-H, s, 1H). ESI/MS: *m/z* 996 $[M\text{-}Cl]^+$.

Synthesis of 4.8 from 4.11 at 48 ℃

12.2 mg (0.012 mmol) of **4.11** was dissolved in d_6-acetone in an NMR tube. The NMR tube was sealed with a rubber septum and vacuum degassed under nitrogen for three times. The sample was then heated at 48 ℃ in a constant temperature oil bath. The reaction progress was monitored by ^1H NMR spectroscopy. After heating for 18 h, the product was

then isolated by TLC by using a hexane/methylene chloride solvent mixture to yield 3.6 mg of **4.8** (32% yield).

Syntheses of $Ru_5(\mu_5\text{-}C)(CO)_{14}[\eta^1\text{-}E\text{-}CH{=}CH(NMe_3)]$, 4.12 and $Ru_5(\mu_5\text{-}C)(CO)_{15}[\eta^1\text{-}E\text{-}CH{=}CH(NMe_3)]$, 4.13 by addition of CO to 4.8

Reaction 1: 11.6 mg (0.0111 mmol) of **4.8** was dissolved in d_6-acetone and then transferred to an NMR tube. The NMR tube was sealed with rubber septum and degassed under nitrogen for three times. CO gas at 1 atm was bubbled through the solution for 30 s. After 22 h at 25 ℃, the reaction mixture passed through a paper filter into a vial and then the solvent removed under a flow of nitrogen. The oily residue was redissolved in a mixture of CH_2Cl_2 and hexane and filtered into a clean vial and was allowed to evaporate in air in a fume hood overnight. A small number of red crystalline plates of $Ru_5(\mu_5\text{-}C)(CO)_{14}[\eta^1\text{-}E\text{-}CH{=}CH(NMe_3)]$, **4.12** formed on the walls of vial. One of these crystals was also used for a single-crystal X-ray diffraction analysis, see below. Compound **4.8** was present on the bottom of the vial. Spectral data for **4.12**: ^{1}H NMR (in acetone-d_6 solvent, δ in ppm): 7.51 (C**H**CHN$(CH_3)_3$, d, $^3J_{H\text{-}H}$ = 12.9 Hz, 1H), 5.47 (CHC**H**N$(CH_3)_3$, d, $^3J_{H\text{-}H}$ = 12.9 Hz, 1H), 3.25 (CHCHN$(C\mathbf{H}_3)_3$, s, 9H).

Reaction 2: In a similar reaction,12.8 mg (0.0132 mmol) of **4.8** was treated with CO and filtered into a clean vial and then sealed with a rubber septum. In a fume hood, CO gas was then passed over the solution to remove the solvent by using two syringe needles (one input/one output) through the septum. Upon removal of the solvent (approx. 1h), red crystals of **4.13** remained in the vial, 11.8 mg of $Ru_5(\mu_5\text{-}C)(CO)_{15}[\eta^1\text{-}E\text{-}CH{=}CH(NMe_3)]$, **4.13** (87% yield). One of these red crystals was also used for a single-crystal X-ray diffraction analysis. Spectral data for **4.13**: IR, ν_{CO} (cm^{-1} in CH_2Cl_2): 2089(w), 2058(s),

2041(vs), 2022(s), 2014(m), 2003(s), 1986(w), 1971(w). ^{1}H NMR (in $(CD_3)_2CO$ solvent, δ in ppm): 6.01 (C**H**CHN$(CH_3)_3$, d, $^3J_{H\text{-}H}$ = 15.2 Hz, 1H), 5.59 (CHC**H**N$(CH_3)_3$, d, $^3J_{H\text{-}H}$ = 15.2 Hz, 1H), 3.16 (CHCHN$(C\mathbf{H}_3)_3$, s, 9H). Elemental analysis: Calculated for $Ru_5NO_{15}C_{21}H_{11}$: C, 24.66%; H, 1.08%; N, 1.37%. Found: C, 25.00%; H, 0.86%; N, 1.34%.

Decarbonylation of 4.13 to 4.12 and 4.8

9.2 mg of (0.0090 mmol) of **4.13** was dissolved in acetone-d_6 and then transferred to an NMR tube under nitrogen at 25 °C. The tube was closed. After 10h, the compound **4.13** was transformed to compounds **4.12** and **4.8** was 35% and 15%, respectively, as determined by ^{1}H NMR analysis. After 24h, the conversion to compounds **4.12** and **4.8** was 40% and 29%, respectively as determined by ^{1}H NMR analysis.

Synthesis of $Ru_5(\mu_5\text{-}C)(CO)_{13}[\mu\text{-}\eta^2\text{-}O{=}C(NMe_2)][\eta^1\text{-}E\text{-}(MeO_2C)C{=}C(H)(NMe_3)](\mu\text{-}H)$, 4.14. Reaction of 4.6 with $HC{\equiv}C(CO_2CH_3)$ and Me_3NO at 25 ℃

28.5 mg (0.0290 mmol) of **4.6** was dissolved in CD_2Cl_2 solvent in an NMR tube. The sample was vacuum degassed and placed under nitrogen. 8.0 μL (0.087 mmol) of methyl propiolate, $HC{\equiv}C(CO_2Me)$, was added to the solution via syringe and mixed thoroughly. 4.3 mg (0.058 mmol) of Me_3NO was then added to the solution and the tube was shaken. The color of the solution changed from yellow to brown. The reaction progress was monitored by ^{1}H NMR after each addition of reagents. The reaction began immediately after addition of Me_3NO as there was no sign of hydride resonances for the starting material after 4h at 25 °C. The solvent was removed in vacuo and the product was then isolated by TLC by using a hexane/methylene chloride/acetone solvent mixture to yield: 9.7 mg of $Ru_5(\mu_5\text{-}C)(CO)_{13}[\mu\text{-}\eta^2\text{-}O{=}C(NMe_2)][\eta^1\text{-}E\text{-}(MeO_2C)C{=}C(H)(NMe_3)](\mu\text{-}H)$, **4.14** (31%

yield). Spectral data for **4.14**: IR νCO (cm^{-1} in CH_2Cl_2): 2079(m), 2040(vs), 2022(s), 2004(w), 1978(m), 1927(vw). ^1H NMR (CD_2Cl_2, δ in ppm): 5.61 (**H**C_2CO_2Me, s, 1H), 3.83 (HC_2CO_2**Me**, s, 3H), 3.26 (N**Me**, s, 3H), 3.23 (N**Me**$_3$, s, 9H), 2.53 (s, 3H, N**Me**), -22.07 (μ-H, s, 1H). Elemental analysis: Calculated for $Ru_5N_2O_{16}C_{24}H_{20}$: C, 26.26%; H, 1.84%; N, 2.55%. Found: C, 26.43%; H, 1.70%; N, 2.50%.

Synthesis of $Ru_5(C)(CO)_{13}[\mu\text{-}\eta^2\text{-}O{=}C(NMe_2)][\mu\text{-}\eta^2\text{-}(MeO_2C)HC{=}CH]$, 4.15 by thermal elimination of NMe_3 from 4.14

12.0 mg (0.00091 mmol) of **4.14** was dissolved in benzene-d_6 in an NMR tube. The solution was then heated in a constant temperature oil bath at 80 ℃ for 4 h. The reaction was monitored by ^1H NMR spectroscopy. The products were then isolated by TLC by using a hexane/methylene chloride mixture to yield in order of elution: 1.9 mg of unreacted **4.6**, 0.6 mg of the new compound $Ru_5(\mu_5\text{-}C)(CO)_{13}[\mu\text{-}\eta^2\text{-}O{=}C(NMe_2)][\mu\text{-}\eta^2\text{-}(MeO_2C)HC{=}CH]$, **4.15** (5% yield), and 0.9 mg of the known compound $Ru_5(\mu_5\text{-}C)(CO)_{13}[\mu\text{-}\eta^2\text{-}O{=}C(NMe_2)](HNMe_2)(\mu\text{-}H)$, **4.16** (8% yield).[12] Spectral data for **4.15**: IR νCO (cm^{-1} in hexane): 2091(m), 2077(w), 2058(w), 2048(vs), 2029(s), 2022(w), 2013(w), 2000(m), 1991(w). ^1H NMR (CD_2Cl_2, δ in ppm): 11.41 ($\mu\text{–}\eta^2$-O=C(OCH_3)HC=C**H**, d, $^3J_{H\text{-}H}$ = 8.4 Hz, 1H), 6.37 ($\mu\text{–}\eta^2$-O=C(OCH_3)**H**C=CH, d, $^3J_{H\text{-}H}$ = 8.7 Hz, 1H), 3.79 ($\mu\text{–}\eta^2$-O=C(OC**H**$_3$)HC=CH, s, 3H), 3.11 ($N(CH_3)_2$, s, 3H), 2.40 ($N(CH_3)_2$, s, 3H). EI/MS *m*/*z*. M^+ = 1039.

Crystallographic Analyses

Crystals of each product suitable for single-crystal X-ray diffraction analyses were grown by slow evaporation of solvent from solutions of the pure compound in the open air except for compound **4.13**. Single crystals of **4.7** (yellow), and **4.14** (yellow) were obtained

from a hexane/methylene chloride solvent mixture at 25˚C. Single crystals of **4.8** (dark red), **4.9** (yellow), and **4.10** (yellow) were obtained from solutions in methylene chloride at 25˚C. Single crystals of **4.11** (yellow) were obtained from a solution in diethyl ether at 25˚C. Single crystals of **4.12** (orange) were obtained from a hexane/methylene chloride solvent mixture at 25˚C. Single crystals of **4.13** (red) were obtained from a CH_2Cl_2/hexane solvent mixture by slow evaporation of solvent under a slow purge of CO at 25˚C. Single crystals of **4.15** (yellow) were obtained from a solution in hexane at 25˚C. X-ray intensity data for all compounds were collected at 100(2) K by using a Bruker D8 QUEST diffractometer equipped with a PHOTON-100 CMOS area detector and an Incoatec microfocus source (Mo $K\alpha$ radiation, λ = 0.71073 Å).[14] The data collection strategy consisted of five 180° ω-scans with different φ settings, with a scan width per image of 0.5°. The crystal-to-detector distance was 5.0 cm. The raw area detector data frames were reduced, scaled and corrected for absorption effects by using the SAINT and SADABS programs. All structures were solved and refined by using the programs SHELX[15] or OLEX.[16] For all structures, all non-hydrogen atoms were refined with anisotropic displacement parameters. The hydrido ligands were located and refined by using and isotropic thermal parameter. Other hydrogen atoms were placed in geometrically idealized positions and included as riding atoms with *d*(C-H) = 0.98 Å and *U*iso(H) = 1.5*U*eq(C).

Compound **4.7** crystallized in the monoclinic system. The pattern of systematic absences in the intensity data was consistent with the space groups *C*c and *C*2/*c*. The acentric group *C*c was found by the solution program XT and was confirmed by structure solution and refinement. Subsequent checking with ADDSYM found no missed symmetry. The asymmetric unit in *C*c consists of one molecule. The hydride atom was located and

refined freely. The final absolute structure (Flack) parameter was 0.16(2), consistent with inversion twinning of the data crystal. An inversion twinning matrix was therefore included in the final refinement cycles, with the Flack parameter representing the minor twin domain volume fraction. Compound **4.8** crystallized in the monoclinic system. The pattern of systematic absences in the intensity data uniquely identified that space group as $P2_1/n$. Compound **4.10** crystallized in the monoclinic system. The pattern of systematic absences in the intensity data uniquely identified the space group as $P2_1/c$ in both cases and both were confirmed by the successful solution and refinement of the structures. The asymmetric unit of **4.10** consists of one complete molecule of $Ru_5(\mu_5\text{-}C)(CO)_{12}(\mu\text{-}\eta^2\text{-}O{=}C(NMe_2)[\mu\text{-}\eta^2\text{-}CH{=}CH(NMe_3)](\mu\text{-}H)$ molecule and one dichloromethane molecule from the crystallization solvent. The dichloromethane was initially refined as fully occupied, which resulted in abnormally large CH_2Cl_2 atomic displacement parameters and deep difference electron density holes (-2.1 e-/Å^3) at the chlorine sites. Refinement of a group occupancy for the dichloromethane lowered the *R*-values from *R*1/*wR*2 = 0.022/0.055 to 0.017/0.036 and flattened the difference map. The dichloromethane occupancy refined to 0.786(2). Hydrogen atoms H1 and H2 and the hydride atom were located and refined freely. Compound **4.11** crystallized in the monoclinic system. The pattern of systematic absences in the intensity data uniquely indicated the space group $P2_1/c$, which was confirmed by the successful solution and refinement of the structure. Compound **4.12** crystallizes in the triclinic system. The space group *P*-1 was selected and confirmed by structure solution and refinement. The asymmetric unit consists of one complete formula unit of the complex $Ru_5(\mu_5\text{-}C)(CO)_{14}[\eta^1\text{-}E\text{-}CH{=}CH(NMe_3)]$ and one molecule of dichloromethane from the crystallization solvent. The dichloromethane is

disordered with one chlorine atom occupying two positions having refined population fractions of 0.51(3)/0.49(3). Compound **4.13** crystallized in the monoclinic system. The pattern of systematic absences in the intensity data was consistent with the space group $P2_1/n$, which was confirmed by structure solution and refinement. The methyl hydrogens were allowed to rotate as a rigid group to the orientation of maximum observed electron density. The two alkene hydrogens were located and refined freely. Compound **4.14** crystallized in the monoclinic system. The pattern of systematic absences in the intensity data was consistent with the space group $P2_1/n$, which was confirmed by structure solution and refinement. Compound **4.15** crystallized in the orthorhombic system. The pattern of systematic absences in the intensity data was uniquely consistent with the space group *P*bca, which was confirmed by the successful solution and refinement of the structure. Crystal data, data collection parameters, and results of the analyses are summarized in Table 4.1-4.4.

4.3 Results

The reaction of **4.5** with C_2H_2 in the presence of Me_3NO and Me_3N at -78 ºC provided the new compound $Ru_5(\mu_5\text{-}C)(CO)_{13}[\mu\text{–}\eta^2\text{–}CHCH(NMe_3)]$, **4.8** in a low yield (5.2%). Compound **4.8** was characterized by IR, ^1H and ^{13}C NMR analyses, single-crystal X-ray diffraction analyses and elemental analyses. An ORTEP diagram of the molecular structure of compound **4.8** is shown in Figure 4.1. Compound **4.8** contains a square-pyramidal shaped Ru_5 cluster of metal atoms with a carbido ligand in the center of the square base and thirteen linear terminal carbonyl ligands distributed as shown in Figure 4.1. The most interesting ligand in **4.8** is a 2-trimethylammonioethenyl ligand, $CH{=}CH(^+NMe_3)$, that bridges the Ru2 – Ru3 edge of the cluster. The positively-charged

2-trimethylammonioethenyl ligand, CH=CH($^{+}$NMe$_3$) ligand is formally a zwitterion that is derived from a 2-trimethylammonioethenide, $^{-}$CH=CH($^{+}$NMe$_3$), that formally has a positive charge on the nitrogen atom and a negative charge on the terminal enyl carbon atom. Upon coordination, the negative charge on the carbon atom is formally transferred to the coordinated metal atom and the complex overall becomes a zwitterion with the negative charge on a metal atom, see below. The CH=CH($^{+}$NMe$_3$) ligand is similar the one recently observed in the hexaruthenium compound **4.1**.[10] It is coordinated in the σ+π coordination fashion that is well established for bridging alkenyl ligands.[17] The C1−C2 double bond is π–bonded to Ru(2), Ru2−C1 = 2.210(2) Å, Ru2−C2 = 2.243(2) Å, and σ-bonded to Ru(3), Ru3−C1 = 2.031(2) Å. The C(1) – C(2) bond length, 1.388(3) Å, is similar in length to that of the CH=CH($^{+}$NMe$_3$) ligand found in **4.1** (1.427(19) Å). Compound **4.8** is formally a zwitterion with a positive charge located on the nitrogen atom. The negative charge would be formally located on Ru(3), but this negative charge will certainly be delocalized via molecular orbitals that spread across the entire Ru$_5$ cluster.[18]

The CH=CH($^{+}$NMe$_3$) ligand in **4.8** exhibits three proton resonances in the ^{1}H NMR spectrum: a pair of doublet at 11.23 ppm and 5.87 ppm, $^{3}J_{H-H}$ = 10.0 Hz, due to the protons on C(1) and C(2), respectively. The latter resonance shows some small unresolved coupling from the nitrogen atom N(1). The N-methyl resonance, a singlet at 3.64 ppm, is shifted downfield due to the positive charge on the nitrogen atom. The ^{13}C NMR spectrum of **4.8** exhibits three resonances for the CH=CH^{+}NMe$_3$ ligand: 170.41 ppm for C(1), 94.80 ppm for C(2) and 54.65 ppm for the methyl groups; the latter is a 1:1:1 triplet, $^{1}J_{C-N}$ = 16 Hz, due to coupling to the nitrogen atom. The bridging CH=CH^{+}NMe$_3$ ligand in **4.8** serves formally as a four electron donors; thus, the complex overall achieves a total of 74 cluster

valence electrons which is in accord with the observation of a square-pyramidal shaped cluster of five metal atoms.[18]

In recent studies, we have synthesized the pentaruthenium complex **4.6** from the reaction of **4.5** with DMF.[12] Compound **4.6** contains an opened, wingtip bridged, butterfly cluster of five ruthenium atoms with a dimethylformamido ligand bridging one of the nonbonded pairs of metal atoms. For comparisons with the reactivity to **4.5**, the reaction of **4.6** with C_2H_2 in the presence of Me_3NO at 25 °C was investigated. This reaction provided two compounds $Ru_5(\mu_5\text{-}C)(CO)_{13}[\mu\text{–}\eta^2\text{–}O{=}C(NMe_2)][\eta^1\text{–}E\text{–}CH{=}CH(NMe_3)](\mu\text{–}H)$, **4.9**[13] (48% yield) and $Ru_5(\mu_5\text{-}C)(CO)_{12}[\mu\text{-}\eta^2\text{-}O{=}C(NMe_2)][\mu\text{-}\eta^2\text{-}CHCH(NMe_3)](\mu\text{-}H)$, **4.10** (6.4% yield). Compound **4.9** was characterized by IR, ^1H and ^{13}C NMR analyses, single-crystal X-ray diffraction analyses and elemental analyses. An ORTEP diagram of the molecular structure of compound **4.9** is shown in Figure 4.2. The metal cluster of compound **4.9** is structurally similar to that of its parent **4.6** having an open, wing-tip bridged butterfly cluster of metal atoms with a carbido ligand in the center and a dimethylformamido ligand bridging one of the nonbonded pairs of metal atoms. Compound **4.9** contains thirteen linear terminal carbonyl ligands distributed as shown in Figure 4.2, but the most interesting ligand in **4.9** is a 2-trimethylammonioethenyl ligand, η^1-*E*-$CH{=}CH(^+NMe_3)$, that is terminally-coordinated to the wing-tip bridged Ru atom, Ru(4), in the equatorial coordination site that is trans to the metal atom Ru(3). NMe_3 was not added to this reaction, so the NMe_3 group that is present in the $CH{=}CH(^+NMe_3)$ ligand is believed to be derived solely from the Me_3NO after it reacted with a CO ligand in **4.6** to form CO_2 and NMe_3. The Ru4 - C4 distance is 2.074(4) Å in length. There is an *E*-stereochemistry at the C – C double bond, C4 - C5 = 1.286(5) Å, and are both distances are slightly shorter

than the corresponding distances, Ru - C = 2.097(2) Å and C1-C2 = 1.306(3) Å, in the terminally-coordinated *E*-CH=CH($^{+}$NMe$_3$) ligand in compound **4.2**.[10] The ethenyl hydrogen atoms appear as two deshielded doublets at δ = 8.25 and 5.90 with a large coupling constant, $^{3}J_{H\text{-}H}$ = 14 Hz, that is consistent with the observed *E*-stereochemistry at the C – C double bond. There is a bridging hydrido ligand H1 on the Ru(1) – Ru(2) bond that exhibits the expected high-field resonance shift, δ = -22.07. The alkenyl carbon atoms, C4 and C5, exhibit significant upfield shifts for their resonances in the ^{13}C NMR spectrum, δ = 141.95 and 133.05, respectively, relative to those observed for the carbon atoms of the bridging CH=CH($^{+}$NMe$_3$) ligand in **4.8**. The terminally-coordinated CH=CH($^{+}$NMe$_3$) ligand in **4.9** serves as a 2-electron donor and the Ru$_5$ cluster achieves a 76-electron configuration as expected for the observed open-square pyramidal structure of metal atoms.[18] Compound **4.9** is formally a zwitterion with a positive charge on the nitrogen atom N(2) and a negative charge on Ru(4).

The coproduct **4.10** has been characterized by IR, ^{1}H NMR, single-crystal X-ray diffraction and elemental analyses. An ORTEP diagram of the molecular structure of compound **4.10** is shown in Figure 4.3. The metal cluster of compound **4.10** is structurally similar to that of its parent **4.6** having an open, wing-tip bridged butterfly cluster of metal atoms with a carbido ligand in the center and a dimethylformamido ligand bridging one of the nonbonded pairs of metal atoms. Compound **4.10** contains only twelve CO ligands and one 2-trimethylammonioethenyl ligand, CH=CH($^{+}$NMe$_3$), that is a η^2-σ+π coordinated, bridging ligand across the metal atoms Ru(2) and Ru(3). The Ru – C bond distances to the coordinated double bond C1 and C2, Ru2 - C1 = 2.0580(15) Å, Ru3 - C1 = 2.2176(15) Å and Ru3 - C2 = 2.2449(15) Å, are very similar to those in **4.8**. The coordinated double

bond in **4.10**, C1 - C2 = 1.394(2) Å, is significantly longer than the uncoordinated C – C double bond in **4.9**, 1.280(5) Å but it is very similar to the coordinated C – C double bond in **4.8**, 1.388(3) Å. The ethenyl hydrogen atoms appear as two deshielded doublets at δ = 10.57, $^{3}J_{H-H}$ = 8.8 Hz) and 4.46, $^{3}J_{H-H}$ = 8.8 Hz). There is a formal positive charge on the nitrogen atom N(1) and the resonance of the N-methyl groups is appropriately deshielded, δ = 3.51. There is a bridging hydrido ligand H(12) on the Ru(1) – Ru(4) bond that exhibits the usual high-field resonance shift, δ = -21.44.

Compound **4.10** is formally a zwitterion with a positive charge on the nitrogen atom N(1) and a negative charge that is formally on Ru(2), but this negative charge may delocalize between Ru(2) and Ru(3). The bridging CH=CH($^{+}$NMe$_3$) ligand in **10** serves as a 4-electron donor and the cluster achieves a 76-electron configuration as expected for the observed open-square pyramidal structure of metal atoms.[18]

Compound **4.9** was converted to **4.8** (73 % yield) by thermal elimination of the dimethylformamido ligand and the hydrido ligand as DMF when solutions of **4.9** were heated to 60 ºC. Compound **4.9** can also be converted to **4.10** in a good yield (41 %) by decarbonylation with Me$_3$NO at 25 ºC. Small amounts of **4.8** (14 %) were also formed in this reaction. Interestingly, **4.10** was easily converted to **4.8** in a good yield (50 %) by very mild heating (50 ºC/13h) of solutions. It thus appears that **4.10** is an intermediate en route to **4.8** from **4.9**. Compound **4.10** was converted back to **4.9** (36% yield) by addition of CO at 35 ºC, together with formation of the new compound Ru$_5$(μ_5-C)(CO)$_{15}$[η^1-*E*-CH=CH(NMe$_3$)], **4.13** (50 % yield) which is a product of the addition of CO to **4.8**, see below.

Because of the interesting results obtained from the reactions of **4.6** with C_2H_2, we also investigated the reaction of compound **4.7** with C_2H_2 and Me_3NO. Compound **4.7** was first reported Johnson and Lewis many years ago,[11] but it has not yet been structurally characterized. For the purpose of knowing its exact structure and for comparisons with the products that we have obtained from it, see below, we have performed a single-crystal X-ray diffraction analysis of **4.7** that we have included in this chapter. An ORTEP diagram of the molecular structure of compound **4.7** is shown in Figure 4.4. The metal cluster of **4.7** is structurally similar to that of **4.6** and **4.9** having an open, wing-tip bridged butterfly cluster of metal atoms with a carbido ligand in the center. The hydrido ligand bridges the hinge bond of the Ru_4 butterfly, Ru(1) – Ru(2), and the chloro ligand Cl(1) is a terminally-coordinated ligand in an axial position on the wing-tip bridging metal atom Ru(4), Ru(4) – Cl(1) = 2.4211(9) Å. Compound **4.7** contains fifteen linear terminal carbonyl ligands distributed as shown in Figure 4.4.

The reaction of **4.7** with C_2H_2 at 1 atm in the presence of Me_3NO for 15 min in CH_2Cl_2 solvent yielded two products: compound **4.8** (9 % yield), and the new compound $Ru_5(\mu_5\text{-}C)(CO)_{14}Cl[\eta^1\text{-}\textit{E}\text{-}CH{=}CH(NMe_3)](\mu{-}H)$, **4.11** (56 % yield). Compound **4.11** was characterized by IR, ^{1}H NMR, single-crystal X-ray diffraction and mass spectral analyses. An ORTEP diagram of the molecular structure of compound **4.11** is shown in Figure 4.5. The metal cluster of compound **4.11** is structurally similar to that of **4.6**, **4.9** and **4.10** having an open, wing-tip bridged butterfly cluster of metal atoms with a carbido ligand in the center. Compound **4.11** contains fourteen linear, terminal carbonyl ligands and one 2-trimethylammonioethenyl, $CH{=}CH(^+NMe_3)$, ligand that is terminally coordinated, to the wing-tip bridging ligand, Ru(4), Ru4−C1 = 2.091(3) Å in an equatorial coordination site.

The C – C double bond distance, C1 - C2 = 1.292(5) Å, is very similar to that found for the terminally-coordinated C(H)=C(H)$^{+}$NMe$_3$ ligand in **4.9**. The chloro ligand, Cl(1), is axially coordinated to Ru(4), Ru(4) - Cl(1) = 2.4612(10) Å. The ^{1}H NMR spectrum of **4.11** exhibits two doublets for the ethenyl hydrogen atoms: δ = 8.51 and 6.17 with a large coupling constant, $^{3}J_{H-H}$ = 14.4 Hz that is consistent with the structurally observed *E*-stereochemistry. The bridging hydrido ligand H(12) exhibits the usual high-field resonance shift, δ = -22.53.

Compound **4.11** is also a zwitterion with a positive charge on atom N(1) and a formal negative charge on atom Ru(4). The C(H)=C(H)$^{+}$NMe$_3$ ligand in **4.11** serves as a 2-electron donor and the cluster achieves a 76-electron configuration as expected for the observed open-square pyramidal structure of metal atoms.[18] When heated to 48 ^{o}C for 18 h, compound **4.11** was converted to compound **4.8** in 32% yield by elimination of CO and a reductive-elimination of HCl, formation of a metal – metal bond between that atoms Ru(1) and Ru(4) and conversion of the CH=CH($^{+}$NMe$_3$) ligand into a σ+π coordinated, bridging ligand.

Treatment of compound **4.8** with CO at 25 ^{o}C yielded two new products: Ru$_5$(C)(CO)$_{14}$[η^{1}-*E*-CH=CH(NMe$_3$)], **4.12** and Ru$_5$(C)(CO)$_{15}$[η^{1}-*E*-CH=CH(NMe$_3$)], **4.13** by the addition of one and two equivalents of CO. Compound **4.12** is an unstable intermediate en route to **4.13**. It can be isolated in very small amounts by allowing filtered solutions of the reaction mixture to evaporate in a vial in the open air in a fume hood. Small red plates of **4.12** will form on the walls of the vial. Solutions of **4.12** eventually convert back fully to **4.8** by loss of CO, but the crystals are more stable and can be analyzed by single-crystal X-ray diffraction analysis at low temperature, see below. Compound **4.12**

adds CO to yield **4.13** at room temperature. Compound **4.13** is stable in solution only when maintained under an atmosphere of CO. Compound **4.13** can be obtained as pure red crystals in a good yield (87%) by filtering the reaction solutions and then carefully removing the reaction solvent under a flow of CO in a fume hood. Solutions of **4.13** slowly lose CO and convert back to **4.8** via **4.12** under an atmosphere of nitrogen. Red crystals of **4.13** were also suitable for single-crystal X-ray diffraction analysis.

ORTEP diagrams of the molecular structures of compounds **4.12** and **4.13** are shown in Figures 4.6 and 4.7, respectively. The metal cluster of compound **4.12** has the shape of a square pyramid like **4.8** with a carbido ligand in the center of the square base. There is a terminally-coordinated C(H)=C(H)$^{+}$NMe$_3$ ligand in an axial position on the basal metal atom Ru(1), Ru1−C1 = 2.041(11) Å. The C – C double bond is short, C1−C2 = 1.290(15) Å, and has an *E*-conformation as observed for the terminal CH=CH($^{+}$NMe$_3$) ligands in **4.9** and **4.11**. Compound **4.12** contains fourteen linear, terminal carbonyl ligands distributed about the cluster as shown in Figure 4.6. The apical - basal Ru – Ru bond, Ru1−Ru5 = 2.9034(13) Å, *trans* to the CH=CH($^{+}$NMe$_3$) ligand is significantly longer than the three other apical – basal Ru – Ru bonds, Ru2−Ru5 = 2.8487(13) Å, Ru3−Ru5 = 2.7771(13) Å, Ru4−Ru5 = 2.8068(12) Å which suggests that the CH=CH($^{+}$NMe$_3$) ligand has a stronger *trans*-effect than a CO ligand.

The ^{1}H NMR spectrum of **4.12** exhibits two doublets for the ethenyl hydrogen atoms: δ = 7.51 and 5.47 with a large coupling constant, $^{3}J_{H\text{-}H}$ = 12.9 Hz, as expected for the *E*-stereochemistry observed in the solid state structure. Compound **4.12** is also a zwitterion with a positive charge on the nitrogen atom N(1) and a negative charge formally

on Ru(1). The metal cluster of compound **4.12** contains a total of 74 valence electrons which is consistent with its square-pyramidal structure.

The structure of **4.13** consists of an opened square-pyramidal cluster (a wing-tipped bridged butterfly cluster) of five Ru atoms similar to that observed for compounds **4.9**, **4.10** and **4.11**. There is a terminally-coordinated CH=CH($^{+}$NMe$_3$) ligand in an axial position on the wing-tip, bridging metal atom Ru(4), Ru4 - C1 = 2.1183(17) Å. The C – C double bond length, C1 - C2 = 1.315(2) Å, is similar to that observed for the terminal CH=CH($^{+}$NMe$_3$) ligands in compounds **4.9**, **4.11** and **4.12**. There are a number of examples of nucleophile-induced opening of square-pyramidal Ru$_5$ cluster complexes by the addition of donor ligands to a basal positioned metal atom.[11,19] The ethenyl hydrogen atoms on C(1) and C(2) in **4.13** appear as two mutually-coupled, deshielded doublets at δ = 6.01 and 5.59 with a large coupling constant, $^{3}J_{H\text{-}H}$ = 15.2 Hz, that is consistent with the *E*-stereochemistry observed in the solid state. Compound **4.13** is a zwitterion with a positive charge on the nitrogen atom N(1) and a formal negative charge on the metal atom Ru(4). The metal cluster of compound **4.13** contains a total of 76 valence electrons which is consistent with its observed open structure.

The reaction of **4.6** with methyl propiolate, HC≡C(CO$_2$Me), and Me$_3$NO in CH$_2$Cl$_2$ at 25 °C yielded the new compound Ru$_5$(μ$_5$-C)(CO)$_{13}$[μ-η^2-O=C(NMe$_2$)][η^1-*E*-(MeO$_2$C)C=CH(NMe$_3$)](μ-H), **4.14** in 31% yield. Compound **4.14** was characterized by IR and ^{1}H NMR spectroscopy and structurally by single-crystal X-ray diffraction analysis. An ORTEP diagram of the molecular structure of compound **4.14** is shown in Figure 4.8. Compound **4.14** is very similar to that of **4.9** having a wing-tipped bridged butterfly Ru$_5$ cluster of metal atoms and a bridging dimethylformamido ligand, but it has a terminally-

coordinated, 1-methoxycarbonyl, 2-trimethylammonioethenyl ligand, η^1-*E*-(1-MeO_2C)C=C(H)(2-$^+NMe_3$), in an equatorial coordination site on Ru(1) in the location of the 2-trimethylammonioethenyl ligand found in **4.9**. The Ru(1) – C(2) distance, 2.1401(18) Å is slightly longer than the corresponding Ru – C bond in **4.9**, 2.097(2) Å. The C – C double bond in the (MeO_2C)C=C(H)$^+NMe_3$ ligand has an *E*-conformation at the double bond and its bond length, C1−C2 = 1.320(3) Å, is similar to that observed in **4.9**, **4.11**, **4.12** and **4.13**.

The resonances of the single ethenyl hydrogen atom on C(1) and the trimethylammonio methyl groups in **4.14** are deshielded at 5.61 ppm and 3.23 ppm, respectively, in the ^{1}H NMR spectrum. A hydrido ligand bridges the Ru(2) – Ru(3) bond in **4.14** and exhibits the expected high-field resonance shift at -22.07 ppm. Compound **4.14** is a zwitterion with a positive charge on the nitrogen atom N2 and a formal negative charge on the metal atom Ru(1). The metal cluster of compound **4.14** contains a total of 76 valence electrons which is consistent with its observed open structure.

When a solution of **4.14** dissolved in benzene-d_6 was heated to 80 ℃ for 4 h, two products were formed in low yields: a new compound $Ru_5(\mu_5\text{-}C)(CO)_{13}[\mu\text{-}\eta^2\text{-}O{=}C(NMe_2)][\mu\text{-}\eta^2\text{-}(MeO_2C)HC{=}CH]$, **4.15** (5% yield), and the known compound $Ru_5(\mu_5\text{-}C)(CO)_{13}[\mu\text{-}\eta^2\text{-}O{=}CNMe_2](HNMe_2)(\mu\text{-}H)$, **4.16** (8% yield).[12] An ORTEP diagram of the molecular structure of compound **4.15** is shown in Figure 4.9. Compound **4.15** was formed from **4.14** by elimination of the NMe_3 grouping from the (MeO_2C)C=C(H)($^+NMe_3$) ligand. The compound contains an open Ru_5 cluster with an approximately trigonal bipyramidal carbido ligand in the center. There is an η^2-bridging dimethylformamido ligand across the open Ru(1) - Ru(2) edge of the cluster, and there is a bridging η^2-(CH_3O_2C)(H)C=C(H)

ligand across the open Ru(1) - Ru(4) edge of the cluster. The carbonyl oxygen atom O(2) of the methoxycarbonyl group asymmetrically bridges the two metal atoms Ru(1) and Ru(4), Ru1−O2 = 2.396(4) Å, Ru4−O2 = 2.199(4) Å. The carbonyl C – O bond is short, C(6) - O2 = 1.245(8) Å, indicating that it still contains considerable double bond character. There is a hydrogen atom on C(5) that was presumably derived from the bridging hydrido ligand in **4.14** by a C – H bond-forming step. The C4 − C5 bond is also short, 1.364(10) Å, and is formally a C – C double bond. The hydrogen atoms on C(4) and C(5) are significantly deshielded in the ^{1}H NMR spectrum, δ = 11.41 and 6.37 with a coupling constant, $^{3}J_{H\text{-}H}$ = 8.4 Hz, that is consistent with the observed *Z*-conformation at the double bond. Compound **4.15** contains a total of 78 cluster valence electrons which is in accord with an electron-precise metal cluster of five metal atoms (n) having six metal – metal bonds (m), according to the formula 18n – 2m. The side product **4.16** was obtained previously by the thermal decomposition of **4.6** which generates Me_2NH by decarbonylation of the dimethylformamido ligand.[12]

4.4 Discussion

A summary of our studies of the reactions of **4.5**, **4.6** and **4.7** with ethyne in the presence of Me_3NO is shown in Scheme 4.1.

The reaction of the square-pyramidal Ru_5 cluster complex **4.5** with the decarbonylation agent Me_3NO in the presence C_2H_2 and NMe_3 provided a low yield of the square-pyramidal Ru_5 cluster complex **4.8** containing a 2-trimethylammonioethenyl ligand, $CH{=}CH^{+}NMe_3$, that bridges a basal edge of a square-pyramidal Ru_5 cluster. Further investigations showed that the open cluster complexes **4.6** and **4.7** provided good yields of open Ru_5 cluster complexes **4.9** and **4.11**, respectively, containing terminally-coordinated,

2-trimethylammonioethenyl ligands having *E*-stereochemistry located on the wing-tip bridging ruthenium atom of the Ru_4C portion of clusters. Compounds **4.9** and **4.11** were both converted to **4.8** thermally in good yields by the elimination of DMF from **4.9** and CO and HCl from **4.11**. An important intermediate, **4.10**, was observed in the conversion of **4.9** to **4.8**. Compound **4.10** was formed from **4.9** by a Me_3NO-induced decarbonylation with a conversion of the terminally-coordinated η^1-CH=CH$^+$NMe$_3$ ligand into a η^2-bridging ligand by coordination of its C – C double bond, a prerequisite to the formation of **4.8**. Compound **4.10** reacted CO to regenerate **4.9** in 36 % yield at 35 ºC in 24 h by adding one CO ligand and by converting the η^2-CH=CH$^+$NMe$_3$ ligand back into a terminal-coordinated η^1-CH=CH$^+$NMe$_3$ ligand. Compound **4.13** was also formed in 50 % yield in this reaction. Compound **4.13** was presumably formed by conversion of some of the **4.9** to **4.8** by loss of DMF (also observed as a reaction product) and subsequent addition of CO to yield **4.13** via **4.12**, see below. It was observed previously that the bridging η^2-trimethylammonioethenyl ligand in **4.1** could be converted to a terminally-coordinated η^1-trimethylammonioethenyl ligand in complex **4.2** by the addition of CO to **4.1** at 25 ºC, eq. (4.1).[10]

It was also observed in a separate reaction that the η^2-bridging CH=CH$^+$NMe$_3$ ligand in **4.8** was converted into a terminally-coordinated, η^1-CH=CH$^+$NMe$_3$ ligand by CO addition; in fact, two CO addition products were obtained. The first one **4.12** was formed by the addition of only one equivalent of CO to **4.8** and it consists of a square-pyramidal cluster of five ruthenium atoms with a terminally-coordinated η^1-CH=CH$^+$NMe$_3$ ligand bonded to one of the Ru atoms in the base of the square pyramid. The second CO addition product **4.13** was formed by a cluster opening addition of CO to the first one, **4.12**, by

cleavage of the axial-basal Ru – Ru bond to the η^1-CH=CH$^+$NMe$_3$ substituted Ru atom. Compounds **4.12** and **4.13** are both unstable in solution in the absence of a CO atmosphere and they both revert back to **4.8** in high yield by loss of CO.

A summary of our reactions of **4.6** with methyl propiolate, HC≡CCO$_2$Me, is shown schematically in Scheme 4.2. The reaction of **4.6** with a combination of methyl propiolate and Me$_3$NO yielded the complex **4.14** containing a terminally-coordinated, 2-trimethylammonio(1-methyoxycarbonyl)ethenyl, η^1-*E*-1-(MeO$_2$C)C=C(H)(2-$^+$NMe$_3$), ligand. The η^1-*E*-(1-CO$_2$Me)C=C(H)(2-$^+$NMe$_3$) ligand in **4.14** is structurally similar to η^1-*E*-1-(MeO$_2$C)C=C(H)(2-$^+$NMe$_3$) ligand found in the complex Ru$_6$C(CO)$_{16}$[η^1-*E*-(1-(MeO$_2$C)C=C(H)(2-$^+$NMe$_3$)], **4.17**[10] which contains an uncoordinated C – C double bond of similar length, 1.304(7) Å. Note: the (MeO$_2$C)C=C(H)(2-$^+$NMe$_3$) ligands in **4.14** and **4.17** were both formed by the addition of the NMe$_3$ molecule to the unsubstituted end of the methyl propiolate, presumably for steric reasons. The mechanism of this coupling has not yet been established.

When a solution of **4.14** was heated to 80 ºC, it eliminated the NMe$_3$ group from the 1-(MeO$_2$C)C=C(H)(2-$^+$NMe$_3$) ligand to yield the compound **4.15**. This process presumably proceeded through an unobserved intermediate containing an alkyne ligand that promptly coupled with the hydrido ligand to yield the observed alkenyl ligand, μ-η^2-HC=C(H)(CO$_2$Me), that subsequently inserted the oxygen of its carbonyl group into one of the Ru – Ru bonds to form the O-bridged carbonyl group, thus, completing the formation of **4.15**. An η^2-HC=C(H)(CO$_2$Me) ligand obtained by a β-CH activation on the vinyl group of methyl acrylate in a reaction with Ru$_5$(μ_5-C)(CO)$_{15}$ was also observed in the Ru$_5$ complex Ru$_5$(μ_5-C)(CO)$_{14}$[η^2-O=C(OMe)CH=CH](μ-H), but in this case, the ligand is

coordinated as a chelate to only one ruthenium atom of the cluster.[20] π-Coordinated bridging η^3-HC=C(H)(CO_2Me) ligands were found in the complexes $Ru_5(\mu_5$-C)$(CO)_{12}(C_2H_4)[\mu$-η^3-O=C(OMe)CHCH]$(\mu$-H)[20] and $Ru_5(\mu_5$-C)$(CO)_{12}[H_2CC(H)CO_2Me][\mu$-$\eta^3$-O=C-(OMe)CHCH]$(\mu$-H)[21] that were obtained from reactions of $Ru_5(\mu_5$-C)$(CO)_{14}[\eta^2$-O=C(OMe)CH=CH]$(\mu$-H) with Me_3NO and ethylene or $H_2C_2(H)CO_2Me$, respectively.

The side product, $Ru_5(\mu_5$-C)$(CO)_{13}[\mu$-η^2-O=C(NMe_2)]($HNMe_2$)$(\mu$-H), **4.16** was also formed in a low yield the thermal transformation of **4.14**. We have shown previously that Me_2NH is formed by decarbonylation of the dimethylformamido ligand in **4.6**.[12] A similar formation of Me_2NH from a dimethylformamido ligand **4.14** accompanied by the complete elimination of the 1-(MeO_2C)C=C(H)(2-$^+NMe_3$) ligand in another molecule of **4.14** and an addition of Me_2NH could have yielded the small amounts of the **4.16** observed in this reaction.

4.5 Conclusion

In this work the first procedures for the synthesis of zwitterionic pentaruthenium carbonyl complexes containing bridging- and terminally-coordinated 2-trimethylammonioethenyl ligands have been established. The bridging trimethylammonioethenyl ligands adopt a σ+π, η^2- coordination of the C – C double bond to two neighboring metal atoms. The bridging and terminally-coordinated trimethylammonioethenyl ligands can be interconverted by the addition and elimination of CO ligands to and from the metal atoms. One zwitterionic pentaruthenium carbonyl complex containing a 1-methyoxycarbonyl-substituted, 2-trimethylammonioethenyl ligand, 1-(MeO_2C)C=C(H)(2-$^+NMe_3$) was obtained from the reaction of **4.6** with methyl

propiolate. The C-N bond in the 1-(MeO_2C)C=C(H)(2-$^+NMe_3$) ligand was cleaved thermally and the NMe_3 group was eliminated from the complex to yield complex **4.15** containing a bridging [μ-η^2-HC=C(H)(CO_2Me)] alkenyl ligand formed by transfer of the hydrido ligand in **4.14** to the resultant alkyne ligand.

4.6 References

1. (a) Wittig, G.; Schollkope, U. *Chem. Ber.-Rec*. **1954**, *87*, 1318 - 1330. (b) Wittig, G.; Haag, W. *Chem. Ber.-Rec.* **1955**, *88*, 1654 - 1666. (c) Bart, J. C. J. *J. Chem. Soc. (B)*, **1969**, 350 – 365.
2. (a) Trost, B. M.; Melvin, L. S., "Sulfur Ylides. Emerging Synthetic Intermediates", Academic Press, New York, **1975**. (b) Neuhaus, J. D.; Oost, R.; Merad, J.; Maulide, N. *Top. Curr. Chem*. **2018**, 376, 15. (c) Lu, L.-Q.; Li, T.-R.; Wang, Q.; Xiao, W.-J. *Chem. Soc. Rev*. **2017**, 46, 4135−4149. (d) Zhang, Y.; Wang, J. *Coord. Chem. Rev*. **2010**, 254, 941−953. (e) Burtoloso, A. C. B.; Dias, R. M. P.; Leonarczyk, I. A. *Eur. J. Org. Chem*. **2013**, 5005−5016. (f) Li, A.-H.; Dai, L.-X.; Aggarwal, V. K. *Chem. Rev*. **1997**, 97, 2341−2372.
3. (a) Maryanoff, B. E.; Reitz, A. B. *Chem. Rev*. **1989**, 89, 863 - 927. (b) Johnson, A. W.; Kaska, W. C.; Starzewski, K. A. O.; Dixon, D. *Ylides and Imines of Phosphorus*; Wiley: New York, **1993**. (c) Dequina, H. J.; Schomaker. J. M. *Trends in Chem*. **2020**, 2, 874 – 887. (d) Huang, Y.; Liao, J.; Wang, W.; Liu, H.; Guo, H. *Chem. Commun*. **2020**, 56, 15235 – 15281.
4. Selected examples include: (a) Pattacini, R.; Jiez, S.; Braunstein, P. *Chem. Commun*. **2009**, 890 – 892. (b) Engelter, C.; Moss, J.R.; Niven, M.L.; Nassimbeni, L.R.; Reid, G. *J. Organomet. Chem*. **1982**, 232, C78 – C80. (c) Kermode, N. J.; Lappert, M.F.; Skelton, B. W.; White, A. H.; Holton, J. *J. Organomet. Chem*. **1982**, *228*, C71 - C75.

(d) Azam, K. A.; Frew, A. A.; Lloyd, B. R.; Manojlovic-Muir, L.; Muir, K. W.; Puddephatt, R. J. *Organometallics* **1985**, 4, 1400 – 1406. (e) Churchill, M. R.; Wasserman, H. J. *Inorg. Chem.* **1982**, *21*, 3913-3916. (f) Toupet, L.; Weinberger, B.; Abbayes, H. D.; Gross, U. *Acta Crystallogr. Sect.C: Cryst.Struct.Commun*. **1984**, *40*, 2056 – 2058. (g) Moss, J. R.; Niven, M. L.; Stretch, P. M. *Inorg. Chim. Acta*, **1986**, *119*, 177 – 186. h) Porter, L. C.; Knachel H.; Fackler, Jr., J. P. *Acta Cryst.* **1987**, C43, 1833-1835. i) Uson, R.; Laguna, A.; Uson, A.; Jones, P. G.; Meyer-Base, K. *J. Chem. Soc., Dalton Trans*. **1988**, 341 – 345. j) Uson, R.; Laguna, A.; Laguna, M.; Gimeno, M. C.; Pablo, A.; Jones, P. G.; Meyer-Base, K., Erdbrugger, C. F. *J. Organomet. Chem*., **1987**, *336*, 461 – 468. k) Hoover J. F.; Stryker, J. M. *Organometallics* **1988**, *7*, 2082 – 2084. l) Cerrada, E.; Gimeno, M. C.; Laguna, A.; Laguna, M.; Orera, V.; Jones, P. G. *J. Organomet. Chem*. **1996**, *506*, 203 – 210.

5. Selected examples include: (a) O'Connor, E. J.; Helquist, P. *J. Am. Chem. Soc.* **1982**, *104*, 1869 - 1874. (b) Hevia, E., Perez, J., Riera, V.; Miguel, D. *Organometallics* **2002**, *21*, 5312 - 5319. (c) Leoni, P.; Marchetti, F.; Paoletti, M. *Organometallics* **1997**, *16,* 2146 - 2151. (d) Kilbourn, B. T.; Felix, D. ***J. Chem. Soc. A,*** **1969**, 163 - 168. (e) Fackler, Jr., J. P., Paparizos, C. *J. Am. Chem. Soc*. **1977**, *99*, 2363 - 2364. (f) Vicente, J.; Chicote, M. -T.; Abrisqueta, M. D.; Alvarez-Falcon, M. M.; de Arellano, M. C. R.; Jones, P. G. *Organometallics* **2003**, *22*, 4327 – 4333.

6. (a) Lappas, D.; Hoffman, D. M.; Folting, K.; Huffman, J. C. *Angew. Chem., Int. Ed. Engl*. **1988**, *27*, 587 – 589. (b) Hoffman, D. M.; Huffman, J. C.; Lappas, D.; Wierda, D. A. *Organometallics* **1993**, *12*, 4312 – 4320. (c) Rogers, R. D.; Alt, H. G.; Maisel, H. E. *J. Organomet. Chem.* **1990**, *381*, 233-238. (d) Chin, C. S.; Lee, S.; Oh, M.; Won,

G.; Kim, M.; Park, Y. J. *Organometallics* **2000,** *19,* 1572 - 1577. (e) Chin, C. S.; Park, Y.; Kim, J.; Byeongno Lee, B. *J. Chem. Soc., Chem. Commun*. **1995**, 1495 – 1496. (f) Takats, J.; Washington, J.; Santarsiero, B. D. *Organometallics* **1994**, *13*, 1078 - 1080. (g) Yang, K.; Bott, S. G. Richmond, M. G. *J. Organomet. Chem.* **1996**, *516*, 65 – 80. (h) Bott, S. G.; Shen, H.; Senter, R. A.; Richmond, M. G. *Organometallics* **2003,** *22,* 1953 - 1959.

7. (a) Boland-Lussier, B. F.; Churchill, M. R.; Hughes, R. P.; Rheingold, A. L. *Organometallics* **1982**, *1*, 628 – 634. (b) Hogarth, G.; Knox, S. A. R., Lloyd, B. R.; Macpherson, K. A.; Morton, D. A. V.; Orpen, A. G. *J. Chem. Soc., Chem. Commun*. **1988**, 360 – 362. (c) Bamber, M.; Froom, S. F. T.; Green, M.; Schulz, M., Werner, H. *J. Organomet. Chem.,* **1992**, *434*, C19-C25.
8. Henrick K.; McPartlin, M.; Deeming, A. J.; Hasso, S.; Manning, P. *J. Chem Soc., Chem. Commum.* 1**982**, 899 – 906.
9. (a) Chin, C. S.; Lee, H.; Oh, M. *Organometallics* **1997**, *16,* 816 – 818. (b) Chin, C. S.; Cho, H.; Won, G.; Oh, M. *Organometallics* **1999**, *18,* 4810-4816.
10. Adams, R. D.; Smith, M. D.; Wakdikar, N. D. *Inorg. Chem.* **2020**, *59*, 1513 – 1521.
11. Johnson, B. F. G.; Lewis, J.; Nicholls, J. N.; Puga, J.; Raithby, P. R.; Rosales, M. J.; McPartlin, M.; Clegg, W. *J. Chem. Soc., Dalton Trans*. **1983**, 277−290.
12. Adams, R. D.; Tedder, J. D. *Inorg. Chem*. **2018**, 57, 5707 – 5710.
13. Tedder, J. D. **2018**, 'Studies of the Activation of Carbon-Gold and Carbon-Hydrogen Bonds by the Pentaruthenium Carbonyl Cluster $Ru_5(\mu_5\text{-}C)(CO)_{15}$', PhD thesis, University of South Carolina, Columbia.

14. APEX3 Version 2016.5-0 and SAINT Version 8.37A. Bruker AXS, Inc. Madison, WI, USA.

15. SHELXT: Sheldrick, G.M., SHELXT - Integrated space-group and crystal-structure determination. *Acta Cryst*. **2015**, *A71*, 3-8.

16. **OLEX2**: a complete structure solution, refinement, and analysis program. Dolomanov, O. V., Bourhis, L. J., Gildea, R. J., Howard J. A. K. and Puschmann, H. *J. Appl. Cryst.* **2009**, *42*, 339 - 341.

17. (a) Orpen, A. G.; Pippard, D.; Sheldrick, G. M.; Rouse, K. D. *Acta Cryst.* **1978**, *B34*, 2466-2472. (b) Iggo, J. A.; Mays, M. J.; Raithby, P. R. *J. Chem. Soc., Dalton Trans*. **1983**, 205 – 215. (c) Dennett, J. N. L.; Knox, S. A. R.; Anderson, K. M.; Charmant, J. P. H.; Orpen. A. G. *Dalton Trans*., **2005**, 63–73. (d) Adams, R. D.; Dhull, P.; Rassolov, V.; Wong, Y. O. *Inorg. Chem.* **2016**, *55*, 10475 – 10483. (e) Adams, R. D.; Wong, Y. O. *J. Organomet. Chem*. **2015**, *784*, 109−113. (f) Adams, R. D.; Dhull, P.; Kaushal, M.; Smith, M. D. *J. Organomet. Chem.* **2019**, *902*, 120969. (g) Zhao, X.; Yang, D.; Zhang, Y.; Wang, B.; Qu, J. *Chem. Commun.* **2018**, *54*, 11112 – 11115.

18. (a) Mingos, D. M. P.; May, A. S., in *The Chemistry of Metal Cluster Complexes*. Shriver, D. F.; Kaesz, H. D.; Adams, R. D., VCH Publishers, New York, 1990, Ch. 2. (b) Mingos, D. M. P., Polyhedral Skeletal Electron Pair Approach, *Acc. Chem. Res.* **1984**,*17*, 311-319.

19. (a) Farrar, D. H.; Poë, A. J.; Zheng, Y. *J. Am. Chem. Soc.* **1994**, *116*, 6252-6261. (b) Freeman, G.; Ingham, S. L.; Johnson, B. F. G.; McPartlin, M.; Scowen, I. J. *J. Chem. Soc., Dalton Trans.*, **1997**, 2705–2711.

20. Adams, R. D.; Smith, M. D.; Tedder, J. D.; Wakdikar, N. D. *Inorg. Chem.* **2019**, 58, 8357−8368.

21. Adams, R. D.; Prince, C.; Smith, M. D.; Tedder, J. D.; Wakdikar, N. D. *J. Organomet. Chem.* **2019**, 901, 120938.

Table 4.1 Crystal data, data collection parameters for compounds **4.7** and **4.8**.

Compound	**4.7**	**4.8**
Empirical formula	$Ru_5ClO_{15}C_{16}H$	$Ru_5O_{13}NC_{19}H_{11}$
Formula weight	973.97	966.64
Crystal system	Monoclinic	Monoclinic
Lattice parameters		
a (Å)	9.9659(3)	9.8955(5)
b (Å)	15.2615(4)	17.7522(9)
c (Å)	15.8976(4)	14.8801(7)
α (deg)	90.00	90.00
β (deg)	90.800(1)	104.191(2)
γ (deg)	90.00	90.00
V (Å^3)	2417.70(11)	2534.2(2)
Space group	Cc	$P2_1/n$
Z value	4	4
ρ_{calc} (g/cm^3)	2.676	2.534
μ (Mo Kα) (mm^{-1})	3.234	2.978
Temperature (K)	100(2)	100(2)
$2\Theta_{max}$ (°)	59.97	60.12
No. Obs. ($I > 2\sigma(I)$)	6594	7440
No. parameters	339	352
Goodness of fit (GOF)	1.044	1.001
Max. shift in cycle	0.001	0.002
Residuals[a]: R1; wR2	0.0158/0.0327	0.0235/0.0362
Absorption correction, Max/min	Multi-scan 0.4932/0.4118	Multi-scan 0.6212/0.5607
Largest peak in Final Diff. Map (e$^-$/Å^3)	0.81	0.665

[a] $R1 = \Sigma_{hkl}(||F_{obs}| - |F_{calc}||)/\Sigma_{hkl}|F_{obs}|$; $wR2 = [\Sigma_{hkl}w(|F_{obs}| - |F_{calc}|)^2/\Sigma_{hkl}wF^2_{obs}]^{1/2}$; $w = 1/\sigma^2(F_{obs})$; $GOF = [\Sigma_{hkl}w(|F_{obs}| - |F_{calc}|)^2/(n_{data} - n_{vari})]^{1/2}$.

Table 4.2 Crystal data, data collection parameters for compounds **4.10** and **4.11**.

Compound	**4.10**	**4.11**
Empirical formula	$Ru_5N_2O_{13}C_{21}H_{18}.0.79CH_2Cl_2$	$Ru_5ClO_{14}NC_{20}H_{12}$
Formula weight	1078.48	1031.11
Crystal system	Monoclinic	Monoclinic
Lattice parameters		
a (Å)	10.0186(3)	19.5839(4)
b (Å)	13.0484(4)	9.2500(2)
c (Å)	25.0707(8)	17.2594(4)
α (deg)	90.00	90.00
β (deg)	92.605(1)	110.136(1)
γ (deg)	90.00	90.00
V (Å^3)	3274.02(17)	2935.46(11)
Space group	$P2_1/c$	$P2_1/c$
Z value	4	4
ρ_{calc} (g/cm^3)	2.188	2.333
μ (Mo Kα) (mm^{-1})	2.442	2.669
Temperature (K)	100(2)	301(2)
$2\Theta_{max}$ (°)	61.06	54.992
No. Obs. ($I > 2\sigma(I)$)	9374	5935
No. parameters	416	385
Goodness of fit (GOF)	1.094	1.061
Max. shift in cycle	0.002	0.001
Residuals[a]: R1; wR2	0.0171/0.0344	0.0241/0.0483
Absorption correction, Max/min	Multi-scan 0.6949/0.6448	Multi-scan 0.7456/ 0.6633
Largest peak in Final Diff. Map (e$^-$/Å^3)	0.86	0.54

[a] $R1 = \Sigma_{hkl}(||F_{obs}| - |F_{calc}||)/\Sigma_{hkl}|F_{obs}|$; $wR2 = [\Sigma_{hkl}w(|F_{obs}| - |F_{calc}|)^2/\Sigma_{hkl}wF^2_{obs}]^{1/2}$; $w = 1/\sigma^2(F_{obs})$; $GOF = [\Sigma_{hkl}w(|F_{obs}| - |F_{calc}|)^2/(n_{data} - n_{vari})]^{1/2}$.

Table 4.3 Crystal data, data collection parameters for compounds **4.12** and **4.13**.

Compound	**4.12**	**4.13**
Empirical formula	$Ru_5O_{14}NC_{20}H_{11}.CH_2Cl_2$	$Ru_5O_{15}NC_{21}H_{11}$
Formula weight	1079.57	1022.66
Crystal system	Triclinic	Monoclinic
Lattice parameters		
a (Å)	8.4918(6)	12.1141(5)
b (Å)	12.8814(8)	15.6769(7)
c (Å)	15.0684(10)	15.3058(7)
α (deg)	75.407(2)	90.00
β (deg)	74.613(2)	91.997(2)
γ (deg)	86.010(2)	90.00
V (Å^3)	1537.92(18)	2905.0(2)
Space group	*P*-1	$P2_1/n$
Z value	2	4
ρ_{calc} (g/cm^3)	2.331	2.338
μ (Mo Kα) (mm^{-1})	2.673	2.610
Temperature (K)	100(2)	100(2)
$2\Theta_{max}$ (°)	50.11	65.214
No. Obs. ($I > 2\sigma(I)$)	4227	9613
No. parameters	401	391
Goodness of fit (GOF)	1.213	1.111
Max. shift in cycle	0.000	0.003
Residuals[a]: R1; wR2	0.0684/0.1109	0.0193/0.0381
Absorption correction, Max/min	Multi-scan 0.0434/0.0230	Multi-scan 0.4950/0.3979
Largest peak in Final Diff. Map (e$^-$/Å^3)	0.99	1.10

[a] $R1 = \Sigma_{hkl}(||F_{obs}| - |F_{calc}||)/\Sigma_{hkl}|F_{obs}|$; $wR2 = [\Sigma_{hkl}w(|F_{obs}| - |F_{calc}|)^2/\Sigma_{hkl}wF^2_{obs}]^{1/2}$; $w = 1/\sigma^2(F_{obs})$; $GOF = [\Sigma_{hkl}w(|F_{obs}| - |F_{calc}|)^2/(n_{data} - n_{vari})]^{1/2}$.

Table 4.4 Crystal data, data collection parameters for compounds **4.14** and **4.15**.

Compound	**4.14**	**4.15**
Empirical formula	$Ru_5O_{16}N_2C_{24}H_{20}$	$Ru_5O_{16}NC_{21}H_{11}$
Formula weight	1097.77	1038.66
Crystal system	Monoclinic	Orthorhombic
Lattice parameters		
a (Å)	15.0536(5)	17.1417(13)
b (Å)	11.4280(4)	16.2241(13)
c (Å)	19.3564(7)	20.9215(17)
α (deg)	90.00	90.00
β (deg)	95.781(2)	90.00
γ (deg)	90.00	90.00
V (Å^3)	3313.0(2)	5818.5(8)
Space group	$P2_1/n$	*P*bca
Z value	4	8
ρ_{calc} (g/cm^3)	2.201	2.371
μ (Mo Kα) (mm^{-1})	2.300	2.611
Temperature (K)	100(2)	100(2)
$2\Theta_{max}$ (°)	60.026	51.594
No. Obs. ($I > 2\sigma(I)$)	8595	4588
No. parameters	435	391
Goodness of fit (GOF)	1.048	1.114
Max. shift in cycle	0.004	0.001
Residuals[a]: R1; wR2	0.0174/0.0319	0.0369/0.0955
Absorption correction, Max/min	Multi-scan 0.6212/0.5585	Multi-scan 0.7453/0.6551
Largest peak in Final Diff. Map (e$^-$/Å^3)	0.50	2.03

[a] $R1 = \Sigma_{hkl}(||F_{obs}| - |F_{calc}||)/\Sigma_{hkl}|F_{obs}|$; $wR2 = [\Sigma_{hkl}w(|F_{obs}| - |F_{calc}|)^2/\Sigma_{hkl}wF^2_{obs}]^{1/2}$; $w = 1/\sigma^2(F_{obs})$; $GOF = [\Sigma_{hkl}w(|F_{obs}| - |F_{calc}|)^2/(n_{data} - n_{vari})]^{1/2}$.

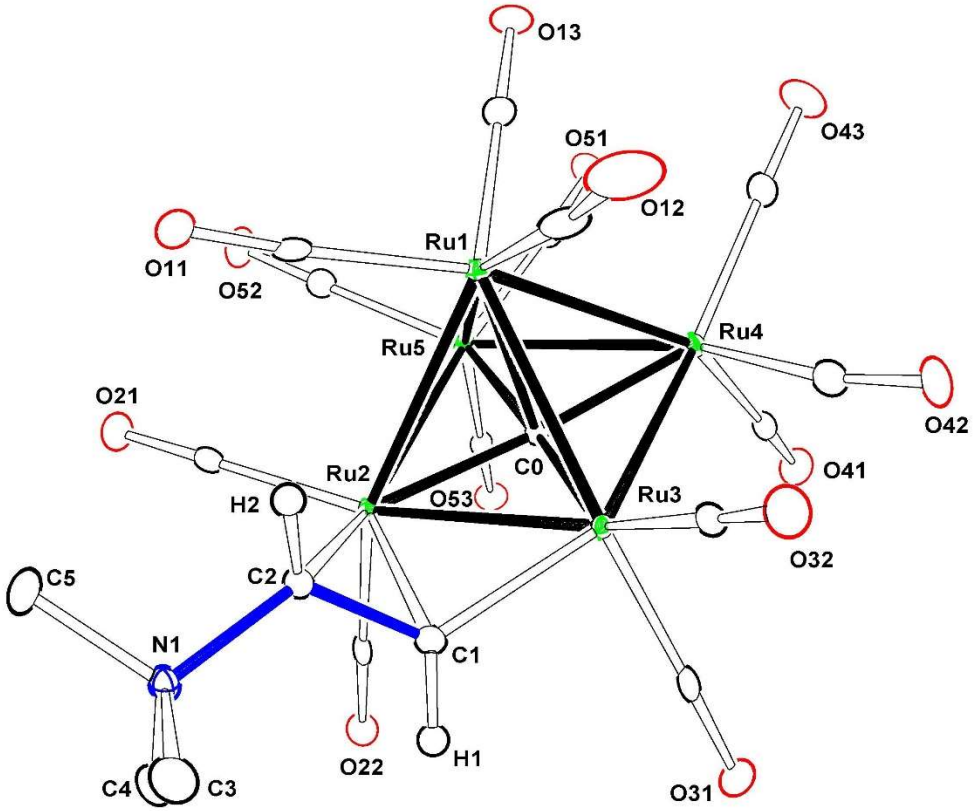

Figure 4.1 An ORTEP diagram of the molecular structure of $Ru_5(\mu_5\text{-}C)(CO)_{13}[\mu\text{-}\eta^2\text{-}HC{=}CH\text{-}N(CH_3)_3]$, **4.8** showing 40% thermal ellipsoid probability. Methyl hydrogen atoms have been omitted for clarity. Selected interatomic bond distances (Å) are as follows: Ru1−Ru2 = 2.8338(3), Ru1−Ru3 = 2.8903(3), Ru1−Ru4 = 2.8026(3), Ru1−Ru5 = 2.7795(3), Ru2−Ru3 = 2.7047(3), Ru2−Ru5 = 2.8795(3), Ru3−Ru4 = 2.8690(3), Ru4−Ru5 = 2.8859(3), Ru1−C0 = 2.134(2), Ru2−C0 = 2.024(2), Ru3−C0 = 2.022(2), Ru4−C0 = 1.993(2), Ru5−C0 = 2.004(2), Ru2−C1 = 2.210(2), Ru2−C2 = 2.243(2), Ru3−C1 = 2.031(2), C1−C2 = 1.388(3), C2−N1 = 1.516(3).

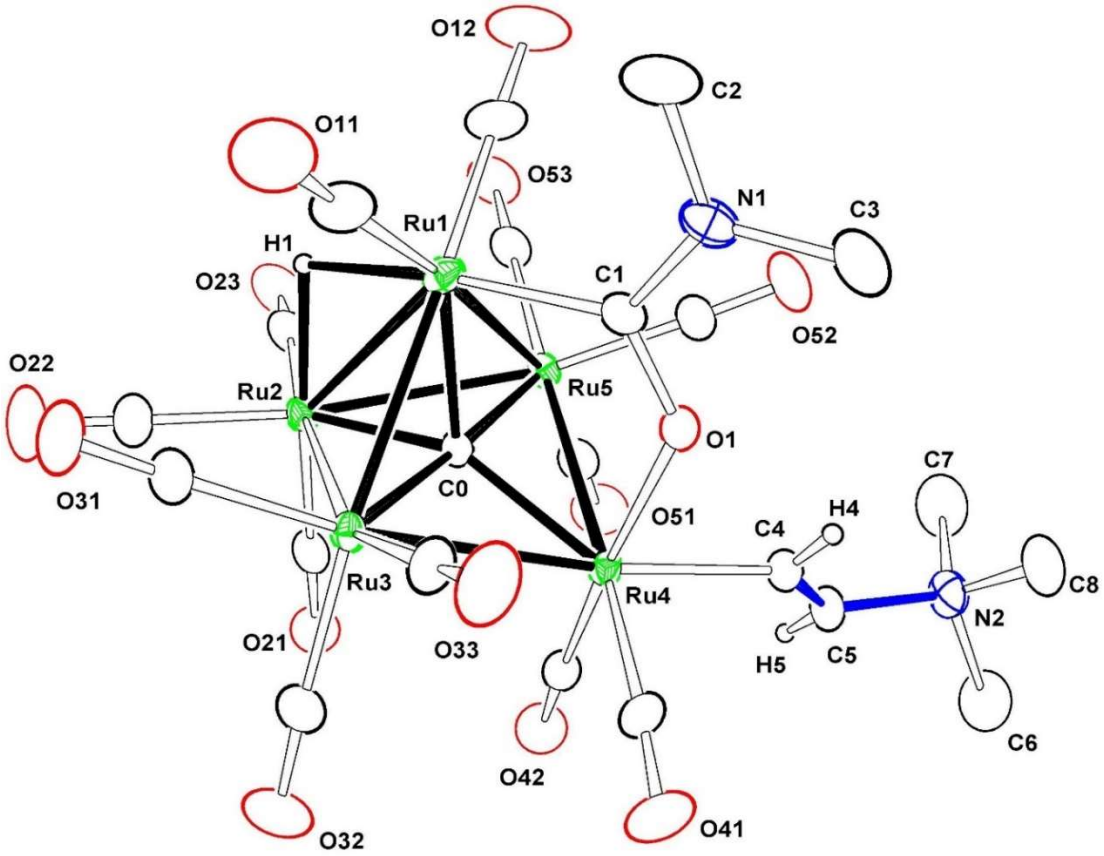

Figure 4.2 An ORTEP diagram of the molecular structure of $Ru_5(\mu_5\text{-}C)(CO)_{13}[\mu\text{-}\eta^2\text{-}O{=}C(NMe_2)][\eta^1\text{-}E\text{-}CH{=}CH(NMe_3)](\mu\text{-}H)$, **4.9**, showing 20% thermal ellipsoid probability.[13] Selected interatomic bond distances (Å) are as follow: Ru1-Ru3 = 2.8176(4), Ru1-Ru5 = 2.8275(4), Ru1-Ru2 = 2.9580(4), Ru2-Ru5 = 2.8635(4), Ru2-Ru3 = 2.8479(4), Ru3-Ru4 = 2.9145(4), Ru4-Ru5 = 2.9087(4), Ru1-H1 = 2.07(4), Ru2-H1 = 2.01(4), Ru4-C4 = 2.074(3), Ru1-C1 = 2.089(4), Ru4-O1 = 2.114(2), C1-O1 = 1.276(4), C4-C5 = 1.286(5), C5-N2 = 1.503(5), Ru1-C0 = 2.071(3), Ru2-C0 = 2.101(3), Ru3-C0 = 1.982(3), Ru4-C0 = 2.068(3), Ru5-C0 = 1.979(3).

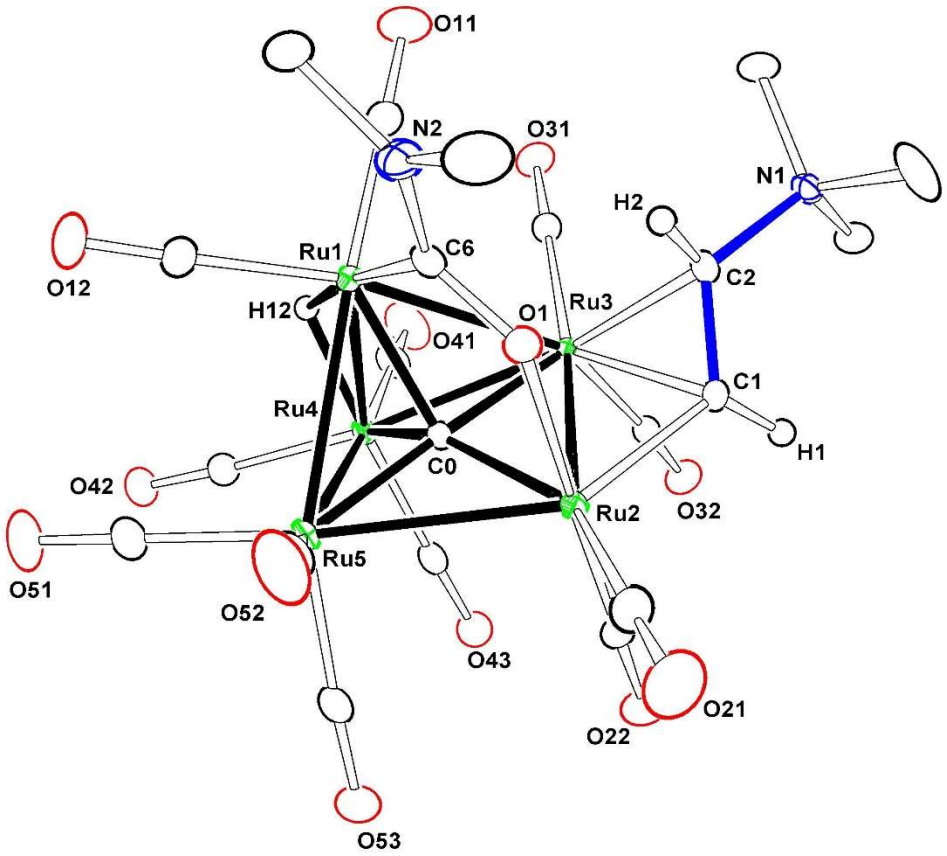

Figure 4.3 An ORTEP diagram of the molecular structure of $Ru_5(\mu_5\text{-}C)(CO)_{12}(\mu\text{-}\eta^2\text{-}O{=}CN(CH_3)_2)(\mu\text{-}\eta^2\text{-}CH{=}CHNMe_3)(\mu\text{-}H)$, **4.10**, showing 40% thermal ellipsoid probability. Selected interatomic bond distances (Å) are as follow: Ru1-Ru3 = 2.88374(18), Ru1-Ru4 = 2.86257(19), Ru1-Ru5 = 2.85533(18), Ru2-Ru3 = 2.74363(17), Ru2-Ru5 = 2.93192(19), Ru3-Ru4 = 2.84052(19), Ru4-Ru5 = 2.91228(19), Ru1-C0 = 2.0448(15), Ru2-C0 = 2.0675(15), Ru3-C0 = 1.9798(15), Ru4-C0 = 2.0898(15), Ru5-C0 = 1.9625(15), Ru1-C6 = 2.0661(17), O1-C6 = 1.2814(19), Ru2-O1 = 2.1135(11), Ru2-C1 = 2.0580(15), Ru3-C1 = 2.2176(15), Ru3-C2 = 2.2449(15), C1-C2 = 1.394(2), N1-C2 = 1.520(2).

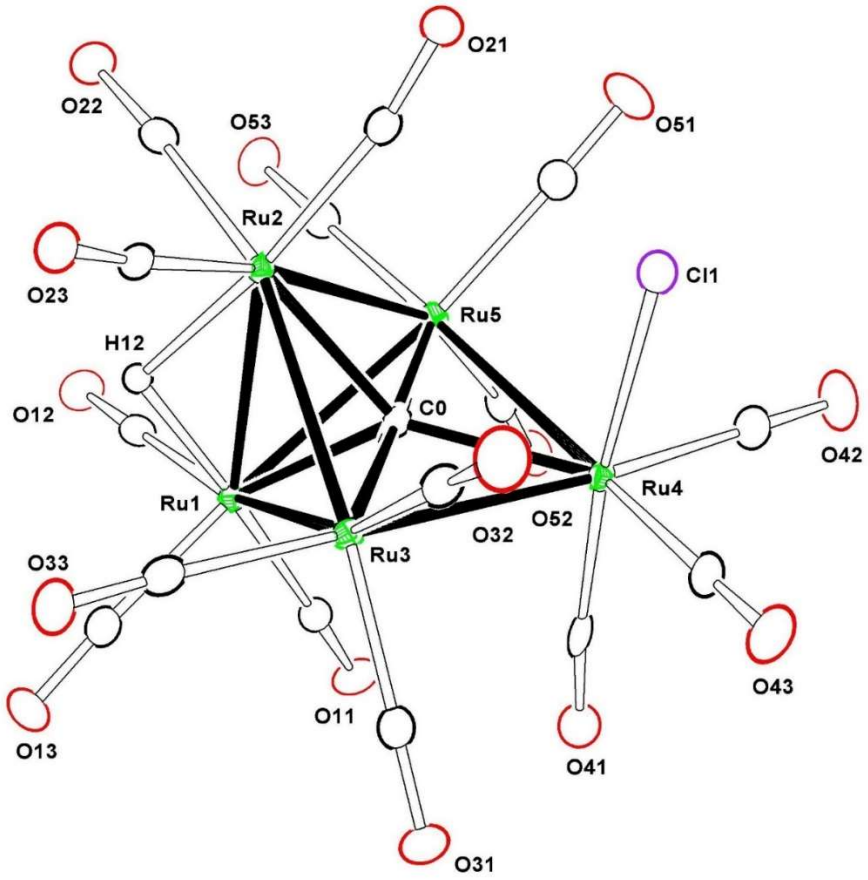

Figure 4.4 An ORTEP diagram of the molecular structure of $Ru_5(\mu_5\text{-}C)(CO)_{15}Cl(\mu\text{-}H)$, **4.7** showing 40% thermal ellipsoid probability. Selected interatomic bond distances (Å) are as follows: Ru1−Ru2 = 2.8349(4), Ru1−Ru3 = 2.8757(4), Ru1−Ru5 = 2.8379(4), Ru2−Ru3 = 2.8601(4), Ru2−Ru5 = 2.8529(4), Ru3−Ru4 = 2.8909(4), Ru4−Ru5 = 2.9429(4), Ru1−C0 = 2.115(4), Ru2−C0 = 2.106(3), Ru3−C0 = 1.961(4), Ru4−C0 = 2.117(4), Ru5−C0 = 1.960(4), Ru4−Cl1 = 2.4211(9).

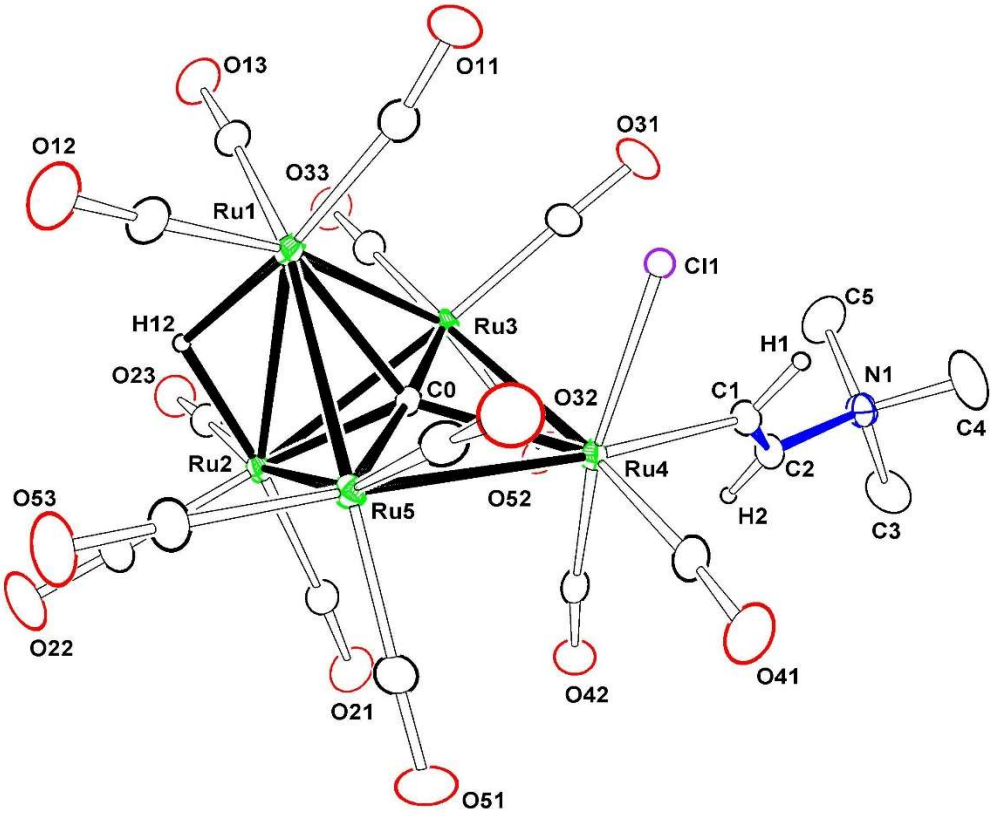

Figure 4.5 An ORTEP diagram of the molecular structure of $Ru_5C(CO)_{14}[\eta^1$-*E*-$HC{=}CHN(CH_3)_3]Cl(\mu$-H), **4.11** showing 15% thermal ellipsoid probability. Methyl hydrogen atoms have been omitted for clarity. Selected interatomic bond distances (Å) are as follows: Ru1−Ru2 = 2.8350(4), Ru1−Ru3 = 2.8413(4), Ru1−Ru5 = 2.8658(4), Ru2−Ru3 = 2.8447(3), Ru2−Ru5 = 2.8521(4), Ru3−Ru4 = 2.9626(3), Ru4−Ru5 = 2.9530(3), Ru1−C0 = 2.122(3), Ru2−C0 = 2.127(3), Ru3−C0 = 1.960(3), Ru4−C0 = 2.141(3), Ru5−C0 = 1.964(3), Ru4−Cl1 = 2.4612(10), Ru4−C1 = 2.091(3), C1−C2 = 1.292(5), C2−N1 = 1.514(4).

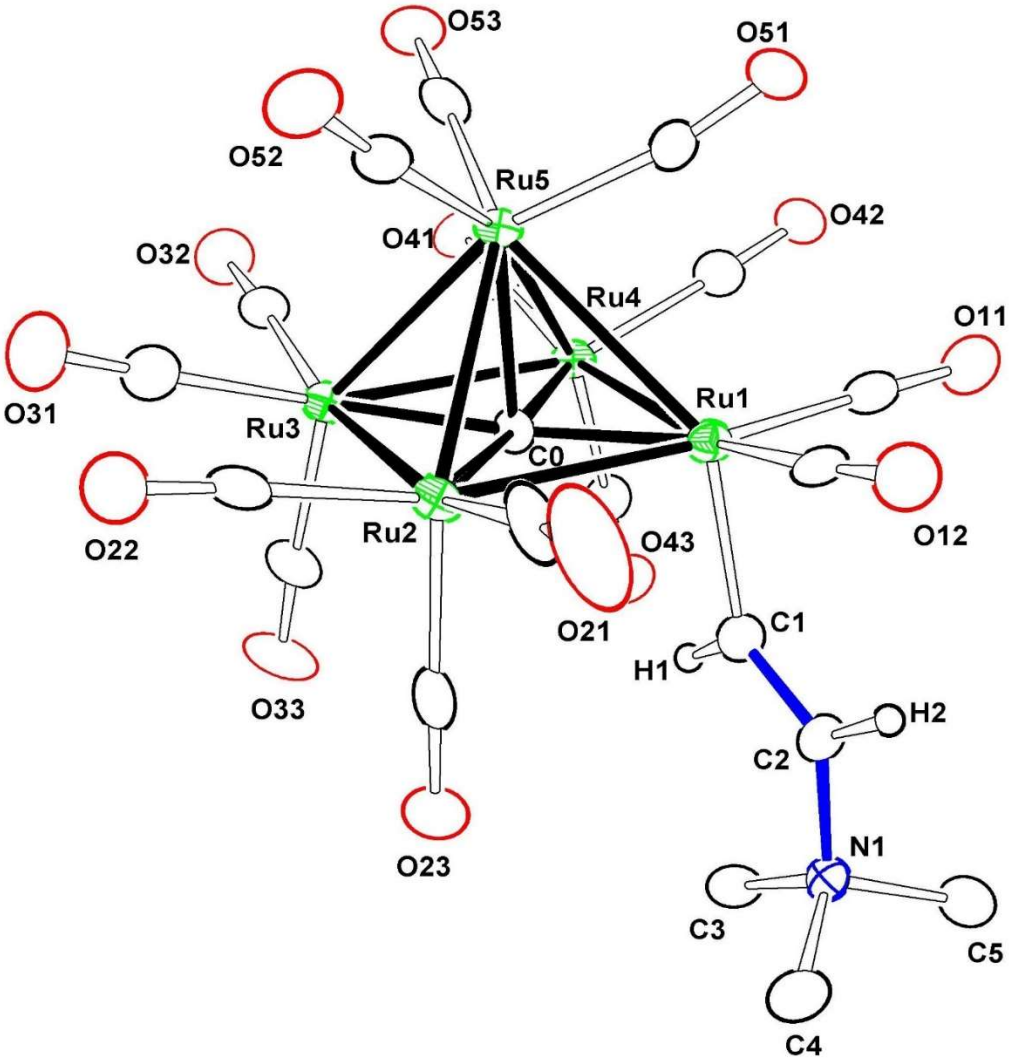

Figure 4.6 An ORTEP diagram of the molecular structure of $Ru_5(\mu_5\text{-}C)(CO)_{14}(\eta^1\text{-}E\text{-}CH{=}CHNMe_3)$, **4.12** showing 35% thermal ellipsoid probability. Selected interatomic bond distances (Å) are as follow: Ru1−Ru2 = 2.8548(14), Ru1−Ru4 = 2.8737(13), Ru1−Ru5 = 2.9034(13), Ru2−Ru3 = 2.8472(13), Ru2−Ru5 = 2.8487(13), Ru3−Ru4 = 2.8616(14), Ru3−Ru5 = 2.7771(13), Ru4−Ru5 = 2.8068(12), Ru1−C0 = 2.037(11), Ru2−C0 = 2.039(10), Ru3−C0 = 2.053(11), Ru4−C0 = 1.970(10), Ru5−C0 = 2.090(11), Ru1−C1 = 2.041(11), C1−C2 = 1.290(15), N1−C2 = 1.505(14).

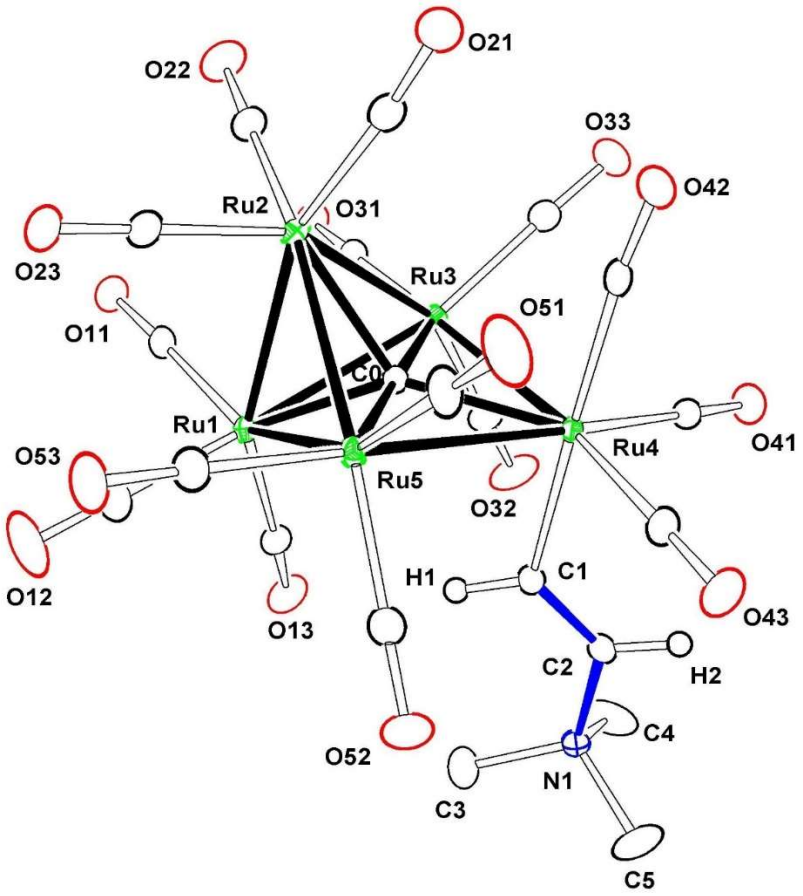

Figure 4.7 An ORTEP diagram of the molecular structure of $Ru_5(\mu_5\text{-}C)(CO)_{15}(\eta^1\text{-}E\text{-}CH{=}CHNMe_3)$, **4.13**, showing 40% thermal ellipsoid probability. Selected interatomic bond distances (Å) are as follow: Ru1-Ru2 = 2.7060(2), Ru1-Ru3 = 2.8718(2), Ru1-Ru5 = 2.8928(2), Ru2-Ru3 = 2.8793(2), Ru2-Ru5 = 2.8716(2), Ru3-Ru4 = 2.8996(2), Ru4-Ru5 = 2.90372(19), Ru1-C0 = 2.0917(15), Ru2-C0 = 2.0959(15), Ru3-C0 = 1.9601(15), Ru4-C0 = 2.1580(15), Ru5-C0 = 1.9617(15), Ru4-C1 = 2.1183(17), C1-C2 = 1.315(2), N1-C2 = 1.504(2).

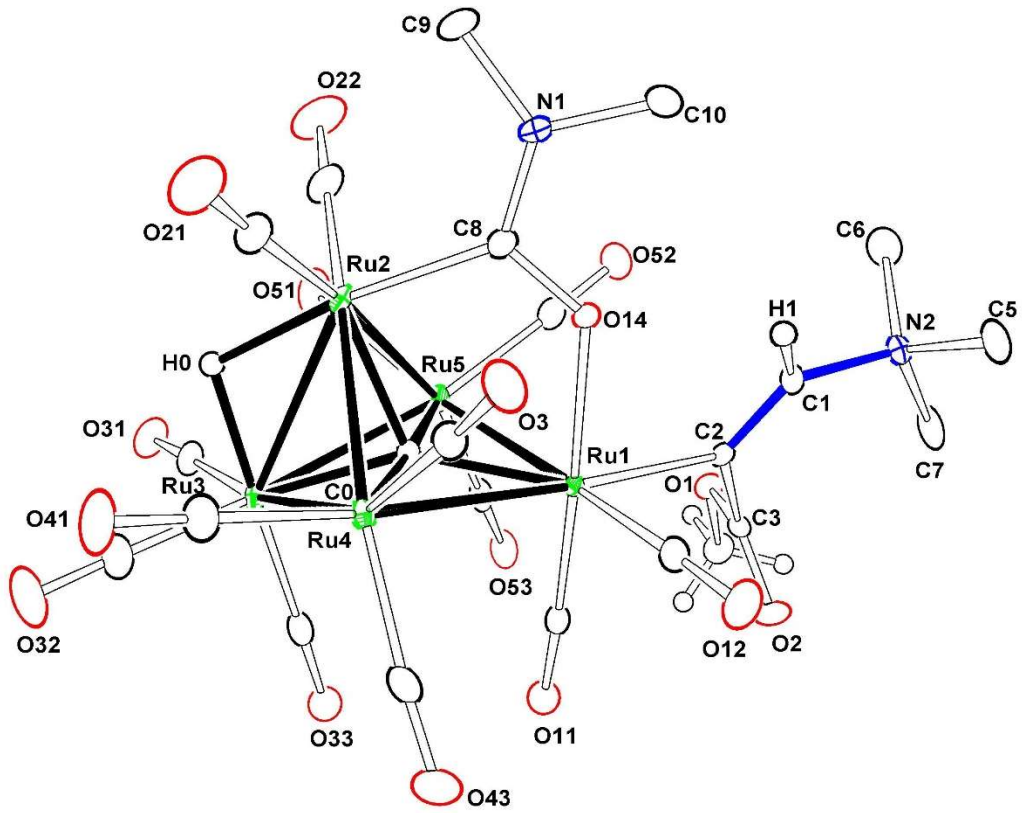

Figure 4.8 An ORTEP diagram of the molecular structure of $Ru_5(\mu_5\text{-}C)(CO)_{13}[\mu\text{-}\eta^2\text{-}O{=}CN(CH_3)_2](\mu\text{-}H)[\eta^1\text{-}HC_2(CO_2CH_3)N(CH_3)_3]$, **4.14** showing 40% thermal ellipsoid probability. Selected interatomic bond distances (Å) are as follows: Ru1−Ru4 = 2.8817(2), Ru1−Ru5 = 2.9036(2), Ru2−Ru3 = 2.8782(2), Ru2−Ru4 = 2.8157(2), Ru2−Ru5 = 2.8317(2), Ru3−Ru4 = 2.8734(2), Ru3−Ru5 = 2.8613(2), Ru1−C0 = 2.0622(18), Ru2−C0 = 2.0545(19), Ru3−C0 = 2.1076(18), Ru4−C0 = 1.9890(18), Ru5−C0 = 1.9705(18), Ru2−C8 = 2.0762(19), C8−N1 = 1.351(2), C8−O14 = 1.285(2), Ru1−O14 = 2.1214(13), Ru1−C2 = 2.1401(18), C2−C1 = 1.320(3), C1−N2 = 1.502(2), N2−C5 = 1.502(3), N2−C6 = 1.491(3), N2−C7 = 1.498(3), C2−C3 = 1.479(3).

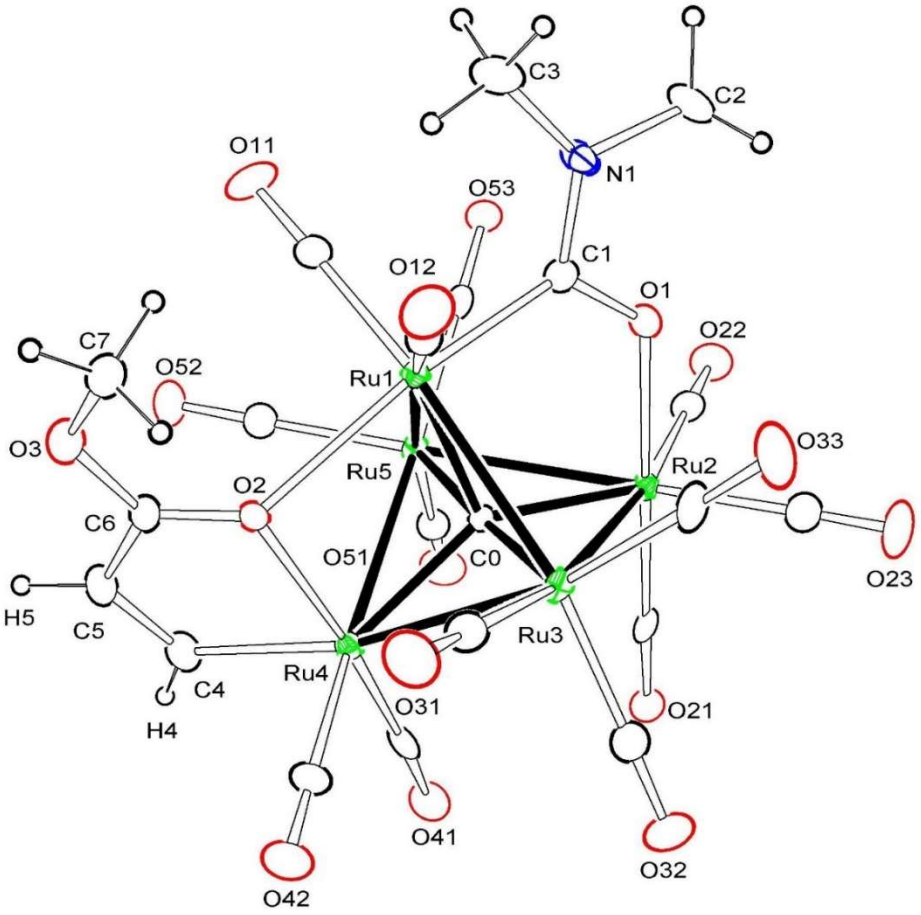

Figure 4.9 An ORTEP diagram of the molecular structure of $Ru_5(\mu_5\text{-}C)(CO)_{13}[\mu\text{-}\eta^2\text{-}O{=}CN(CH_3)_2][\mu\text{-}\eta^2\text{-}(CH_3O_2C)HC{=}CH]$, **4.15** showing 30% thermal ellipsoid probability. Selected interatomic bond distances (Å) are as follows: Ru1−Ru3 = 2.8591(7), Ru1−Ru5 = 2.8493(7), Ru2−Ru3 = 2.8453(7), Ru2−Ru5 = 2.8516(7), Ru3−Ru4 = 2.8959(7), Ru4−Ru5 = 2.9195(7), Ru1−C0 = 2.106(6), Ru2−C0 = 2.108(6), Ru3−C0 = 1.950(6), Ru4−C0 = 2.098(6), Ru5−C0 = 1.960(6), Ru1−C1 = 2.005(6), C1−O1 = 1.261(8), C1−N1 = 1.349(8), Ru2−O1 = 2.107(4), Ru1−O2 = 2.396(4), Ru4−O2 = 2.199(4), Ru4−C4 = 2.041(7), C4−C5 = 1.364(10), C5−C6 = 1.419(10), O2−C6 = 1.245(8), O3−C6 = 1.323(8), O3−C7 = 1.448(8).

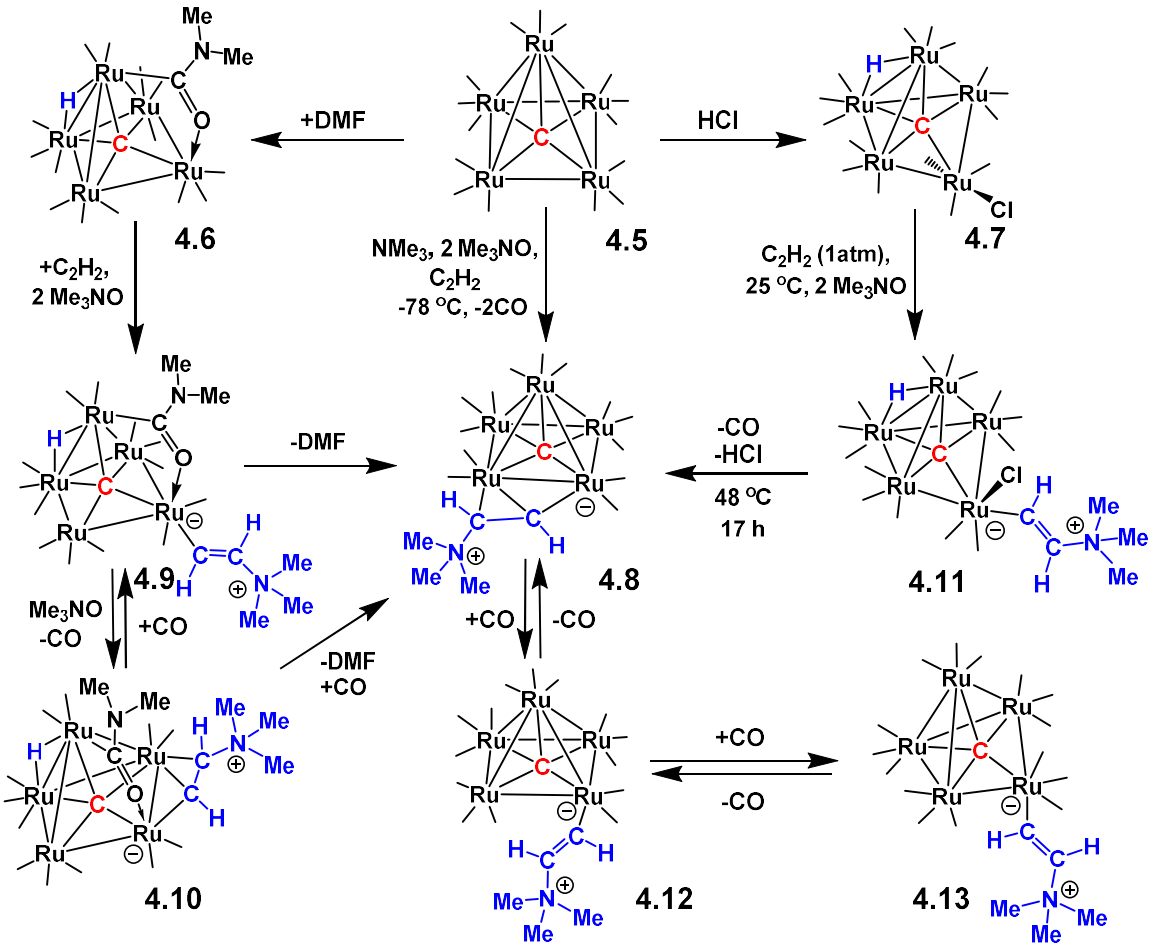

Scheme 4.1 A schematic of the structures and chemical relationships of compounds **4.5-4.13** that were investigated in this study. CO ligands are represented only as lines from the Ru atoms.

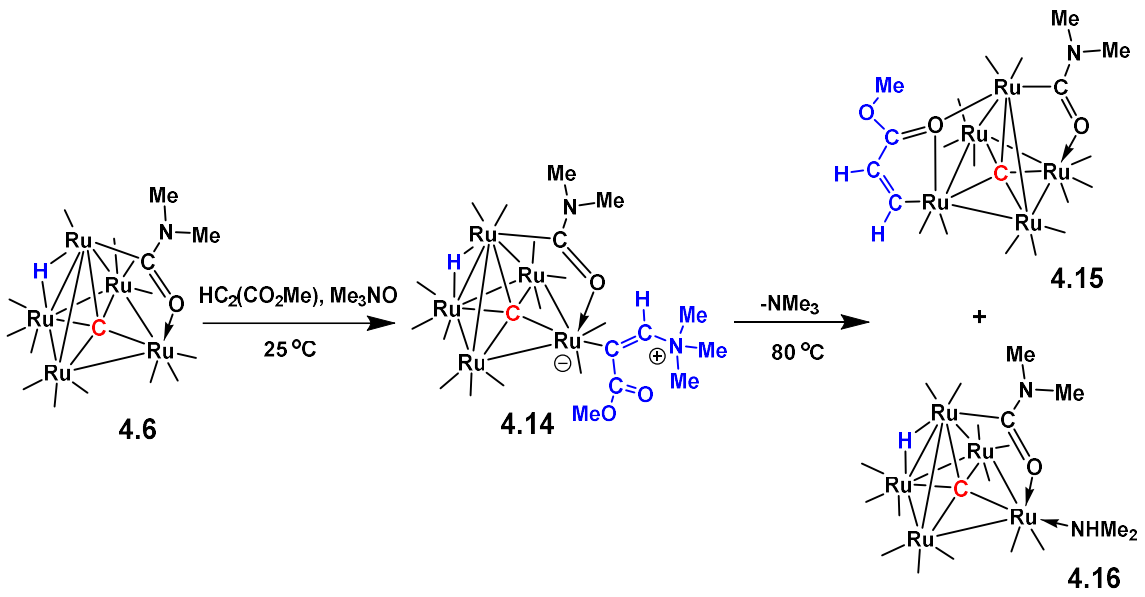

Scheme 4.2 A schematic of the structures and relationships of compounds **4.6** and **4.14** – **4.16**. CO ligands are represented only as lines from the Ru atoms.

Chapter 5

A (μ_5-C) Carbido Carbon Initiated C – C Coupling of Ethyne on $Ru_5(\mu_5\text{-}C)(CO)_{15}$ Cluster

5.1 Introduction

Long chain hydrocarbons are manufactured from syngas (a mixture of CO and H_2 gas) by the Fischer–Tropsch synthesis (FTS) processes.[1] FTS is a heterogeneous process, where catalytic conversion occurs through a surface polymerization reaction.[2] The initiation of the FTS involves the absorption of CO and H_2 gas followed by the formation of metal–carbide (M-C), metal–oxide (M-O) and metal–hydride (M-H) bonds (see Scheme 5.1).[3] There are several well established mechanisms of chain propagation, of which the carbide mechanism is the most widely-accepted one. [1(a), 4]

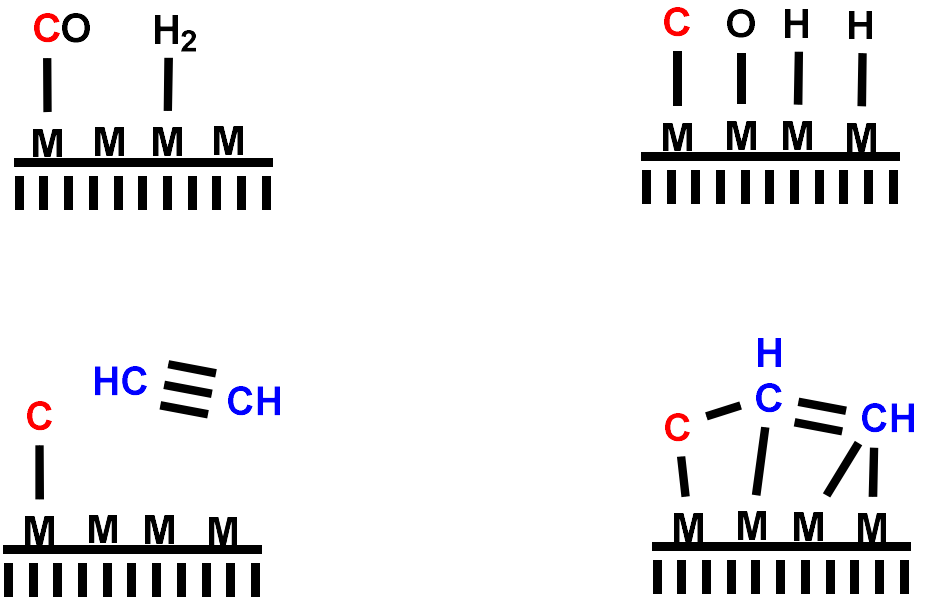

Scheme 5.1 CO and H_2 adsorption on a supported metal surface. Formation of metal-carbide (M-C), metal-oxide (M-O), and metal-hydride (M-H) bonds. The reactivity of M-C with the unsaturated molecule such as ethyne (C_2H_2).

Transition metal (TM) complexes containing an exposed carbido carbon atom may serve as models for the study of the reactivity M-C bonds in homogeneous systems. A terminal carbide complex having M≡C units coordinates to metal fragments via σ-donating and π-accepting bonding interactions. The terminal carbide may also act as a bridging

ligand in late transition metal complexes through the formation of M≡C−M′ bonding interactions.[5] A μ_3-carbido ligand can have a trigonal planar or a trigonal pyramidal geometry. Takemoto and his group reported the synthesis and structure of a bimetallic Ru_2Pt complex that contains a trigonal-planar μ_3-carbido ligand. The μ_3-carbido complex was found to show the first example of an intramolecular C–C coupling reaction between the μ_3-carbide and the methyl ligand.[6] Shriver *et al*. demonstrated the formation of a μ_3-trigonal pyramidal carbido ligand on a Fe_3 metal cluster that was found to form C-C bond upon alkylation to produce an ethylidyne.[7] The μ_4-carbido ligand being well exposed can show a great deal of reactivity. Chung *et al*. demonstrated the formation of a C–C bond between the carbide ligand and an electron deficient alkyne in a WOs_3 cluster complex.[8] Adams *et al*. observed the formation of a C-C bond between a μ_5-carbido carbon and a phenyl group to yield a bridging benzylidyne ligand in a Ru_5C cluster complex.[9]

In an effort to study the reactivity of (μ_5 – C) carbido carbon of the pentaruthenium cluster complex $Ru_5(\mu_5\text{-}C)(CO)_{15}$, **5.1**, we have investigated reactions between **5.1** and the unsaturated hydrocarbon ethyne (C_2H_2). The direct C – C coupling between the (μ_5 – C) carbide carbon and the C_2H_2 was observed to yield four new ethyne-bound Ru_5 cluster complexes. A novel [2+2+1] type cycloaddition of C_2H_2 to the carbide carbon on a multinuclear metal site was also observed. The structures, bonding, and the transformations of these new complexes will be described and discussed in this chapter.

5.2 Experimental Section

General Data

All reactions were performed under an atmosphere of nitrogen. Reagent grade solvents were dried by standard procedure and were freshly distilled prior to use. Infrared spectra were recorded on a Thermo Scientific Nicolet IS10 spectrophotometer. ^{1}H NMR spectra were recorded on Varian Mercury spectrometers operating at 300.1 MHz and 400.1 MHz. Mass spectrometric (MS) measurements were performed by a direct-exposure probe by using electron impact (EI) ionization. $Ru_3(CO)_{12}$ used to make $Ru_5(\mu_5\text{-}C)(CO)_{15}$, **5.1** was obtained from STREM and was used without further purification. $Ru_5(\mu_5\text{-}C)(CO)_{15}$, **5.1** was prepared according to a previously reported procedure.[10] Ethyne gas (HC_2H) was obtained from National Welders and used without further purification. Carbon Monoxide (CO) was purchased from Airgas Specialty Chemicals and was used without further purification. **WARNING**: Carbon Monoxide and ethyne are hazardous gases that should be used only in a well-ventilated fume hood. Product separations were performed by TLC in the air on Analtech 0.25 mm and 0.50 mm silica gel 60 Å F254 glass plates, and silica gel column chromatography on silica gel 60, 0.606 - 0.2 mm (70 – 230 mesh).

Reaction of $Ru_5(\mu_5\text{-}C)(CO)_{15}$, 5.1, with C_2H_2 at 48 °C

A 49.9 mg (0.053 mmol) amount of **5.1** was dissolved in 4 mL of CD_2Cl_2 solvent and was then transferred to three NMR tubes. The NMR tubes were closed with rubber septa and sealed with parafilm. C_2H_2 (g) at 1 atm bubbled through the solution for 30 seconds. The tubes were sealed under an atmosphere C_2H_2 (g). After shaking for few times tubes were kept in a constant temperature oil bath at 48 °C. The reaction progress was

monitored by both ^{1}H NMR and IR spectroscopy. After purging with C_2H_2 four times and heating at 48 °C for 60 h the reaction was complete. The products were then separated by TLC by using a solvent mixture of hexane/methylene chloride to yield four bands in the order of elution: 3.7 mg of orange red $Ru_5[\mu_4\text{-}\eta^3\text{:}\eta^1\text{-}CC(H)C(H)C(H)C(H)](CO)_{13}(\mu_4\text{-}\eta^2\text{:}\eta^1\text{:}\eta^2\text{:}\eta^1\text{-}HCCH)$, **5.2** (7% yield), 1.0 mg of red $Ru_5[\mu_4\text{-}\eta^4\text{:}\eta^1\text{-}CC(H)C(H)C(H)C(H)](CO)_{12}(\mu_4\text{-}\eta^2\text{:}\eta^1\text{:}\eta^2\text{:}\eta^1\text{-}HCCH)$, **5.3** (2% yield), 0.9 mg of orange $Ru_5[\mu_4\text{-}\eta^4\text{:}\eta^1\text{-}CC(H)C(H)C(H)C(H)](CO)_{12}(\mu_4\text{-}\eta^2\text{:}\eta^1\text{:}\eta^2\text{:}\eta^1\text{-}HCCH)$, **5.4** (2% yield), 6.0 mg of orange $Ru_4(CO)_{11}(\mu_4\text{-}\eta^2\text{:}\eta^1\text{:}\eta^2\text{:}\eta^1\text{-}HCCH)Ru(CO)_3(C_5H_4)$, **5.5** (11% yield). Spectral data for **5.2**: IR, ν_{CO} (cm^{-1} in hexane): 2093 (w), 2073 (vs), 2048 (s), 2028 (m), 2021 (w), 2014 (s), 2003 (w), 1984 (vw), 1969 (w). ^{1}H NMR (in acetone-d_6, δ in ppm): 9.28 (CC**H**CHCHC**H,** d, $^3J_{H\text{-}H}$ = 7.2 Hz, 1H), 7.80 (CC**H**CHCHC**H,** d, $^3J_{H\text{-}H}$ = 7.2 Hz, 1H), 7.24 (μ_4-C**H**CH, d, $^3J_{H\text{-}H}$ = 6.6 Hz, 1H), 5.70 (CCHC**H**C**H**CH**,** m, 1H), 5.34 (CCHC**H**C**H**CH**,** m, 1H), 4.80 (μ_4-CHC**H**, d, 4.80, $^3J_{H\text{-}H}$ = 6.6 Hz, 1H). EI/MS m/z. M^+ = 959.5. The isotope distribution pattern is consistent with the presence of five ruthenium atoms. Spectral data for **5.3**: IR, ν_{CO} (cm^{-1} in hexane): 2089 (w), 2080 (vw), 2059 (s), 2049 (w), 2034 (vs), 2014 (s), 2004 (w), 1983 (w), 1967 (w). ^{1}H NMR (in acetone-d_6, δ in ppm): 10.02 (μ_4-C**H**CH, d, $^3J_{H\text{-}H}$ = 6.0 Hz, 1H), 9.23 (CC**H**CHCHC**H,** d, $^3J_{H\text{-}H}$ = 7.5 Hz, 1H), 7.56 (μ_4-CHC**H**, d, $^3J_{H\text{-}H}$ = 6.0 Hz, 1H), 7.25 (CC**H**CHCHC**H,** d, $^3J_{H\text{-}H}$ = 7.2 Hz, 1H), 6.80 (CCHC**H**C**H**CH**,** t, $^3J_{H\text{-}H}$ = 6.6 Hz, 1H), 6.48 (CCHC**H**C**H**CH**,** t, $^3J_{H\text{-}H}$ = 1.2 Hz, 1H). Spectral data for **5.4**: IR, ν_{CO} (cm^{-1} in Hexane): 2092 (w), 2073 (vs), 2051 (vs), 2039 (w), 2031 (m), 2016 (m), 1998 (w), 1981 (w), 1945 (w). ^{1}H NMR (in CD_2Cl_2 solvent, δ in ppm): 9.90 (CHCHCC**H**CHCHC**H**, d, $^3J_{H\text{-}H}$ = 6.6 Hz, 1H), 7.96 (CHC**H**CCHCHCHCH, d, $^3J_{H\text{-}H}$ = 7.5 Hz, 1H), 6.76 (CHCHCC**H**CHCHC**H**, d, $^3J_{H\text{-}H}$ = 6.3 Hz, 1H), 6.28 (CHCHCCHC**H**C**H**CH,

m, 1H), 6.13 (C**H**CHCCHCHCHCH, d, $^{3}J_{H\text{-}H}$ = 7.8 Hz, 1H), 5.88 (CHCHCCHC**H**C**H**CH, m, 1H). Spectral data for **5.5**: IR, ν_{CO} (cm^{-1} in CH_2Cl_2): 2116 (w), 2086 (vw), 2069 (m), 2060 (m), 2029 (s), 2011 (vs), 1989 (w), 1970 (w). ^{1}H NMR (in acetone-d_6, δ in ppm): 9.93 (μ_4-C**H**C**H,** s, 2H), 6.26 (CC**H**CHCHC**H**, t, $^{3}J_{H\text{-}H}$ = 1.8 Hz, 2H), 5.91 (CCHC**H**C**H**CH, t, $^{3}J_{H\text{-}H}$ = 1.8 Hz, 2H).

Thermal transformation of 5.2 to 5.3 and 5.5 at 48 °C

A 9.1 mg (0.0095 mmol) amount of **5.2** was dissolved in CD_2Cl_2 solvent in an NMR tube. The NMR tube was sealed with a rubber septum and degassed under nitrogen three times. Then the tube was heated at 48 °C in a constant temperature oil bath. Reaction progress was monitored by ^{1}H NMR spectroscopy. After heating for 18 h, the solvent was removed, and the products were isolated by TLC by using a hexane/methylene chloride solvent mixture to yield in order of elution: 1.3 mg of unreacted **5.2**, 1.4 mg of **5.3** (16% yield), and 2.5 mg of **5.5** (27% yield).

Carbonylation of 5.3 at 25 °C

3.4 mg (0.0036 mmol) of **5.3** was taken in an NMR tube in 3.0 ml CD_2Cl_2 solvent. The NMR tube was sealed with rubber septa and degassed under nitrogen for three times. CO at 1 atm pressure was then purged through the solution for 30 sec at room temperature. The progress of the reaction was by monitored ^{1}H NMR spectroscopy. After 2 h at room temperature, the reaction was complete. The reaction mixture was then separated by TLC plate by using a hexane/methylene chloride solvent mixture to yield in order of elution: 2.6 mg of **5.2** (74% yield) and 0.3 mg of **5.5** (8% yield).

Thermal Conversion of 5.2 to 5.5 and $Ru_4(CO)_{12}(\mu_4\text{-}C_2H_2)$, 5.6 at 68 °C

10.5 mg (0.011 mmol) of **5.2** was taken in 50 mL three neck flask in dry distilled hexane. The progress of the reaction was monitored by IR spectroscopy. After refluxing at 68 °C for 50 min., the solvent was removed in *vacuo.* The reaction mixture was purified on a TLC plate using hexane/methylene chloride mixture to yield in order of elution: 4.1 mg of the known compound $Ru_4(CO)_{12}(\mu_4\text{-}C_2H_2)$, **5.6** (48% yield)[11], and 0.5 mg of **5.5** (5% yield).

Formation of 5.6 and 5.7 from 5.5 at 70 °C

4.6 mg (0.0046 mmol) of **5.5** was dissolved in d_8-toluene solvent and then transferred to an NMR tube. The tube was sealed and degassed under nitrogen for three times. Then the tube was heated in a constant temperature oil bath at 70 °C for 6.5 days. The progress of the reaction was monitored by ^{1}H NMR spectroscopy. After heating the reaction, the solvent wass removed *in vacuo.* The reaction mixture was then separated by TLC plate by using a hexane/methylene chloride/acetone solvent mixture to yield in order of elution: 1.2 mg of **5.6** (39% yield), and 0.6 mg of **5.5** was recovered. The formation of a known compound $[Ru_2(\eta^5\text{-}C_5H_5)_2(CO)_4]$, **5.7** (7.7% conversion by NMR integration) was also observed in the reaction.[12]

Crystallographic Analyses

Single crystals of compounds **5.2**-**5.5** suitable for X-ray diffraction analyses obtained by slow evaporation of solvent from solutions of the pure compounds at room temperature. Red crystals of compound **5.2** were obtained from a CH_2Cl_2/hexane solvent mixture. Dark red crystals of compound **5.3** were obtained from a CH_2Cl_2/heptane solvent

mixture. Red crystals of compound **5.4** were obtained from a benzene/heptane solvent mixture. Red crystals of compound **5.5** were obtained from a benzene/heptane solvent mixture. X-ray intensity data for compounds **5.2**-**5.5** were measured by using a Bruker D8 QUEST diffractometer equipped with a PHOTON-100 CMOS area detector and an Incoatec microfocus source (Mo Kα radiation, λ = 0.71073 Å).[13] The raw area detector data frames for compounds **5.2**-**5.5** were reduced, scaled, and corrected for absorption effects using the SAINT[13] and SADABS[14] programs. All structures were solved by using SHELXT.[15] Subsequent difference Fourier calculations and full-matrix least-squares refinement against F^2 were performed with SHELXL-2018[15] by using OLEX2[16]. All non-hydrogen atoms were refined with anisotropic displacement parameters.

Compound **5.2** crystallized in the monoclinic system. The pattern of systematic absences in the intensity data indicated the space group $P2_1/c$, which was confirmed by structure solution. The asymmetric unit consists of one complete molecule. All hydrogen atoms were located in difference Fourier maps and were refined freely. Compound **5.3** crystallized in the triclinic system. The space group *P*-1 was selected and subsequently confirmed by the successful solution and refinement of the structure. The asymmetric unit consists of one complete molecule. The six unique hydrogen atoms were located in difference Fourier maps. Their coordinates were refined freely with displacement parameters treated as Uiso(H) = 1.2Ueq(C). Compound **5.4** crystallized in the triclinic system. The space group *P*-1 was selected and confirmed by the successful solution and refinement of the structure. The asymmetric unit consists of one complete molecule. The six unique hydrogen atoms bonded to the carbon atoms were located in difference Fourier maps and were refined freely. Compound **5.5** crystallized in the monoclinic system. The

pattern of systematic absences in the intensity data was uniquely consistent with the space group $P2_1/n$, which was confirmed by successful solution and refinement of the structure. The asymmetric unit consists of one complete molecule. The hydrogen atoms bonded to carbon atoms were located in difference Fourier maps and were refined freely. Crystal data, data collection parameters, and refinement results for each analysis are listed in Table 5.1 and 5.2.

5.3 Results

The reaction of **5.1** with C_2H_2 at 48 °C for 60 h yielded four new pentaruthenium carbonyl cluster compounds in order of elution: $Ru_5[\mu_4\text{-}\eta^3\text{:}\eta^1\text{-}CC(H)C(H)C(H)C(H)](CO)_{13}(\mu_4\text{-}\eta^2\text{:}\eta^1\text{:}\eta^2\text{:}\eta^1\text{-}HCCH)$, **5.2** (7% yield), $Ru_5[\mu_4\text{-}\eta^4\text{:}\eta^1\text{-}CC(H)C(H)C(H)C(H)](CO)_{12}(\mu_4\text{-}\eta^2\text{:}\eta^1\text{:}\eta^2\text{:}\eta^1\text{-}HCCH)$, **5.3** (2% yield), $Ru_5(CO)_{13}[\mu_4\text{-}\eta^1\text{:}\eta^3\text{:}\eta^1\text{:}\eta^4\text{-}C(H)C(H)CC(H)C(H)C(H)C(H)]$, **5.4** (2% yield), and $Ru_4(CO)_{11}(\mu_4\text{-}\eta^2\text{:}\eta^1\text{:}\eta^2\text{:}\eta^1\text{-}HCCH)Ru(CO)_3(C_5H_4)$, **5.5** (11% yield). Compound **5.2** was characterized by IR, and ^1H NMR spectroscopy, mass spectrometry, and single-crystal X-ray diffraction analysis. An ORTEP diagram of the molecular structure of **5.2** is shown in Figure 5.1. Compound **5.2** consists of a Ru-spiked Ru_4 metal core where atoms Ru(2), Ru(3), Ru(4), and Ru(5) form a square, and atom Ru(1) is bonded to atom Ru(2) as a "spike". The square Ru_4 is bridged by an ethyne ligand in an $\eta^2\text{:}\eta^1\text{:}\eta^2\text{:}\eta^1$ fashion. Similar bonding and coordination were reported previously for tetranuclear metal clusters with bridging alkyne ligands.[17] The C5–C6 distance is 1.416(4) Å. The considerable lengthening happens due to the incorporation of all π electrons of the alkyne into the cluster bonding. The metal – metal bonds between Ru1 – Ru3, Ru1 – Ru4, Ru1 – Ru5 cleaved in the parent cluster. The most

interesting ligand in compound **5.2** is the bridging metalla-penta-1,3-dienyl ligand, CC(H)C(H)C(H)C(H), where two C_2H_2 molecules have been coupled to the carbido carbon of the cluster by a C – C bond formation. The C0 – C1 and C2 – C3 bond distances are 1.444(3) and 1.438(4) Å respectively and are longer than the bond distances of C1 – C2 = 1.407(4) Å and C2 – C4 = 1.409(4) Å. The bond between Ru(1) and C(0) is also cleaved. However, the carbido carbon C(0) remains bonded to Ru(2), Ru(3), Ru(4), and Ru(5) in a quadruply-bridging manner. The C(H)C(H)C(H)C(H) portion of the ligand is π-bonded to Ru(1) and σ-bonded to Ru(2) through a bridging η^3:η^1 fashion. The bond distance between Ru1 – C1 is 2.499(3) is longer than the bond lengths of Ru1 – C2, Ru1 – C3, and Ru1 – C4 (see Figure 5.2). There is a bridging carbonyl ligand across the metals Ru(2) and Ru(5).

The ^{1}H NMR spectrum of compound **5.2** shows a pair of doublets at δ = 7.24 and 4.81 due to the hydrogens on atom C(5) and C(6), and the $^3J_{H\text{-}H}$ is 6.6 Hz, which is consistent with the observed *Z*-conformation at the double bond. The resonances at δ = 9.28 and 7.80 are assigned due to the hydrogens at C(1)/C(2) or C(3)/C(4). These two hydrogen atoms are coupled by $^3J_{H\text{-}H}$ of 7.2 Hz. There is some unresolved coupling at 9.28 due to the long-distance coupling of the hydrogen atoms. The multiplets at δ = 5.70 and 5.34 are due to the hydrogens on C(2)/C(3) or C(3)/C(2). The C_2Ru_4C portion of the compound **5.2** can be viewed as closo-pentagonal bipyramid with Ru(3) and Ru(5) at the apices and C(0), Ru(2), C(5), C(6), and Ru(4) in the equatorial positions. Hence, for such an eight skeletal-electron pair (SEP) count, the cluster should and does have a total of 86 cluster valence electrons.[18]

Compound **5.3** was characterized by IR, ^{1}H NMR spectroscopy, and single-crystal X-ray diffraction analyses. An ORTEP diagram of the molecular structure of **5.3** is shown in Figure 5.2. Compound **5.3** consist of a pentanuclear metal core where, atoms Ru(1), Ru(3), Ru(4), and Ru(5) form a butterfly cluster structure and the wingtip atoms Ru(3) and Ru(5) are bridged by the fifth metal atom Ru(2). An ethyne ligand is bridged to the metals Ru(1), Ru(3), Ru(2), and Ru(5) by a η^2:η^1:η^2:η^1 fashion.[17] The C(5)–C(6) distance is 1.420(5) Å, which is similar to the C – C bond distance of ethyne ligand in compound **5.2**.

To form **5.3** the metal – metal bond between Ru1 – Ru2 in the parent cluster was cleaved. The most interesting ligand in compound **5.3** is the bridging metalla-penta-1,3-dienyl ligand, CC(H)C(H)C(H)C(H), where two ethyne molecules coupled and bonded to the carbido carbon C(0) of the cluster by a C – C bond formation. The C0 – C1 and C2 – C3 bond distances are 1.426(5) and 1.432(5) Å respectively and are longer than the bond distances of C1 – C2 = 1.418(4) Å and C2 – C4 = 1.410(4) Å. In addition, the C – C bond distances in the bridging penta-1,3-dienyl ligand in compound **5.3** are very similar to the bond distances in the corresponding ligand of compound **5.2**. The bond between Ru(1) and C(0) was also cleaved. However, the carbido carbon C(0) remains bonded to the metal atoms Ru(2), Ru(3), Ru(4), and Ru(5) in a bridging manner. The C(H)C(H)C(H)C(H) chain of the ligand is π-bonded to Ru(4) and σ-bonded to Ru(3) by carbon atom C(4), Ru3−C4 = 2.060(4) Å. The bond distances of Ru4 – C1, Ru4 – C2, Ru4 – C3, Ru4 – C4 are 2.297(3) Å, 2.249(4) Å, 2.208(4) Å and 2.176(4) Å, respectively and are similar to the bond distances of Ru1 – C2, Ru1 – C3, Ru1 – C4 in compound **5.2** (see figure 5.2).

The ^{1}H NMR spectrum of compound **5.3** shows a pair of doublets at δ = 10.02 and 7.56 due to the hydrogen on atoms on C5 and C6, with $^{3}J_{H-H}$ is 5.7 Hz, that is consistent

with the observed *Z*-conformation at the double bond. The resonances at δ = 9.23 and 7.25 are assigned due to the hydrogens at C1/C4 or C4/C1. There is some small, unresolved coupling at 9.23 due to the long-distance coupling of hydrogen atoms. Doublets of doublets at δ = 6.80 and 6.48 are assigned due to the hydrogen atoms on C2/C3 or C3/C2. There is a bridging carbonyl ligand C(13)-O(13) spanning the metal atoms Ru1 and Ru4. The C_2Ru_5C portion of the compound **5.3** can be viewed as closo dodecahedron with Ru(3) and Ru(5) at the apices and Ru(1), Ru(4), C(0), Ru(5), C(6), and C(5) in the equatorial positions. Hence, for nine skeletal electron pair (SEP) count, the cluster achieves the expected 84 cluster valence electron count.[18]

Compound **5.4** was characterized by IR, ^{1}H NMR spectroscopy, and by a single-crystal X-ray diffraction analysis. An ORTEP diagram of the molecular structure of **5.4** is shown in Figure 5.3. Compound **5.4** consists of a Ru-spiked tetrahedron having an Ru_4 metal core where, atoms Ru(1), Ru(2), Ru(3), and Ru(4) form a tetrahedron, and the fifth metal Ru(5) is bonded to Ru(3). The bond length between Ru3 – Ru5 is 2.866(2) Å and is slightly longer than all the other Ru – Ru bond distances in the cluster (see caption in Figure 5.3).

The hydrocarbon ligand in **5.4** can be viewed as an ethyne ligand coupled to the carbido carbon C(3) by a C – C bond formation reaction that forms a chain of a bridging metalla-hepta-1,3,6-trienyl ligand, C(H)C(H)CC(H)C(H)C(H)C(H). The C(H)C(H)CC(H)C(H)C(H)C(H) ligand is bonded to the cluster in a bridging μ_4-η^1:η^3:η^1:η^4 fashion. The carbido carbon atom C3 bridges two metal atoms, i. e., Ru2 and Ru3. The bond distance between Ru(3) – C(3), 2.026(19) Å, is similar to the Ru - C bond

distances in the parent cluster **5.1**. There are two bridging carbonyl ligands spanning Ru1 and Ru3, and Ru2 and Ru4.

The ^{1}H NMR spectrum of compound **5.4** shows six resonances for the -C_7H_6 chain. A pair of doublets at δ = 9.90 and 6.76 are attributed to the hydrogen atoms on atom C4/C5 or C5/C4, $^{3}J_{H-H}$ is 6.6 Hz. The resonances at δ = 7.96 and 6.13 are assigned due to the hydrogen atoms on C2 and C1, respectively, with $^{3}J_{H-H}$ is 7.8 Hz. The multiplets at δ = 6.28 and 5.88 are assigned to the hydrogen atoms on C6/C7 or C7/C6. Compound **5.4** contains a total of 76 cluster valence electrons which is in accord with an electron-precise metal cluster of five transition metal atoms (n) having seven metal – metal bonds (m), according to the formula 18n – 2m.

Compound **5.5** was characterized by IR, ^{1}H NMR spectroscopy, and single-crystal X-ray diffraction analyses. An ORTEP diagram of the molecular structure of **5.5** is shown in Figure 5.4. Compound **5.5** consists of a butterfly structure of four metal atoms, and one of the wingtip Ru atoms Ru(3) is coordinated to a $Ru(CO)_3(C_5H_4)$ fragment by a Ru-C bond to a metallated cyclopentadienyl ligand (C_5H_4), C(3) – C(7) that was formed by a cyclization of the open C0 – C4 ligand in **5.2** from which it was made. This metallated-cyclopentadienyl ligand is π-coordinated to Ru(5). There is a quadruply bridging ethyne ligand coordinated to the four metal atoms Ru(1), Ru(3), Ru(2), and Ru(4) in a $\eta^2:\eta^1:\eta^2:\eta^1$ coordination mode. The C – C bond of the ethyne ligand is oriented parallel to the hinge bond of the Ru_4 core. Similarly coordinated ethyne ligands were observed in other butterfly tetranuclear metal cluster compounds.[11, 19] The Ru – C bonds fall into two categories: the longer bonds involving the wing-tip Ru atoms [2.182(13)–2.198(13) Å] and

the shorter bonds to the hinge Ru atoms [2.109(14) Å, and 2.098(14) Å]. The C(1)–C(2) bond distance is 1.451(19) Å, and the considerable lengthening is due to the incorporation of all of the πelectrons of the alkyne into the metal cluster framework.

The ^{1}H NMR spectrum of compound **5.5** shows three resonances. A low-field singlet at δ = 9.93 is due to the two hydrogen atoms on the ethyne ligand coordinated to the butterfly Ru_4 metal core. Besides, there is a pair of doublet of doublet at δ = 6.26 and 5.91 where, $^{3}J_{H\text{-}H}$ = 1.8 Hz due to the four hydrogens on -C_5H_4 ligand which is coordinated to the single Ru atom, Ru(3). The C_2Ru_4 portion of the compound **5.5** can be viewed as closo octahedron with Ru(3) and Ru(4) at the apices and Ru(1), Ru(2), C(2), and C(1) in the equatorial positions. Hence, for seven a skeletal electron pair (SEP) count, the cluster achieves the expected 66 valence electron count.[18]

5.4 Discussion

A summary of our studies of the thermal reaction of square pyramidal pentaruthenium carbido carbonyl cluster **5.1** with ethyne is shown in Scheme 5.2 (see below for atom numbering scheme). The reaction yielded four new ethyne containing cluster compounds. Compound **5.2** has a pentanuclear metal core of Ru_5 where an ethyne ligand is bound to Ru(2), Ru(3), Ru(4), and Ru(5) in a bridging η^2:η^1:η^2:η^1 fashion. There is a bridging metalla-penta-1,3-dienyl ligand, CC(H)C(H)C(H)C(H), where two C_2H_2 molecules are coupled and bonded to the carbido carbon of the cluster by C – C bond formations. The carbido carbon bridges the metal atoms Ru(2), Ru(3), Ru(4), and Ru(5). In addition, the C(H)C(H)C(H)C(H) chain of the ligand bridges Ru(1) and Ru(2) in a η^3:η^1 fashion. When heated to 48 °C for 18h, compound **5.2** was converted to compound

5.3 in 16% yield by elimination and rearrangement of CO and the formation of two metal – metal bonds between Ru(1) and Ru(3), and Ru(1) and Ru(5), and a switch in the bonding of C(0) from Ru(2) to Ru(1). In addition, the C(H)C(H)C(H)C(H) ligand converted to bridging η^4:η^1 ligand from bridging η^3:η^1 ligand and switching the bond between C4-Ru2 to C4-Ru3. Compound **5.5** was also formed in 27 % yield by the addition of CO to Ru(2) and a cleavage of the metal – metal bond between Ru(1) and Ru(2) in this reaction. In this transformation, bonds between C(0) – Ru(3), C(0) – Ru(4), and C(0) – Ru(5) also cleaved while C(0) remains bonded to Ru(2). However, the bridging metalla-penta-1,3-dienyl lilgand in **5.2** changes its coordination mode from bridging η^3:η^1 mode to a η^5–metalla-cyclopenta-1,3-dienyl ligand on Ru(1). One ethyne ligand remains bonded to Ru(2), Ru(3), Ru(4), and Ru(5) in a quadruply-bridging η^2:η^1:η^2:η^1 fashion similar to the one in compound **5.2**. Thermal carbonylation of compound **5.3** at 25 °C yielded compound **5.2** (yield 74%) together with the formation of compound **5.5** (yield 8%). Thus, it can be concluded that **5.2** is an intermediate en route to **5.5** from **5.3**.

When a solution of compound **5.2** was heated to reflux in hexane at 68 °C for 50 minutes, the reaction yielded two compounds. A low yield (5%) of compound **5.5** together with high yield (48% yield) of a known compound $Ru_4(CO)_{12}(\mu_4\text{-}C_2H_2)$, **5.6**. It was assumed that compound **5.5** is the intermediate en route from **5.3** to **5.6**. To confirm the formation of compound **5.6** from compound **5.5** and to study the fate of the fragment $Ru(CO)_3(\eta^5\text{-}C_5H_4)$ in compound **5.5**, we have studied the thermal transformation of compound **5.5** by NMR spectroscopy. When a solution of compound **5.5** was heated at 68 °C for 6.5 days, the formation of compound **5.6** was observed in 39% yield together with

the formation of a known compound $[Ru_2(\eta^5\text{-}C_5H_5)_2(CO)_4]$, **5.7**. The formation of compound **5.7** was confirmed by IR and ^1H NMR spectroscopy, and mass spectrometry.

The formation of **5.6** and **5.7** from **5.5** can be explained by thermally cleaving the Ru2 – C0 bond, and a transfer of a carbonyl ligand from Ru1 to Ru2 completes the formation of **5.6**. The fragment $Ru(CO)_2(\eta^5\text{-}C_5H_4)$ adds a proton to C0 to make the $\eta^5\text{-}C_5H_5$ ligand which then dimerizes to yield **5.7**. It was found that the source of the proton was a small amount of water (H_2O) present in the reaction mixture. A ^2D NMR in d_8-toluene showed no resonances for deuterium in the region of the formation of compound **5.7**. Later in another experiment increased conversion of **5.5** to **5.7** was observed in the presence of added water. Additionally, compound **5.7** was purified by using preparative TLC and was detected by IR and ^1H NMR spectroscopy. Finally, a direct probe mass spectrum was obtained and confirmed a parent ion M^+ for $[Ru_2(\eta^5\text{-}C_5H_5)_2(CO)_4]$, which has only 10 protons.

5.5 Conclusion

The reaction of ethyne (HC≡CH) with the compound **5.1** yields novel ethyne-coordinated complexes **5.2** – **5.5** where ethyne is not only coordinated to the cluster but also connected to the (μ_5-C) carbido carbon atom of the compound **5.1**. The ethyne-ethyne coupling with the carbido carbon of **5.1** yields two pentaruthenium cluster complexes **5.2** and **5.3** containing metalla-penta-1,3-dienyl ligands. Compound **5.2** and **5.3** can be converted to compounds **5.5**, **5.6**, and **5.7** thermally by the addition of CO and the rearrangement of the metalla-penta-1,3-dienyl ligand within the cluster. In addition, compound **5.4** was obtained which is an isomer of compound **5.2** having metalla-hepta-

1,3,5-trienyl ligand. These conversions show the key processes that might happen during the alkyne-alkyne coupling on a carbide containing metal surface.

5.6 References

1. (a) Fischer, F.; Tropsch, H. *Brennstoff-Chem.* **1926**, 7, 97. (b) Fischer, F.; Tropsch, H. *Brennstoff-Chem.* **1930**, 11, 489. (c) H. Pichler, in: W. Frankenburg, E. Rideal, V. Komarewsky (Eds.), Advances in Catalysis, vol. IV, Academic Press, New York, **1952**, p. 271. (d) Anderson, R. B. The Fischer-Tropsch Synthesis, Academic Press, New York, **1984**. (e) Somorjai, G. A. Introduction to Surface Chemistry and Catalysis, Wiley, New York, **1994**. (f) Khodakov, A. Y.; Chu, W.; Fongarland, P. *Chem. Rev.* **2007**, 107, 1692−1744. (g) Maitlis, P. M.; Zanotti, V. *Chem. Commun.* **2009**, 1619–1634.
2. (a) Dry, M. E. *Appl. Catal. A Gen.* **1996**, 138, 319–344. (b) Overett, M. J.; Hill, R. O.; Moss, J. R. *Coord. Chem. Rev.* **2000**, 581, 206–207.
3. Ponec, V.; van Barneveld, W. A. *Ind. Eng. Chem. Prod. Res. Dev.* **1979**, 18, 268–271.
4. (a) Dictor, R. A.; Bell, A. T. *J. Catal.* **1986**, 97, 121–136. (d) Biloen, P.; Helle, J. N.; Sachtler, W. M. H. *J. Catal.* **1979**, 58, 95–107. (e) Mousavi, S.; Zamaniyan, A.; Irani, M.; Rashidzadeh, M. *Applied Catalysis A: General* **2015**, 506, 57–66.
5. (a) Mansuy, D.; Lecomte, J. P.; Chottard, J. C.; Bartoli, J. F. *Inorg. Chem.* **1981**, 20, 3119−3121. (b) Goedken, V. L.; Deakin, M. R.; Bottomley, L. A. *J. Chem. Soc., Chem. Commun.* **1982**, 11, 607−608. (c) Rossi, G.; Goedken, V. L.; Ercolani, C. *J. Chem. Soc., Chem. Commun.* **1988**, 1, 46−47. (d) Beck, W.; Knauer, W.; Robl, C. *Angew. Chem., Int. Ed. Engl.* **1990**, 29, 318−320. (e) Miller, R. L.; Wolczanski, P. T.; Rheingold, A. L. *J. Am. Chem. Soc.* **1993**, 115, 10422−10423. (f) Caselli, A.; Solari, E.; Scopelliti,

R.; Floriani, C. *J. Am. Chem. Soc.* **2000**, 122, 538−539. (g) Hong, S. H.; Day, M. W.; Grubbs, R. H. *J. Am. Chem. Soc.* **2004**, 126, 7414−7415. (h) Solari, E.; Antonijevic, S.; Gauthier, S.; Scopelliti, R.; Severin, K. *Eur. J. Inorg. Chem.* **2007**, 367−371. (i) Hill, A. F.; Sharma, M.; Willis, A. C. *Organometallics* **2012**, 31, 2538−2542. (j) Borren, E. S.; Hill, A. F.; Shang, R.; Sharma, M.; Willis, A. C. *J. Am. Chem. Soc.* **2013**, 135, 4942−4945.

6. Takemoto, S.; Morita, H.; Karitani, K.; Fujiwara, H.; Matsuzaka, H. *J. Am. Chem. Soc.* **2009**, 131, 18026−18027.
7. Kolis, J. W.; Holt, E. M.; Drezdzon, M.; Whitmire, K. H.; Shriver, D. F. *J. Am. Chem. Soc.* **1982**, 104, 6134-6135.
8. Chung, C.; Tseng, W.-C.; Chi, Y.; Peng, S.-M.; Lee, G.-H. *Organometallics* **1998**, 17, 2207-2214.
9. Adams, R. D.; Captain, B.; Fu, W.; Smith, M. D. *Inorg. Chem.* **2002**, 41, 5593-5601.
10. Johnson, B. F. G.; Lewis, J.; Nicholls, J. N.; Puga, J.; Raithby, P. R.; Rosales, M. J.; McPartlin, M.; Clegg, W., *J. Chem. Soc. Dalton Trans.* **1983**, 277-290.
11. Bruce, M. I.; Skelton, B. W.; White, A. H.; Zaitseva, N. N. *J. Chem. Soc., Dalton Trans*. **1999**, 1445–1453.
12. Abrahamson, H. B.; Palazzotto, M. C.; Reichel, C. L.; Wrighton, M. S. *J. Am. Chem. Soc.* **1979**, 101, 4123–4127.
13. APEX3 Version 2016.5-0 and SAINT Version 8.37A. Bruker AXS, Inc. Madison, WI, USA.
14. SADABS Version 2016/2. Krause, L., Herbst-Irmer, R., Sheldrick G.M. & Stalke D. *J. Appl. Cryst*. **2015**, *48*, 3-10.

15. (a) SHELXT: Sheldrick, G.M. *Acta Cryst.* **2015**, *A71*, 3-8. (b) SHELXL: Sheldrick, G.M. *Acta Cryst.* **2015**, *C71*, 3-8.

16. **OLEX2**: a complete structure solution, refinement and analysis program. Dolomanov, O. V., Bourhis, L. J., Gildea, R. J., Howard J. A. K. and Puschmann, H. *J. Appl. Cryst.* **2009**, *42*, 339-341.

17. (a) Sappa, E.; Tiripicchio, A.; Tiripicchio Camellini, M. *J. Chem. Soc., Dalton Trans.* **1978**, 419. (b) Aime, S.; Nicola, G.; Osella, D.; Manotti Lanfredi, A. M.; Tiripicchio, A. *Inorg. Chim. Acta* **1984**, 85, 161. (c) Davies, J. E.; Johnson, B. F. G.; Martion, C. M.; Pearson, R. H. H.; Dyson, P. J. *J. Organomet. Chem.* **1998**, 550, 431. (d) Bruce, M. I.; Zaitseva, N. N.; Skelton, B. W.; White, A. H. *J. Chem. Soc., Dalton Trans.* **2002**, 3879–3885.

18. (a) Mingos, D. P. M. *Acc. Chem. Res.* **1984**, 17, 311-319. (b) Mingos, D. M. P.; May, A. S., in *The Chemistry of Metal Cluster Complexes*. Shriver, D. F.; Kaesz, H. D.; Adams, R. D., VCH Publishers, New York, **1990**, Ch. 2.

19. (a) Okazaki, M.; Ohtani, T.; Takano, M.; Ogino, H.; *Inorg. Chem.* **2002**, 41, 6726−6730. (b) Zuno-Cruz, F. J.; Sa´nchez-Cabrera, G.; Rosales-Hoz, M. J.; No¨th, H. *J. Organomet. Chem.* **2002**, 649, 43–49. (c) Ferrand, V.; Süss-Fink, G.; Neels, A.; Stoeckli-Evans, H. *J. Chem. Soc., Dalton Trans.* **1998**, 3825–3831.

Table 5.1 Crystal data, data collection parameters for compounds **5.2** and **5.3**.

Compound	**5.2**	**5.3**
Empirical formula	$Ru_5O_{13}C_{20}H_6$	$Ru_5O_{12}C_{19}H_6$
Formula weight	959.60	931.59
Crystal system	Monoclinic	Triclinic
Lattice parameters		
a (Å)	11.6680(5)	9.5052(8)
b (Å)	10.2320(4)	9.9126(8)
c (Å)	20.7513(8)	14.6411(12)
α (deg)	90.00	96.529(2)
β (deg)	99.651(2)	103.350(2)
γ (deg)	90.00	117.827(2)
V (Å^3)	2442.37(17)	1147.01(16)
Space group	$P2_1/c$	*P*-1
Z value	4	2
ρ_{calc} (g/cm^3)	2.610	2.697
μ (Mo Kα) (mm^{-1})	3.088	3.280
Temperature (K)	100(2)	100(2)
$2\Theta_{max}$ (°)	56.71	56.756
No. Obs. ($I > 2\sigma(I)$)	5480	4955
No. parameters	368	343
Goodness of fit (GOF)	1.035	1.047
Max. shift in cycle	0.002	0.001
Residuals*: R1; wR2	0.0193/0.0426	0.0261/0.0472
Absorption correction, Max/min	Multi-scan 0.7457/0.6476	Multi-scan 0.6205/0.5766
Largest peak in Final Diff. Map (e$^-$/Å^3)	1.127	1.317

$R1 = \Sigma_{hkl}(||F_{obs}| - |F_{calc}||)/\Sigma_{hkl}|F_{obs}|$; $wR2 = [\Sigma_{hkl}w(|F_{obs}| - |F_{calc}|)^2/\Sigma_{hkl}wF^2_{obs}]^{1/2}$; $W = 1/\sigma^2(F_{obs})$; $GOF = [\Sigma_{hkl}w(|F_{obs}| - |F_{calc}|)^2/(n_{data} - n_{vari})]^{1/2}$.

Table 5.2 Crystal data, data collection parameters for compounds **5.4** and **5.5**.

Compound	**5.4**	**5.5**
Empirical formula	$Ru_5O_{13}C_{20}H_6$	$Ru_5O_{14}C_{21}H_6$
Formula weight	959.60	987.61
Crystal system	Triclinic	Monoclinic
Lattice parameters		
a (Å)	8.8115(4)	12.0677(5)
b (Å)	10.6704(5)	17.0832(7)
c (Å)	13.4282(6)	13.4170(6)
α (deg)	102.952(2)	90.00
β (deg)	93.294(2)	103.619(2)
γ (deg)	94.093(2)	90.00
V (Å^3)	1223.78(10)	2688.2(2)
Space group	*P*-1	$P2_1/n$
Z value	2	4
ρ_{calc} (g/cm^3)	2.604	2.440
μ (Mo Kα) (mm^{-1})	3.082	2.812
Temperature (K)	100(2)	100(2)
$2\Theta_{max}$ (°)	58.48	65.354
No. Obs. ($I > 2\sigma(I)$)	5885	9050
No. parameters	368	386
Goodness of fit (GOF)	1.051	1.095
Max. shift in cycle	0.001	0.002
Residuals*: R1; wR2	0.0172/0.0305	0.0169/0.0317
Absorption correction, Max/min	Multi-scan 0.7458/0.6496	Multi-scan 0.5655/0.4066
Largest peak in Final Diff. Map (e$^-$/Å^3)	0.713	0.544

$R1 = \Sigma_{hkl}(\,|\,|F_{obs}|-|F_{calc}|\,|)/\Sigma_{hkl}|F_{obs}|$; $wR2 = [\Sigma_{hkl}w(|F_{obs}|-|F_{calc}|)^2/\Sigma_{hkl}wF^2_{obs}]^{1/2}$; $W = 1/\sigma^2(F_{obs})$; $GOF = [\Sigma_{hkl}w(|F_{obs}|-|F_{calc}|)^2/(n_{data} - n_{vari})]^{1/2}$.

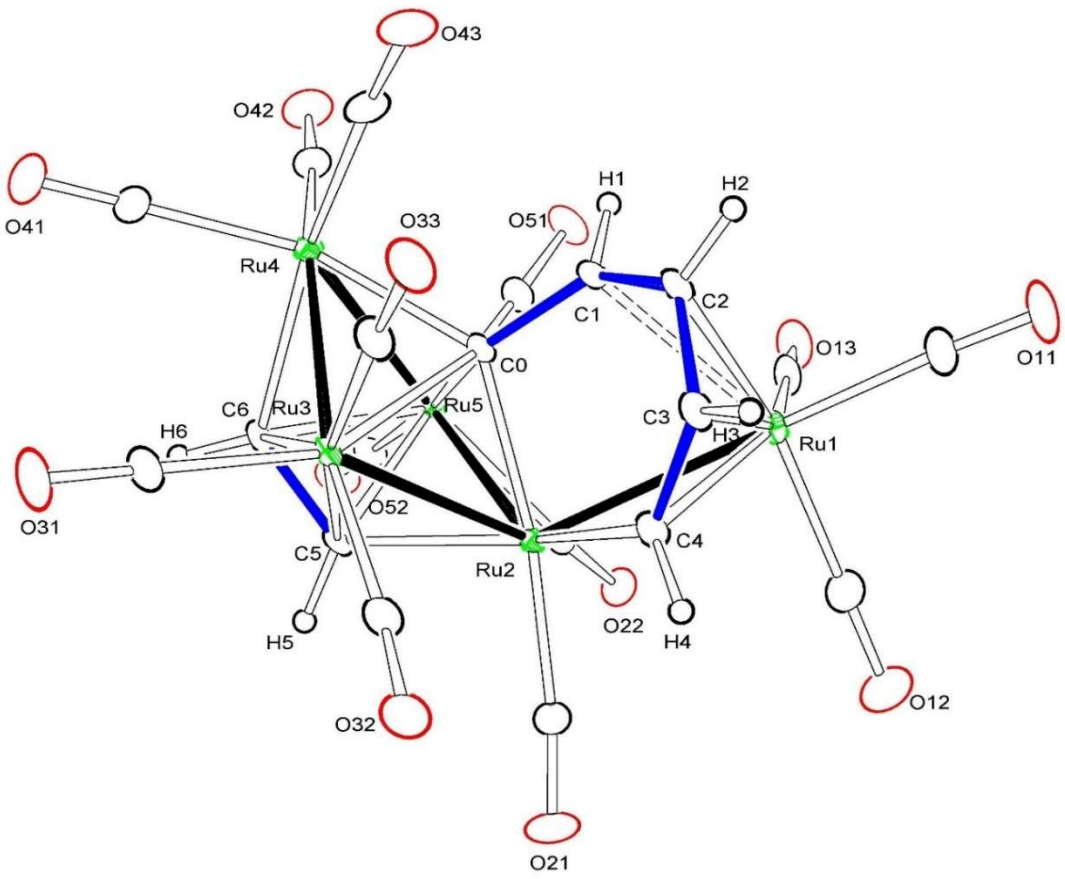

Figure 5.1 An ORTEP diagram of the molecular structure of $Ru_5[\mu_4\text{-}\eta^3\text{:}\eta^1\text{-}CC(H)C(H)C(H)C(H)](CO)_{13}(\mu_4\text{-}\eta^2\text{:}\eta^1\text{:}\eta^2\text{:}\eta^1\text{-}HCCH)$, **5.2** showing 25% thermal ellipsoid probability. Selected interatomic bond distances (Å) are as follows: Ru1−Ru2 = 2.8328(3), Ru2−Ru5 = 2.6920(3), Ru2−Ru3 = 2.7121(3), Ru4−Ru5 = 2.7849(3), Ru3−Ru4 = 2.7398(3), C0−C1= 1.444(3), C1−C2 = 1.407(4), C2−C3 = 1.438(4), C3−C4 = 1.409(4), C5−C6 = 1.416(4), Ru2−C4 = 2.050(3), Ru1−C1 = 2.499(3), Ru1−C2 = 2.227(3), Ru1−C3 = 2.205(3), Ru1−C4 = 2.191(3), Ru2−C0 = 2.099(2), Ru3−C0 = 2.324(2), Ru4−C0 = 2.144(3), Ru5−C0 = 2.284(2), Ru3−C6 = 2.290(2), Ru4−C6 = 2.117(2), Ru5−C6 =2.304(2), Ru2−C5 = 2.152(2), Ru3−C5 = 2.244(2), Ru5−C5 =2.278(2).

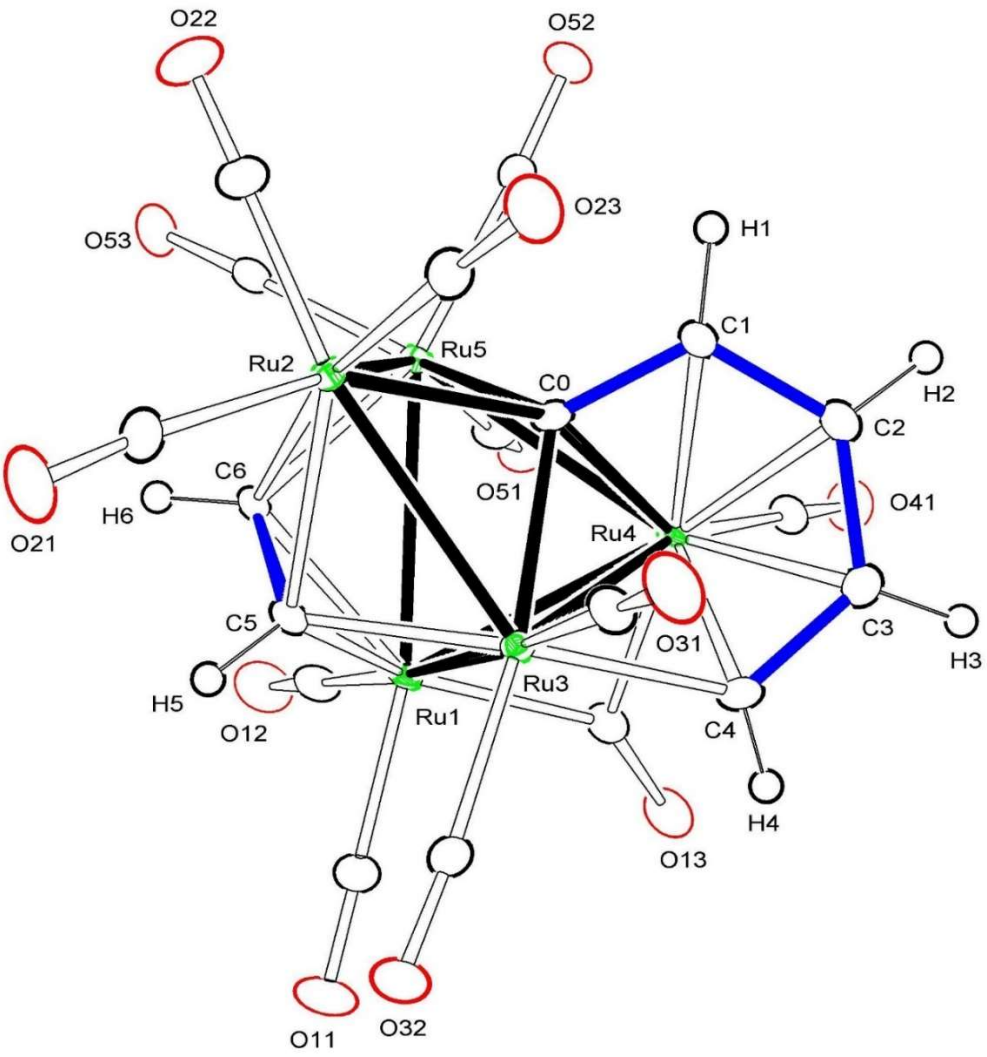

Figure 5.2 An ORTEP diagram of the molecular structure of $Ru_5[\mu_4\text{-}\eta^4\text{:}\eta^1\text{-}CC(H)C(H)C(H)C(H)](CO)_{12}(\mu_4\text{-}\eta^2\text{:}\eta^1\text{:}\eta^2\text{:}\eta^1\text{-}HCCH)$, **5.3** showing 35% thermal ellipsoid probability. Selected interatomic bond distances (Å) are as follows: Ru1−Ru3 = 2.9087(4), Ru1−Ru4 = 2.7999(4), Ru1−Ru5 = 2.8856(4), Ru2−Ru3 = 2.7920(4), Ru2−Ru5 = 2.8486(4), Ru3−Ru4 = 2.8106(4), Ru4−Ru5 = 2.8658(4), C0−C1 = 1.426(5), C1−C2 = 1.418(5), C2−C3 = 1.432(5), C3−C4 = 1.410(5), C5−C6 = 1.420(5), Ru3−C4 = 2.060(4), Ru4−C1 = 2.297(3), Ru4−C2 = 2.249(4), Ru4−C3 = 2.208(4), Ru4−C4 = 2.176(4), Ru2−C0 = 2.119(3), Ru3−C0 = 2.114(3), Ru4−C0 = 2.159(3), Ru5−C0 = 2.300(3), Ru1−C5 = 2.273(3), Ru2−C5 = 2.281(3), Ru3−C5 = 2.112(4), Ru1−C6 =2.286(3), Ru2−C6 = 2.283(3), Ru5−C6 = 2.134(3).

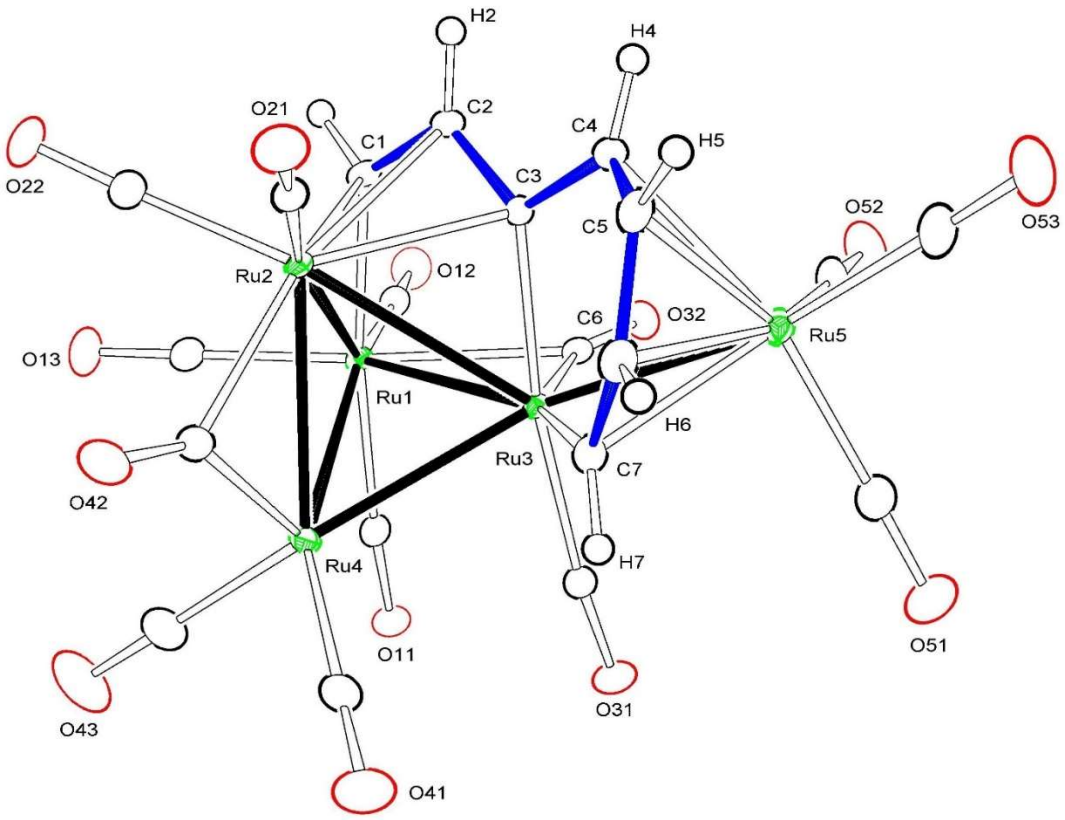

Figure 5.3 An ORTEP diagram of the molecular structure of $Ru_5(CO)_{13}[\mu_4\text{-}\eta^1\text{:}\eta^3\text{:}\eta^1\text{:}\eta^4\text{-}C(H)C(H)CC(H)C(H)C(H)C(H)]$, **5.4** showing 40% thermal ellipsoid probability. Selected interatomic bond distances (Å) are as follows: Ru1−Ru2 = 2.8253(2), Ru1−Ru3 = 2.8146(2), Ru1−Ru4 = 2.8161(2), Ru2−Ru3 = 2.8330(2), Ru2−Ru4 = 2.8299(2), Ru3−Ru4 = 2.7213(2), Ru3−Ru5 = 2.8655(2), C1−C2 = 1.411(3), C2−C3 = 1.427(3), C3−C4 = 1.457(3), C4−C5 = 1.410(3), C5−C6 = 1.419(3), C6−C7 = 1.416(3), Ru1−C1 = 2.080(2), Ru2−C1 = 2.226(2), Ru2−C2 = 2.2725(19), Ru2−C3 = 2.2606(18), Ru3−C3 = 2.0259(19), Ru3−C7 = 2.029(2), Ru5−C4 = 2.344(2), Ru5−C5 = 2.218(2), Ru5−C6 = 2.237(2), Ru5−C7 = 2.254(2).

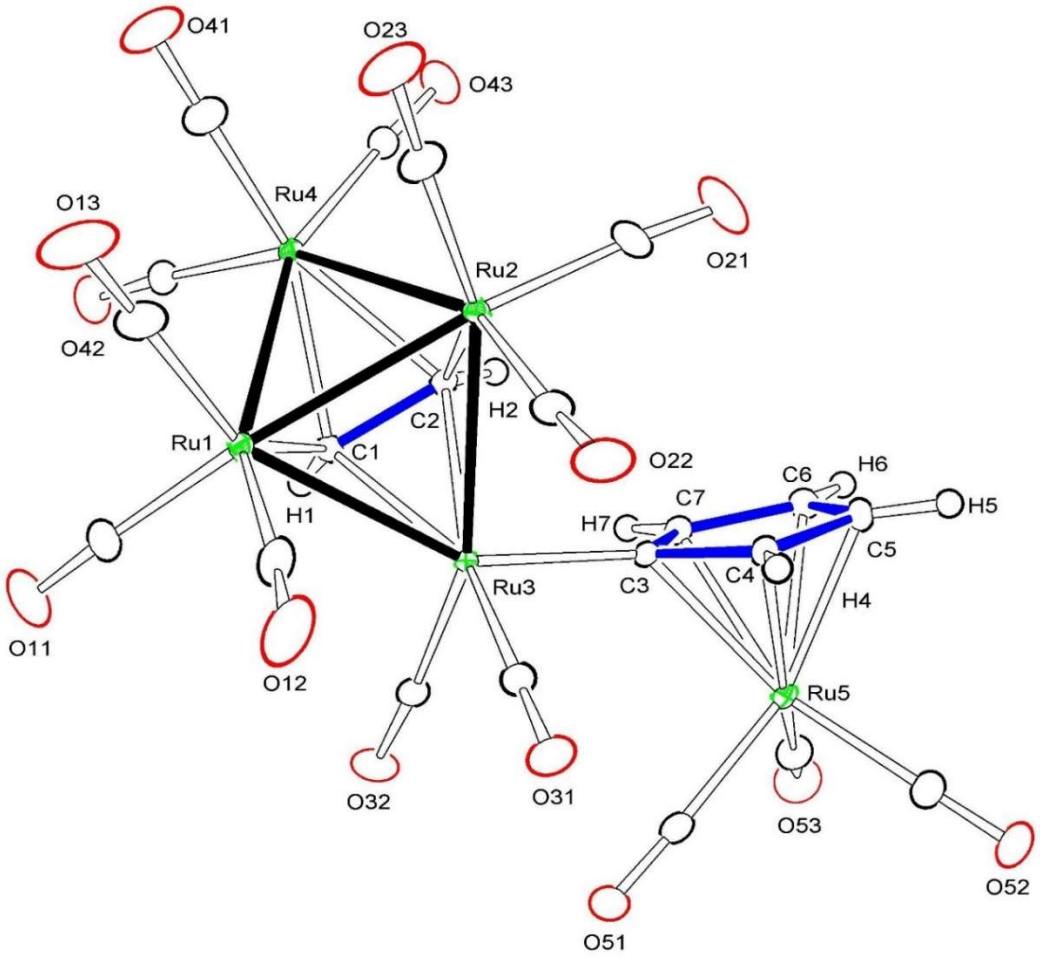

Figure 5.4 An ORTEP diagram of the molecular structure of $Ru_4(CO)_{11}(\mu_4\text{-}\eta^2\text{:}\eta^1\text{:}\eta^2\text{:}\eta^1\text{-}HCCH)Ru(CO)_3(C_5H_4)$, **5.5** showing 40% thermal ellipsoid probability. Selected interatomic bond distances (Å) are as follows: Ru1−Ru2 = 2.81061(18), Ru1−Ru3 = 2.78310(17), Ru1−Ru4 = 2.75114(19), Ru2−Ru3 = 2.77635(18), Ru2−Ru4 = 2.75564(17), C1−C2 = 1.4511(19), Ru1−C1 = 2.1087(14), Ru3−C1 = 2.1878(13), Ru4−C1 = 2.1841(13), Ru2−C2 = 2.0984(14), Ru3−C2 = 2.1984(13), Ru4−C2 = 2.1824(13), Ru3−C3 = 2.0670(13), C3−C4 = 1.4437(19), C4−C5 = 1.434(2), C5−C6 = 1.413(2), C6−C7 = 1.441(2), C7−C3 = 1.437(2), Ru5−C3 = 2.3181(13), Ru5−C4 = 2.2289(14), Ru5−C5 = 2.2310(15), Ru5−C6 = 2.2187(15), Ru5−C7 = 2.2190(14).

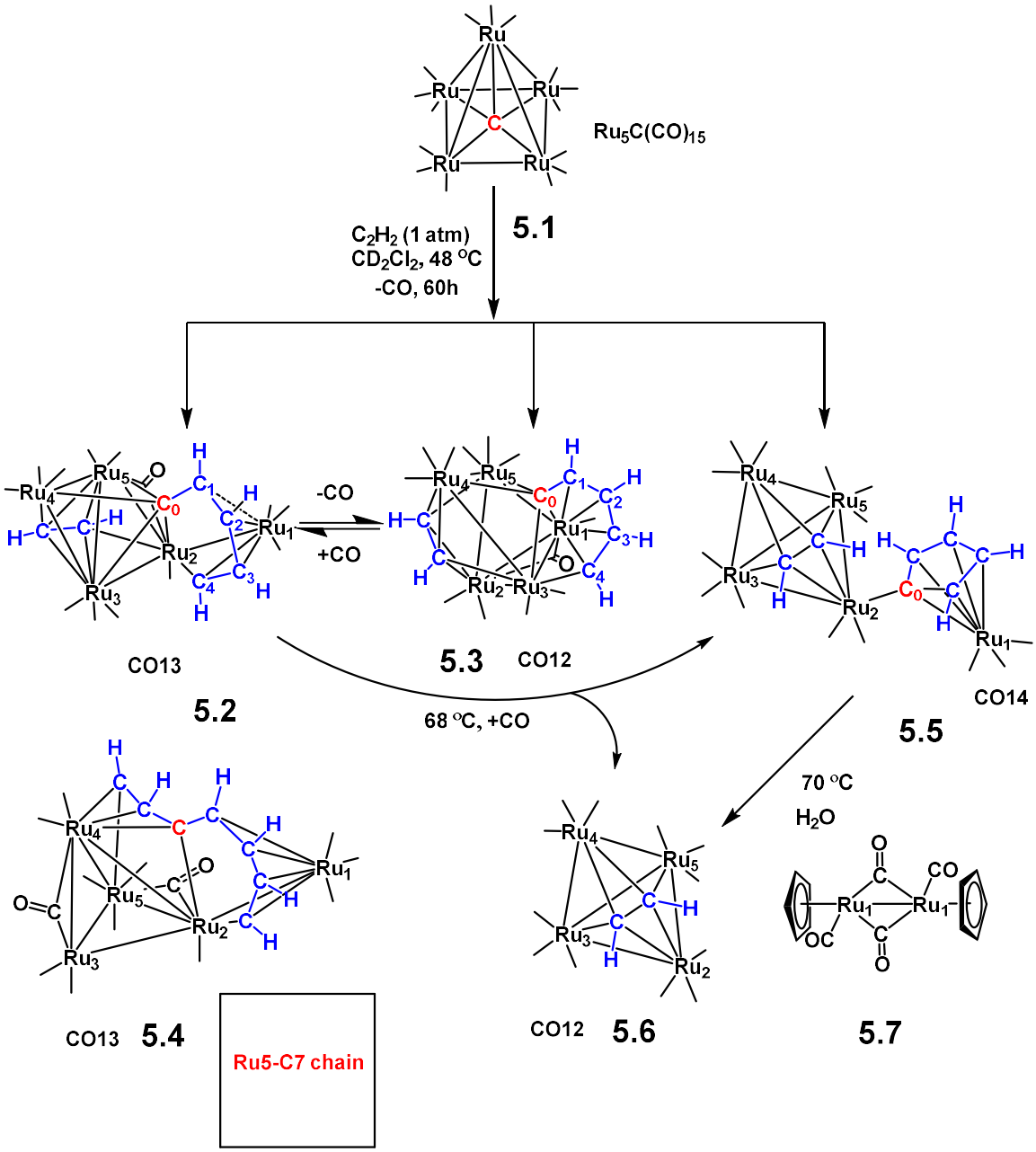

Scheme 5.2 Products obtained from the reaction of **5.1** with ethyne (C_2H_2), and a summary of conversion **5.2** to **5.7**. The CO ligands are represented only as lines from the Ru atoms.

Chapter 6

Trans-Stereochemistry from the Insertion of Alkynes into a Ruthenium–Carbon Bond to a Bridging-Phenyl Ligand[4]

[4] Adams, R. D.; Akter, H.; Smith, M. D.; Tedder, J. D. *Manuscript in progress*.

6.1 Introduction

Insertion reactions have been one of the most useful chemical processes for transforming small unsaturated organic molecules into more complex and valuable derivatives.[1, 2] The migratory 1,2-insertion mechanism of coordinated alkynes into metal – hydrogen and metal – carbon bonds generally proceeds with *cis*-stereochemistry at the alkenyl group, eq. (6.1),[3-5] and has been used in the synthesis of functionalized alkenes and polymers.[6,7]

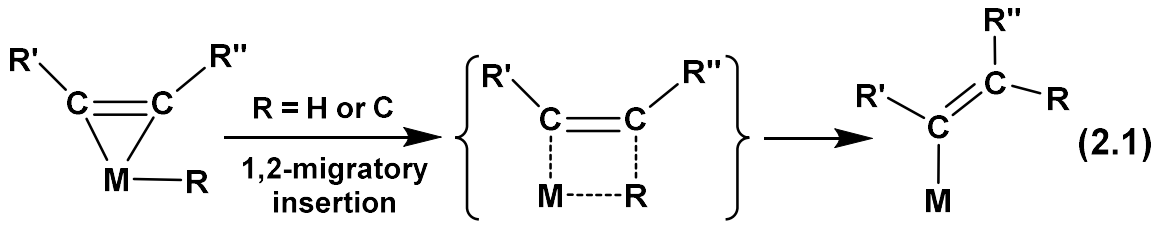

(2.1)

With only a few exceptions,[8,9] *cis*-olefins are the standard products formed by the semi-hydrogenation of alkynes by metal catalysts involving this mechanism.[10] *Trans*-olefins have been observed, but these are often a result of subsequent facile *cis*/*trans* isomerizations that follow for formation of *cis*-olefin products.[10(i), 11]

Insertion reactions of alkynes in di- and polynuclear metal complexes generally provide bridging alkenyl ligands formed by *cis*-insertion stereochemistry,[10(h), 12] although there has been one report of insertion of diphenylacetylene in a dirhodium complex yielding a bridging alkenyl ligand having a *trans*-phenyl groups.[9] Most examples of alkyne insertions involving metal complexes have involved metal-hydrogen bonds.[4, 12] Alkyne insertions into metal – aryl bonds are rare.[5(a), 5(b)]

In recent studies we have prepared a number of transition metal – gold cluster complexes that contain bridging phenyl ligands, e.g. $Os_3(CO)_{10}(\mu\text{-}\eta^1\text{-Ph})[\mu\text{-Au}(PPh_3)]$,[13] $Re_2(CO)_8(\mu\text{-}\eta^1\text{-Ph})[\mu\text{-Au}(PPh_3)]$,[14] $Ru_5(\mu_5\text{-C})(CO)_{13}(\mu\text{-}\eta^2\text{-Ph})[\mu\text{-Au(NHC)}]$, **6.1**, NHC = 1,3-bis(2,6-diisopropylphenyl-imidazol-2-ylidene).[15] In some of these cases, the phenyl ligands have adopted unusual bridging η^1- and η^2-coordination modes that result in interesting chemical and physical properties, including hindered rotation of the phenyl ligand about the metal – carbon bonds.[15, 16] In earlier studies, it was shown that CO readily inserted into the metal – carbon bond of the bridging η^2-phenyl ligand in **6.1** to yield the carbido-pentaruthenium complex $Ru_5(\mu_5\text{-C})(CO)_{13}[\mu\text{-}\eta^2\text{-C(=O)Ph}][\mu\text{-Au(NHC)}]$ containing a bridging benzoyl ligand, see Scheme 6.1.

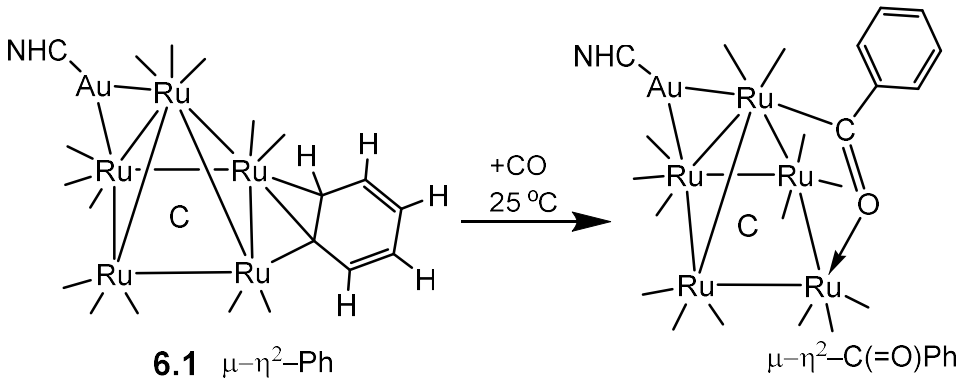

Scheme 6.1 A schematic showing the insertion coupling of CO to the bridging η^2-phenyl ligand of compound **6.1** to from the compound $Ru_5(\mu_5\text{-C})(CO)_{13}[\mu\text{-}\eta^2\text{-C(=O)Ph}][\mu\text{-Au(NHC)}]$.[15] CO ligands are shown only as lines to the Ru atoms.

In a continuation of this work described herein, we have now investigated the reactions of the pentaruthenium complex **6.1** with the alkynes C_2H_2 and HC_2Ph to yield the new alkenyl complexes $Ru_5(\mu_5\text{–C})(CO)_{13}[\mu\text{-}\eta^2\text{-}E\text{-C(H)C(H)Ph}][\mu\text{-Au(NHC)}]$, **6.2** and $Ru_5C(CO)_{13}[\mu\text{-}\eta^2\text{-}E\text{-C(Ph)C(H)Ph}][\mu\text{-Au(NHC)}]$, **6.3** by insertion of the alkyne into the

metal – carbon σ-bond of the phenyl ring in **6.1**. The synthesis, structures and bonding of these new complexes are described in this report.

6.2 Experimental Section

General Data

All reactions were performed under nitrogen atmosphere. Reagent grade solvents were dried by standard procedures and were freshly distilled prior to use. Infrared spectra were recorded on a Thermo Scientific Nicolet IS10. ^{1}H NMR spectra were recorded on a Varian Mercury 300 spectrometer operating at 300.1 MHz. Mass spectrometric (MS) measurements were performed by a direct-exposure probe by using electron impact (EI) ionization on a VG 70S instrument. Ethyne gas (HC_2H) (industrial grade) was purchased from Praxair and was used without further purification. Phenylacetylene (PhC_2H) was purchased from Sigma-Aldrich and was used without further purification. $Ru_5(\mu_5\text{–}C)(CO)_{13}(\mu\text{–}\eta^2\text{–}Ph)[\mu\text{–}Au(NHC)]$, **6.3** where NHC = 1,3-bis(2,6-diisopropylphenyl-imidazol-2-ylidene) was prepared according to previously reported procedures.[15] Product separations were performed by TLC in the air on Analtech 0.25 mm and 0.50 mm silica gel 60 Å F254 glass plates.

Reaction of $Ru_5(\mu_5\text{–}C)(CO)_{13}(\mu\text{–}\eta^2\text{–}Ph)[\mu\text{–}Au(NHC)]$, 6.1 with C_2H_2

10.0 mg (0.0065 mmol) of $Ru_5(\mu_5\text{–}C)(CO)_{13}(\mu\text{–}\eta^2\text{–}Ph)[\mu\text{–}Au(NHC)]$, **6.1** was dissolved in 20 mL of hexane and transferred in three-neck flask. C_2H_2 gas at 1 atm pressure was purged through the solution for 0.5 h at 25 °C. The progress of the reaction was followed by IR spectroscopy. The solvent was then removed *in vacuo*, and 9.0 mg of $Ru_5(\mu_5\text{–}C)(CO)_{13}(\mu\text{-}\eta^2\text{-}E\text{-}CHCHPh)[\mu\text{-}Au(NHC)]$, **6.2** (yield 89%) was isolated by a TLC

by using a 6/3 of hexane/methylene chloride solvent mixture. The product **6.2** recrystallized from a hexane/methylene chloride solvent mixture. Spectral data for **6.2**: IR νCO (cm^{-1} in hexane): 2072(m), 2039(vs), 2027(s), 2017(s), 2008(s), 1990(w), 1979(w), 1957(vw), 1937(vw). ^1H NMR (CD_2Cl_2, in ppm): δ = 10.90 (d, 12 Hz, 1H, C**H**=CH), 7.46 (t, 8 Hz, 2H, para C**H**–$(CH)_2$), 7.21-7.37 (m, 9H, meta H (C_6H_5)), 7.14 (s, 2H, N(C**H**)$_2$), 5.28 (d, 12 Hz, 1H, CH=C**H**), 2.78 (sept, 7 Hz, 4H, C**H**–$(CH_3)_2$), 1.37 (d, 6 Hz, 12H, CH–(C**H**$_3)_2$), 1.14 (d, 6.9 Hz, 12H, CH–(C**H**$_3)_2$). EI+/MS: m/z 1572 (M+).

Reaction of 6.1 with PhC_2H

12.8 mg (0.0083 mmol) of $Ru_5(\mu_5–C)(CO)_{13}(\mu–\eta^2–Ph)[\mu–Au(NHC)]$, **6.1** was dissolved in toluene-d_8 solvent in a NMR tube. 10.0 μL (0.9105 mmol) of PhC_2H was added to the solution. The reaction mixture was heated in a constant temperature oil bath at 80 ºC for 45 min. The progress of the reaction was followed by ^1H NMR spectroscopy. The solvent was removed *in vacuo* and 13.2 mg of $Ru_5C(CO)_{13}(\mu–\eta^2–E–C(Ph)C(H)Ph)[\mu–Au(NHC)]$, **6.3** (yield 96%) was isolated by TLC by using a 2/1 of hexane/methylene chloride solvent mixture for elution. The product was then crystallized from an octane/methylene chloride solvent mixture. Spectral data for **6.3**: IR νCO (cm^{-1} in hexane): 2071(m), 2040(vs), 2028(s), 2018(s), 2009(s), 1992(vw), 1987(vw), 1977(vw), 1969(vw), 1959(vw), 1940(vw). ^1H NMR (CD_2Cl_2, in ppm): 7.45–6.84 (m, 16H, (-C_6H_5), 7.14 (s, 2H, N(C**H**)$_2$), 5.26 (s, 1H, PhC=C**H**), 2.79 (sept, 7.2 Hz, 4H, C**H**–$(CH_3)_2$), 1.37 (d, 5.7 Hz, 12H, CH–(C**H**$_3)_2$), 1.14 (d, 6.9 Hz, 12H, CH–(C**H**$_3)_2$).

Crystallographic Analyses

Single crystals of compound **6.2** suitable for X-ray diffraction analyses were obtained by slow evaporation of solvent from solutions of the pure compounds in a hexane/methylene chloride solvent mixture at room temperature. Single crystals of compound **6.3** suitable for X-ray diffraction analyses were obtained by slow evaporation of solvent from a solution of the pure compound in octane/methylene chloride solvent at room temperature. Crystals for compounds **6.2** and **6.3** were glued onto the end of a thin glass fiber. X-ray intensity data for compounds **6.2** was measured by using a Bruker SMART APEX CCD-based diffractometer by using Mo Kα radiation (λ = 0.71073 Å). The raw data frames were integrated with the SAINT+ program by using a narrow frame integration algorithm. Correction for Lorentz and polarization effects were also applied with SAINT+.[17] An empirical absorption correction based on the multiple measurements of equivalent reflections was applied by using the program SADABS in each analysis.[18]

X-ray intensity data for compound **6.3** was measured by using a Bruker D8 QUEST diffractometer equipped with a PHOTON-100 CMOS area detector and an Incoatec microfocus source (Mo Kα radiation, λ = 0.71073 Å).[10] The data collection strategy for compound **6.3** consisted of five 180° ω-scans at different φ settings and two 360° φ-scans at different ω angles, with a scan width per image of 0.5°. The crystal-to-detector distance was 8.2 cm, and each image was measured for 12 s. The raw area detector data frames were reduced, scaled, and corrected for absorption effects using the SAINT[19] and SADABS[18] programs (Estimated minimum/maximum transmission = 0.2555/0.3343). Both structures were solved by a combination of direct Methods and difference Fourier syntheses, and refined by full-matrix least-squares refinement on F^2 by using the SHELXTL software

package.[20] All hydrogen atoms were placed in geometrically idealized positions. Compound **6.2** crystallized in the monoclinic crystal system. The space group *P*2/n was identified for compound **6.2** based on systematic absences observed in the intensity data. Compound **6.3** crystallized in the orthorhombic crystal system. The space group *P*bca was identified for compound **6.3** based on systematic absences observed in the intensity data. Crystal data, data collection parameters, and results for the refinements for all the structural analyses are listed in Table 6.1.

6.3 Results and Discussion

The reaction of **6.1** with ethyne (C_2H_2) in hexane solvent at 25 ℃ for 30 min yielded the new compound $Ru_5(\mu_5\text{-}C)(CO)_{13}[\mu\text{-}\eta^2\text{-}E\text{-}C(H)C(H)Ph][\mu\text{-}Au(NHC)]$, **6.2** in 89 % yield. Compound **6.2** was characterized by a combination of IR, ^{1}H NMR, mass spectrometry, and single-crystal X-ray diffraction analyses. Crystals of **6.2** contain two structurally similar molecules of the complex in the asymmetric crystal unit. An ORTEP diagram of the molecular structure of one of these molecules of **6.2** is shown in Figure 6.1.

Compound **6.2** is structurally very similar to the structure of **6.1**[15] containing a square pyramidal cluster of five ruthenium atoms with a carbido ligand in the base of the square pyramid and thirteen linear terminal carbonyl ligands distributed about the cluster as shown in Figure 6.1. An Au(NHC) group bridges the apical–basal Ru(1)–Ru(2) bond of the cluster. The Ru–Au bond distances in **6.2**, Ru1–Au1 = 2.7848(7) Å, Ru2–Au1 = 2.8282(7) Å, are similar to its parent cluster **6.1**, Ru - Au = 2.7906(4) Å and 2.8338(4) Å, respectively. The most interesting ligand in **6.2** is a σ, π-coordinated 2-phenylvinyl ligand, $\mu\text{–}\eta^2\text{-}E$-CHCHPh, which was formed by insertion of C_2H_2 into the Ru-C bond of an $\mu\text{-}\eta^2$-

Ph ligand in **6.1**. The alkenyl carbon atoms, C(2) and C(3), are π-coordinated to Ru(3) and Ru3–C2 = 2.205(8) Å, Ru3–C3 = 2.315(9) Å. Atom C(2) is also σ-bonded to Ru(4), Ru4–C2 = 2.053(9) Å. There is an *E*-stereochemistry at the coordinated double bond C2 – C3 due to its σ-coordination to Ru4. The C2 – C3 bond distance is 1.390(12) Å. The alkenyl hydrogen atoms in **6.2** have a *trans*-relationship and appear as two deshielded doublets at δ = 10.90 and 5.28 with a large coupling constant, $^{3}J_{H\text{-}H}$ = 12 Hz in the ^{1}H NMR spectrum. The μ–η^{2}-CHCHPh ligand in **6.2** is unusual because the two alkenyl hydrogen atoms have a *trans*-stereochemistry, see Scheme 6.2 and Figure 6.1.

There are a number of reports of polynuclear metal carbonyl cluster complexes containing similar bridging σ, π-coordinated 2-phenylvinyl ligands,[21] but all have been synthesized by reactions of phenylacetylene, PhC≡CH, with hydride-containing polynuclear metal complexes by insertion of the alkyne into an M – H bond yielding 2-phenylvinyl ligands having an overall *cis*-stereochemistry of the vinyl hydrogen atoms. The μ–η^{2}-CHCHPh ligand in **6.2** serves formally as a three-electron neutral donor to the Ru_5 cluster, and the Au(NHC) group formally donates only one electron. Overall the Ru_5 cluster contains a total of 74 valence electrons, which is exactly the number required for a square pyramidal cluster of five metal atoms.[22]

The reaction of **6.1** with mono-phenylacetylene (PhC_2H), in d_8-toluene solvent at 80 °C for 45 min yielded the new compound **6.3** in 96 % yield. Compound **6.3** was also characterized by a combination of IR, ^{1}H NMR, and single-crystal X-ray diffraction analyses. Crystals of **6.3** contain two structurally similar molecules of the complex in the asymmetric crystal unit. An ORTEP diagram of the molecular structure of one of these molecules of **6.3** is shown in Figure 6.2.

Compound **6.3** is very similar to **6.2** containing of a square pyramidal Ru_5C cluster as shown in Figure 6.2, and an Au(NHC) group bridging the apical–basal Ru(1)–Ru(2) bond of the cluster. The Ru–Au bond distances in **6.3**, Ru1a–Au1a = 2.7701(2) Å, Ru2a–Au1a = 2.8463(2) Å, are very similar to those distances **6.1** and **6.2**. Compound **6.3** contains a σ+π-coordinated, η^2-1,2-diphenylvinyl ligand, η^2-*E*-C(Ph)C(H)Ph, bridging the Ru3 – Ru4 edge of the Ru_5 cluster. Compound **6.3** was formed by the insertion of PhC_2H into the Ru-C bond of the μ–η^2-Ph ligand in compound **6.1**, Ru3a–C2a = 2.246(2) Å, Ru3a–C3a = 2.262(2) Å. Atom C2a remains σ-coordinated to Ru4a, Ru4a–C2a = 2.083(2) Å. Most interestingly, the phenyl groups on the C(Ph)C(H)Ph ligand exhibit a pseudo-*cis*-stereochemistry at the C – C double bond. The C(Ph)C(H)Ph ligand is not completely planar. The Ph-C2a-C3a-Ph torsion angle is 17.1(4)°.

The single hydrogen atom on the coordinated double bond of the alkenyl ligand in **6.3** exhibits a deshielded, singlet resonance in the ^{1}H NMR spectrum at 5.26 ppm. Assuming that the PhCC(H)Ph ligand donates three electrons and the Au(NHC) group donates one electron to the cluster, the Ru_5 cluster of **6.3** then contains a total of 74 cluster valence electrons, which is exactly the number required for a square-pyramidal cluster of five metal atoms.[21]

Assuming that it was the phenyl group on C3a is the one that was originally on the Ru atoms in **6.1**, this would imply that the insertion of the PhC≡CH molecule into the Ru – C σ-bond of the phenyl ligand proceeded with transfer of the phenyl ligand to the unsubstituted carbon atom of the PhC≡CH molecule resulting in an overall *trans*-stereochemistry, i. e. the phenyl group on C2a and the H atom on C3a are *trans* to one

another. The C2a – C3a bond length in in **6.3**, 1.421(3) Å, is slightly longer than the corresponding C – C bond length (1.390(12) Å) in **6.2**, see below.

There are many examples of σ+π-coordinated, bridging C(Ph)C(H)Ph ligands in the literature.[12(c)-12(f), 23] All of these were synthesized by the addition and insertion of diphenylacetylene into a metal – hydrogen bond in a polynuclear metal complexes. All of these exhibit a *cis*-stereochemistry of the two phenyl rings and were presumably formed by *cis*-insertion into the M-H bonds, except for one. The one exception is the compound $Rh_2[P(O\text{-}i\text{-}C_3H_7)_3]_4[\mu\text{-}\eta^2\text{-}C(Ph)C(H)Ph](\mu\text{-}H)$, **6.4** that was obtained by the reaction of $\{Rh[P(O\text{-}i\text{-}C_3H_7)_3]_2(\mu\text{-}H)\}_2$ with diphenylacetylene, PhC≡CPh and was reported by Muetterties and others in 1983.[9] Compound **6.4** contains *trans*-oriented phenyl groups on its bridging C(Ph)C(H)Ph ligand. The bridging η^2-C(Ph)C(H)Ph ligand in **6.4** clearly contains *trans*-oriented phenyl rings. The mechanism of the formation of **6.4** was not established and it cannot be ruled out that the mechanism may involved an unobserved *cis*-insertion step that was followed by an unobserved *cis-trans* isomerization of the alkenyl ligand in a transient intermediate.[24]

Similarly, it cannot be ruled out at this time that the formations of **6.2** and **6.3** may have involved *cis*-alkyne insertion steps involving the phenyl ligand in **6.1** which were followed by *cis-trans* isomerization of the incipient alkenyl ligands in unobserved intermediates.

6.4 Conclusion

The insertion of the alkynes, HC≡CH and HC≡CPh, into the Ru - C bond of the bridging phenyl ligand of the complex **6.1** leads to the formation of bridging 2-phenylvinyl

and bridging 1,2-diphenylvinyl ligands in the complexes **6.2** and **6.3**, respectively, by C – C bond formation. Most notably, the overall stereochemistry of both alkenyl ligands is formally a result of an overall *trans*-insertion coupling of the alkyne to the bridging phenyl ligand of **6.1**. The mechanism of the formation of these vinyl ligands is not yet established. It is possible that both reactions proceed via *cis*-insertions of the alkynes via unobserved intermediate(s) that subsequently isomerize to the observed products **6.2** and **6.3**.

6.5 References

1. (a) Collman, J. P.; Hegedus, L. S.; Norton, J. R.; Finke, R. G. *in Principles and Applications of Organotransition Metal Chemistry*, University Science Books, Mill Valley, CA, **1987**, Ch. 6. (b) Cotton, F. A.; Wilkinson, G.; Murillo, C. A.; Bochmann, M. *in Advanced Inorganic Chemistry*, 6th Ed. John Wiley & Sons, Inc., New York, **1999**, Ch. 21-5.
2. (a) Sinn, H.; Kaminsky, W. Ziegler-Natta Catalysis. *Adv. Organomet. Chem*. **1980**, 18, 99−149. (b) Pruett, R. L. *J. Chem. Ed.* **1986**, 63, 196 – 198. (c) Forster, D.; Dekleva, T. W. *J. Chem. Ed.* **1986**, 63, 204 – 206. (d) Severin, R.; Doye, S. *Chem. Soc. Rev*. **2007**, 36, 1407–1420.
3. (a) Thorn, D. L.; Hoffmann, R. *J. Am. Chem. Soc.* **1978**, 100, 2079 – 2090. (b) Selmeczy, A. D.; Jones, W. D. *Inorg. Chim. Acta* **2000**, 300–302, 138–150. (c) Burch, R. R.; Shusterman, A. J.; Muetterties, E. L.; Teller, R. G.; Williams, J. M. *J. Am. Chem. Soc.* 1983, 105, 3546-3556.
4. (a) Clark, H. C.; Wong, C. S. *J. Organomet. Chem*. **1975**, 92, C31- C34. (b) Attig, T. G.; Clark, H. C.; Wong, C. S. *Can. J. Chem.* **1977**, 55, 189 - 198.

5. (a) Huggins, J. M.; Bergman, R. G., *J. Am. Chem. Soc*. **1981**, 103, 3002 - 3011. (b) Booth, B. L.; Hargreaves, R. G. *J. Chem. Soc. (A)* **1970**, 308 – 314. (c) Carmona, E.; Gutlérrez-Puebla, E.; Monge, A.; Marín, J. M.; Peneque, M.; Poveda, M. L. *Organometallics* **1984**, 3, 1438-1440.
6. (a) Norton, J. R.; Murray, T. F. *J. Am. Chem. Soc*. **1979**, 101, 4107 – 4119.
7. (a) Maitlis, P. M. *Acc. Chem. Res*. **1976**, 9, 93 - 99. (b) Ginsburg, E. J.; Gorman, C. B.; Grubbs, R. H. in *Modern Acetylene Chemistry*, Stang, P. J.; Diederich, F. Eds., VH Pubs., Weinheim, **1995**, Ch. 10, pp 353 – 383.
8. (a) Fürstner, A. *J. Am. Chem. Soc*. **2019**, 141, 11−24. (b) Radkowski, K.; Sundararaju, B.; Fürstner, A. *Angew. Chem. Int. Ed. Engl*. **2013**, 52, 355-360. (c) Leutzsch, M.; Wolf, M. L.; Gupta, P.; Fuchs, M.; Thiel, W.; Farès, C.; Fürstner, A. *Angew. Chem., Int. Ed*. **2015**, 54, 12431−12436. (d) Schleyer, D.; Niessen, H. G.; Bargon, J. *New J. Chem*. **2001**, 25, 423−426.
9. Burch, R. R.; Shusterman, A. J.; Muetterties, E. L.; Teller, R. G.; Williams, J. M. *J. Am. Chem. Soc.* 1983, 105, 3546-3556.
10. (a) Kluwer, A. M.; Elsevier, C. J. *In Handbook for Homogeneous Hydrogenation*, 1st ed.; de Vries, J. G., Elsevier, C. J., Eds.; Wiley-VCH: Weinheim, **2007**; Vol. 1, pp 375-411. (b) (a) Schrock, R. R.; Osborn, J. A. *J. Am. Chem. Soc.***1976**, 98, 2143–2147. (c) Sprengers, J. W.; Wassenaar, J.; Clement, N. D.; Cavell, K. J.; Elsevier, C. J. *Angew. Chem. Int. Ed*. **2005**, 44, 2026 –2029. (d) Hauwert, P.; Boerleider, R.; Warsink, S.; Weigand, J. J.; Elsevier, C. J. *J. Am. Chem. Soc.* **2010**, 132, 16900–16910. (e) Kluwer, A. M.; Koblenz, T. S.; Jonischkeit, T.; Woelk, K.; Elsevier, C. J. *J. Am. Chem. Soc.* **2005**, 127, 15470–15480. (f) Sodeoka, M.; Shibasaki, M. *J. Org. Chem*. **1985**, 50, 1147

– 1149. (g) La Pierre, H. S.; Arnold, J.; Toste, F. D. *Angew. Chem. Int. Ed*. **2011**, 50, 3900 – 3903. (h) Adams, R. D.; Barnard, T. S.; Li, Z.; Wu, W.; Yamamoto, J. *J. Am. Chem. Soc.* **1994**, 116, 9103-9113. (i) Tokmic, K.; Fout, A. R. *J. Am. Chem. Soc*. **2016**, 138, 13700 – 13705.

11. Molnár, Á.; Sárkány, A.; Varga, M. *J. Molec. Catal. A: Chem*. **2001**, 173, 185–221.
12. (a) Knorr, M.; Jourdain, I. *Coord. Chem. Rev*. **2017**, 350, 217–247. (b) Adams, R. D.; Dhull, P.; Rassolov, V.; Wong, Y. O. *Inorg. Chem.* **2016**, 55, 10475 − 10483. (c) Caffyn, A. J. M.; Mays, M. J.; Raithby, P. R. *J. Chem. Soc., Dalton Trans*. **1992**, 515 – 519. (d) Clauss, A. D.; Tachikawa, M.; Shapley, J. R.; Pierpont, C. G. *Inorg. Chem*. **1981**, 20, 1528-1533. (e) Aime, S.; Osella, D.; Milone, L.; Lanfredi, A. M. M.; Tiripicchio, A. *Inorg. Chim. Acta* **1983**, 71, 141 – 147. (f) Ferrand, V.; Süss-Fink, G.; Neels, A.; Stoeckli-Evans, H. *J. Chem. Soc*., *Dalton Trans*. **1998**, 3825–3831.
13. Adams, R. D.; Rassolov, V.; Zhang, Q. *Organometallics* **2013**, 32, 6368−6378.
14. Adams, R. D.; Rassolov, V.; Wong, Y. O. *Angew. Chem. int. Ed. Engl.* **2014**, 53, 11006 - 11009.
15. Adams, R. D.; Tedder, J.; Wong, Y. O. *J. Organomet. Chem.* **2015**, 795, 2 – 10.
16. Adams, R. D.; Rassolov, V.; Zhang, Q. *Organometallics* **2013**, 32, 1587 – 1590.
17. Saint+, Version 6.2a, Bruker Analytical X-ray System, Inc, Madison, WI, **2001**.
18. SADABS Version 2016/2. Krause, L.; Herbst-Irmer, R.; Sheldrick, G. M.; Stalke, D. J. Appl. Cryst. **2015**, 48, 3-10.
19. APEX3 Version 2016.5-0 and SAINT Version 8.37A. Bruker AXS, Inc. Madison, WI, USA.

20. G.M. Sheldrick, SHELXTL, Version 6.1, Bruker Analytical X-ray Systems, Inc, Madison, WI, **1997**.

21. (a) Adams, R. D.; Captain, B.; Trufan, E.; Zhu, L. *J. Am. Chem. Soc.* **2007**, 129, 7545-7556. (b) Adams, R. D.; Captain, B.; Zhu, L. *J. Am. Chem. Soc.* **2006**, 128, 13672-13673. (c) Hogarth, G.; Lavender, M. H.; Shukri, K. *J. Organomet. Chem.***1997**, 527, 247-258 (d) Fujita, K.; Nakaguma, H.; Hanasaka, F.; Yamaguchi, R. Organometallics **2002**, 21, 3749-3757. (e) Tschan, M. J.-L.; Süss-Fink, G.; Cherioux, F.; Therrien, B. *Chem. Eur. J.* **2007**, 13, 292 – 299. (f) Tahara, A.; Kajigaya, M.; Takao, T.; Suzuki, H. *Organometallics* **2013**, 32, 260−271.

22. Mingos, D. M. P. *Acc. Chem. Res.* **1984**, 17, 311 – 319.

23. (a) Adams, R. D.; Chen, G. *Organometallics* **1992**, 11, 837-845. (b) Adams, R. D.; Chen, G. *Organometallics* **1991**, 10, 3028-3035. (c) Cabeza, J. A.; del Rio, I.; Moreno, M.; Riera, V. *Organometallics* **1998**, 17, 3027-3033.

24. Hart, D. W.; Schwartz, J. *J. Organomet. Chem*. **1975**, 81, C11 - C14.

Table 6.1 Crystal data, data collection parameters for compounds **6.2** and **6.3**.

Compound	**6.2**	**6.3**
Empirical formula	$Ru_5AuO_{13}N_2C_{49}H_{43}$	$Ru_5AuO_{13}N_2C_{55}H_{47}$
Formula weight	1570.17	1646.28
Crystal system	Monoclinic	Orthorhombic
Lattice parameters		
a (Å)	33.0470(9)	19.6303(7)
b (Å)	10.6332(3)	34.9241(12)
c (Å)	33.3022(9)	36.2726(13)
α (deg)	90.00	90.00
β (deg)	109.248(1)	90.00
γ (deg)	90.00	90.00
V ($Å^3$)	11048.1(5)	24867.4(15)
Space group	*P*2/n	*P*bca
Z value	8	16
ρ_{calc} (g/cm^3)	1.888	1.850
μ (Mo Kα) (mm^{-1})	4.037	2.406
Temperature (K)	294(2)	100(2)
2Θmax (°)	50.06	60.20
No. Obs. ($I > 2\sigma(I)$)	19541	9265
No. Parameters	1293	433
Goodness of fit (GOF)	1.030	1.029
Max. shift in cycle	0.003	0.006
Residuals*: R1; wR2	0.0404; 0.0908	0.0239, 0.0413
Absorption Correction, Max/min	Multi-scan 1.00/0.749	Multi-scan 0.5969/0.3924
Largest peak in Final Diff. Map ($e^-/Å^3$)	1.275	0.857

*$R1 = \Sigma_{hkl}(||F_{obs}| - |F_{calc}||)/\Sigma_{hkl}|F_{obs}|$; $wR2 = [\Sigma_{hkl}w(|F_{obs}| - |F_{calc}|)^2/\Sigma_{hkl}wF^2_{obs}]^{1/2}$; $w = 1/\sigma^2(F_{obs})$; $GOF = [\Sigma_{hkl}w(|F_{obs}| - |F_{calc}|)^2/(n_{data} - n_{vari})]^{1/2}$.

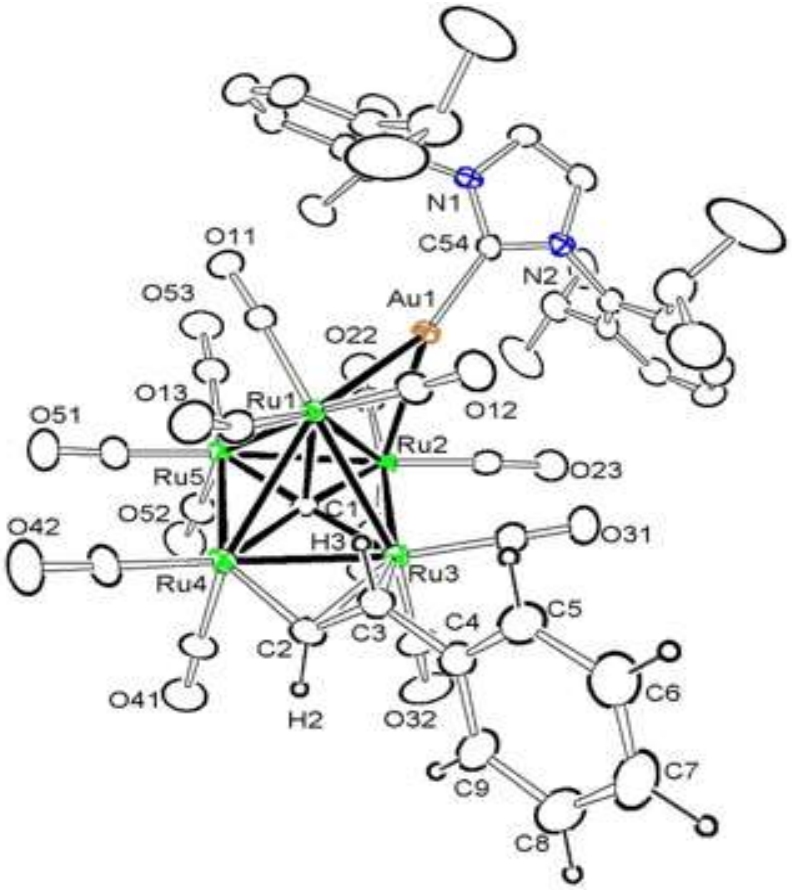

Figure 6.1 An ORTEP diagram of the molecular structure of $Ru_5C(CO)_{13}(\mu\text{-}\eta^2\text{-}E\text{-}CHCHPh)[\mu\text{-}Au(NHC)]$, **6.2**, showing 15% thermal ellipsoid probability. The hydrogen atoms on the carbene ligand are omitted for clarity. Selected interatomic distances in (Å) for molecule 1 in the crystal are as follows: Ru1-Au1 =2.7848 (7), Ru2-Au1 = 2.8282 (7), Ru1-Ru2 = 2.9511 (9), Au1-C54 = 2.014(7), Ru2-Ru3 = 2.8688 (10), Ru4-Ru3 = 2.6828 (9), Ru4-C2 = 2.053 (9), Ru3-C3 = 2.315 (9), Ru3-C2 = 2.205 (8), C2-C3 = 1.390 (12), C3-C4 = 1.482 (12).

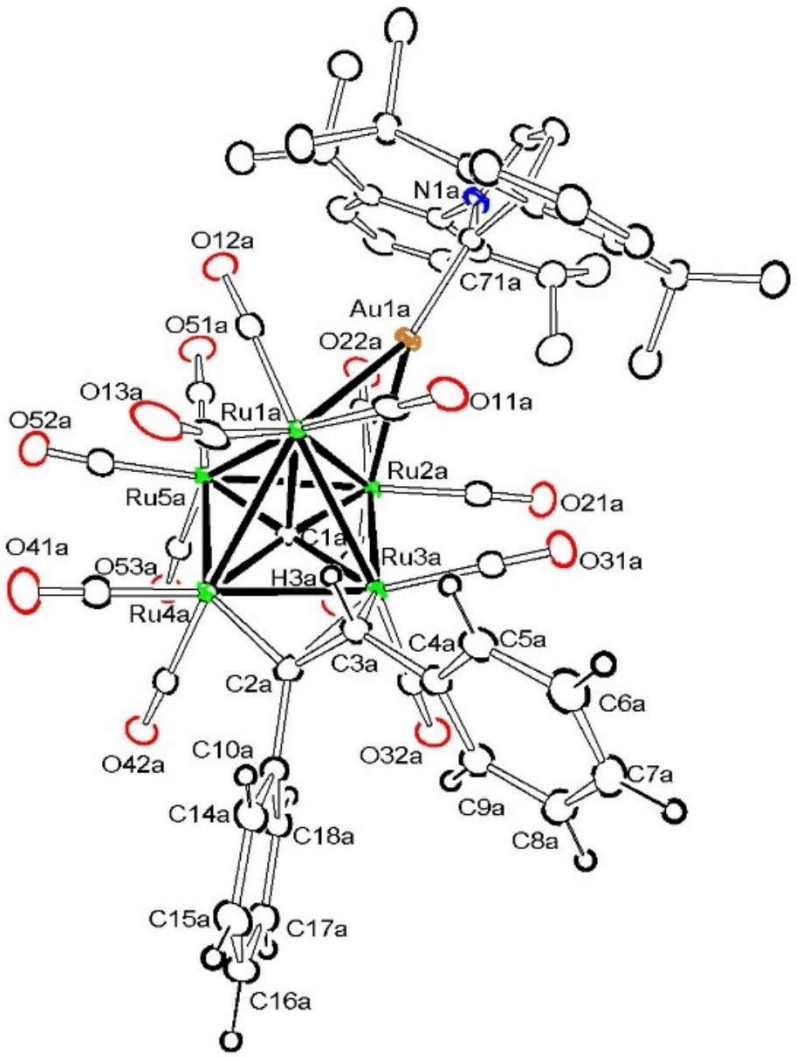

Figure 6.2 An ORTEP diagram of the molecular structure of one of the two similar, independent molecules in the unit cell of $Ru_5C(CO)_{13}(\mu\text{-}\eta^2\text{-}E\text{-}C(Ph)C(H)Ph)[\mu\text{-}Au(NHC)]$, **6.3** showing 40% thermal ellipsoid probability. The hydrogen atoms on the carbene ligand are omitted for clarity. Selected interatomic distances in (Å) for molecule "**a**" in the crystal are as follows: Ru1a-Au1a =2.7701(2), Ru2a-Au1a = 2.8463(2), Ru1a-Ru2a = 2.9175(3), Au1a-C71a = 2.050(2), Ru2a-Ru3a = 2.8574(3), Ru4a-Ru3a = 2.6859(3), Ru4a-C2a = 2.083(2), Ru3a-C3a = 2.262(2), Ru3a-C2a = 2.246(2), C2a-C3a = 1.421(3), C3a-C4a = 1.490 (3), C2a-C10a = 1.493(3); torsion angle Ph-C2a-C3a-Ph = 17.1(4)º.

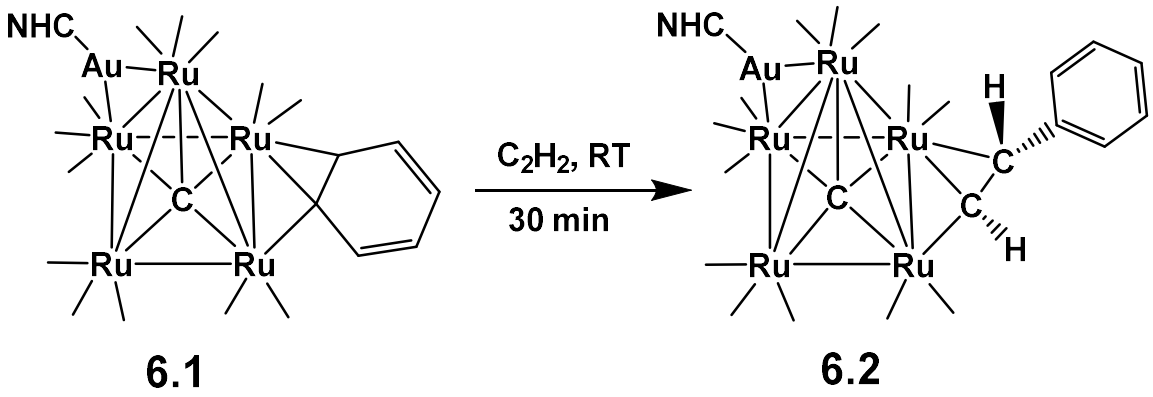

Scheme 6.2 A schematic of the formation of **6.2** by a formal *trans*-insertion of C_2H_2 into the bridging Ph ligand of **6.1**. The CO ligands are represented only as lines from the Ru atoms.

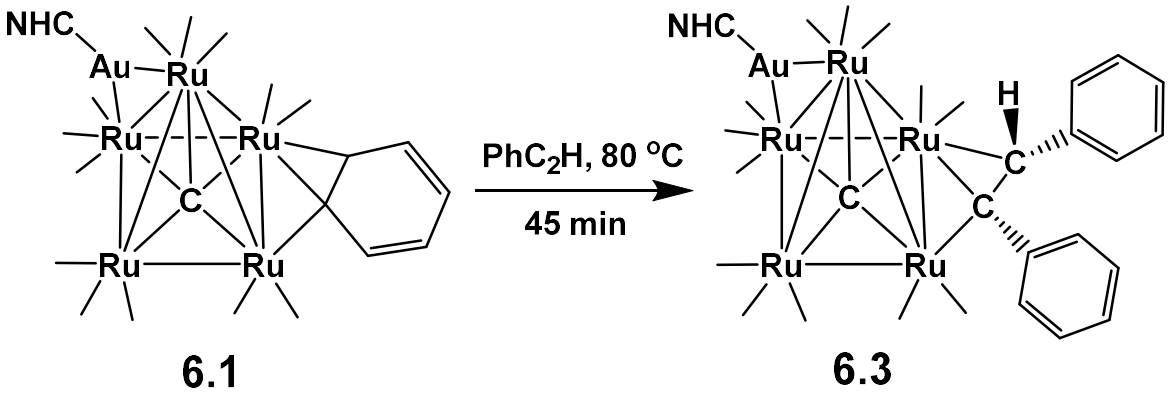

Scheme 6.3 A schematic of the formation of **6.3** by a formal trans-insertion of PhC_2H into the bridging Ph ligand of **6.1**. The CO ligands are represented only as lines from the Ru atoms.

Appendix A

Copyright Releases

Permission for reprint from publisher of Chapter 2.

Adams, R. D.; Akter, H.; Tedder, J. D. *J. Organomet. Chem.* **2018**, *871*, 159-166.

Permission for reprint from publisher of Chapter 3.

Adams, R. D.; Akter, H.; Smith, M. D.; Tedder, J. D. *J. Organomet. Chem.* **2018**, *878*, 77-83.

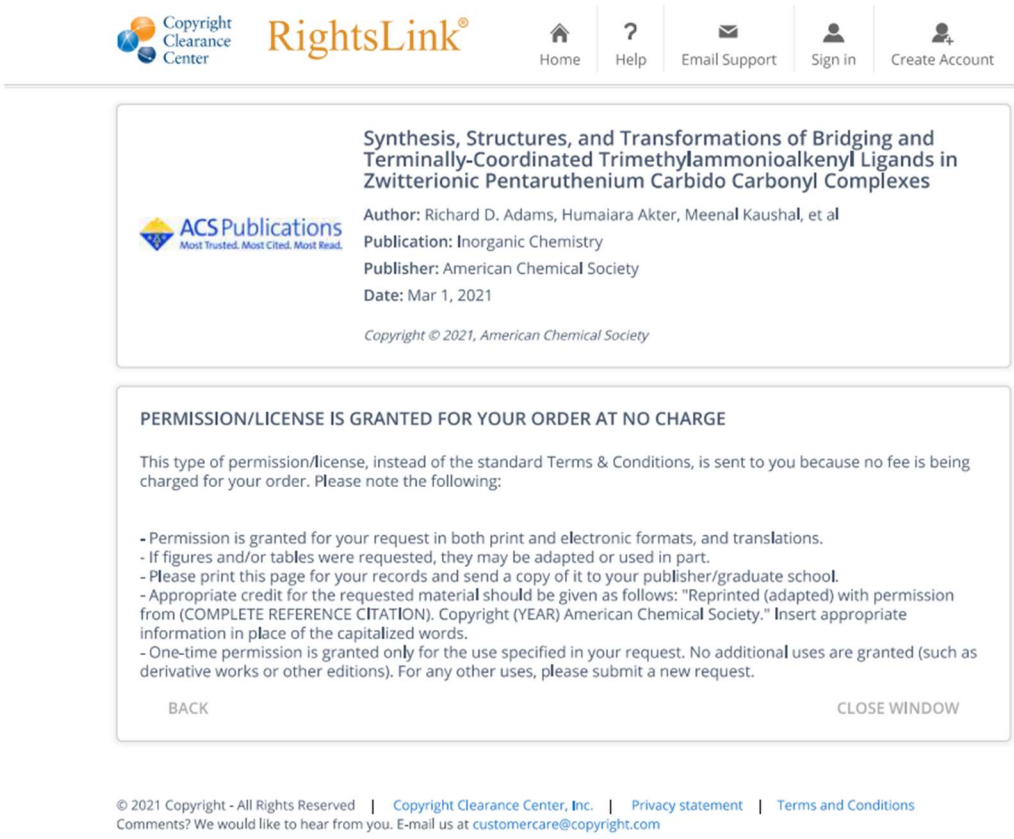

Permission for reprint from publisher of Chapter 4.

Adams, R. D.; Akter, H.; Kaushal, M.; Smith, M. D.; Tedder, J. D. *Inorg. Chem.* **2021**, 60, 6, 3781–3793.